

Volpicella, Alessio

**Working Paper**

## SVARs identification through bounds on the forecast error variance

Working Paper, No. 890

**Provided in Cooperation with:**

School of Economics and Finance, Queen Mary University of London

*Suggested Citation:* Volpicella, Alessio (2019) : SVARs identification through bounds on the forecast error variance, Working Paper, No. 890, Queen Mary University of London, School of Economics and Finance, London

This Version is available at:

<https://hdl.handle.net/10419/210447>

**Standard-Nutzungsbedingungen:**

Die Dokumente auf EconStor dürfen zu eigenen wissenschaftlichen Zwecken und zum Privatgebrauch gespeichert und kopiert werden.

Sie dürfen die Dokumente nicht für öffentliche oder kommerzielle Zwecke vervielfältigen, öffentlich ausstellen, öffentlich zugänglich machen, vertreiben oder anderweitig nutzen.

Sofern die Verfasser die Dokumente unter Open-Content-Lizenzen (insbesondere CC-Lizenzen) zur Verfügung gestellt haben sollten, gelten abweichend von diesen Nutzungsbedingungen die in der dort genannten Lizenz gewährten Nutzungsrechte.

**Terms of use:**

*Documents in EconStor may be saved and copied for your personal and scholarly purposes.*

*You are not to copy documents for public or commercial purposes, to exhibit the documents publicly, to make them publicly available on the internet, or to distribute or otherwise use the documents in public.*

*If the documents have been made available under an Open Content Licence (especially Creative Commons Licences), you may exercise further usage rights as specified in the indicated licence.*

# SVARs Identification through Bounds on the Forecast Error Variance

Alessio Volpicella

Working paper No. 890

July 2019

ISSN1473-0278

## School of Economics and Finance



Queen Mary  
University of London

# SVARs Identification through Bounds on the Forecast Error Variance<sup>\*†</sup>

Alessio Volpicella<sup>‡</sup>

**Job Market Paper**  
Latest Version Here

## Abstract

Sign-restricted Structural Vector Autoregressions (SVARs) are increasingly common. However, they usually result in a set of structural parameters that have very different implications in terms of impulse responses, elasticities, historical decomposition and forecast error variance decomposition (FEVD). This makes it difficult to derive meaningful economic conclusions, and there is always the risk of retaining structural parameters with implausible implications. This paper imposes bounds on the FEVD as a way of sharpening set-identification induced by sign restrictions. Firstly, in a bivariate and trivariate setting, this paper analytically proves that bounds on the FEVD reduce the identified set. For higher dimensional SVARs, I establish the conditions in which the placing of bounds on the FEVD delivers a non-empty set and sharpens inference; algorithms to detect non-emptiness and reduction are also provided. Secondly, under a convexity criterion, a prior-robust approach is proposed to construct estimation and inference. Thirdly, this paper suggests a procedure to derive theory-driven bounds that are consistent with the implications of a variety of popular, but different, DSGE models, with real, nominal, and financial frictions, and with sufficiently wide ranges for their parameters. The methodology is generalized to incorporate uncertainty about the bounds themselves. Fourthly, a Monte-Carlo exercise verifies the effectiveness of those bounds in identifying the data-generating process relative to sign restrictions. Finally, a monetary policy application shows that bounds on the FEVD tend to remove unreasonable implications, increase estimation precision, sharpen and also alter the inference of models identified through sign restrictions.

**Keywords:** Bounds, Forecast Error Variance, Monetary Policy, Set Identification, Sign Restrictions, Structural Vector Autoregressions (SVARs). **JEL:** C32, C53, E10, E52.

---

<sup>\*</sup>I am indebted to Andrea Carriero and Haroon Mumtaz for invaluable guidance and support.

<sup>†</sup>I also thank Raffaella Giacomini, Christiane Baumeister, Serena Ng, Dario Caldara, Toru Kitagawa, Mikkel Plagborg-Møller, Wouter Den Haan, Matthias Meier, Emmanuel Guerre, Michel van der Wel, Mathias Trabandt, Renato Faccini, Filippo Ferroni, Ron Smith, Konstantinos Theodoridis, George Kapetanios, Liudas Giraitis, Daniele Bianchi, Sylvain Barde, Emanuele Bacchiocchi, Mark Bognanni, Yuliya Lovcha, Alejandro Perez-Laborda, Marta Boczon, and Alexander Mayer for discussions and insightful suggestions. I would like to thank conference and seminar participants at the Econometric Institute International PhD Conference (Erasmus University Rotterdam), 2019 Workshop in Structural VAR models (QMUL), 6th Money, Macroeconomics and Finance PhD conference (MMF PhD conference, City University), 2019 Royal Economic Society (RES) Conference (University of Warwick), 24th Spring Meeting of Young Economists (SMYE, Université libre de Bruxelles), 12th International Conference on Computational and Financial Econometrics (CFE, University of Pisa), Empirical Macroeconomics seminar at Freie Universität Berlin, 71st European Meeting of the Econometric Society (ESEM, University of Cologne), 33rd Annual Congress of the European Economic Association (EEA, University of Cologne), 2018 International Association for Applied Econometrics annual conference (IAAE, Université du Québec à Montréal and Université de Montréal), 5th Money, Macroeconomics and Finance PhD conference (MMF PhD conference, University of Kent), and QMUL Reading Groups and PhD Conference for valuable comments and beneficial discussions. Financial support from Queen Mary University of London, School of Economics and Finance, International Association for Applied Econometrics (IAAE), and Royal Economic Society (RES) is gratefully acknowledged. All errors are mine.

<sup>‡</sup>Queen Mary University of London, School of Economics and Finance. Email: a.volpicella@qmul.ac.uk

# 1 Introduction and Related Literature

Since the work of Sims (1980), structural vector autoregressions (SVARs) are the commonest tool for studying the dynamics caused by macroeconomic shocks. Early studies employed zero short-run, medium-run or long-run restrictions on impulse response functions (IRFs) for the identification of structural shocks (Sims, 1980; Uhlig, 2004a; Blanchard and Quah, 1989). However, more recent research has relaxed controversial restrictions and has attempted to rely on weaker assumptions. Specifically, since the works of Faust (1998), Canova and Nicolo (2002) and Uhlig (2005), it has become increasingly common to identify structural shocks with sign restrictions on either the impulse response functions or the structural parameters. Such restrictions are usually weaker than classical identification schemes, and are therefore more likely to generate agreement amongst researchers. Additionally, because structural parameters and IRFs are set-identified (or bounded), conclusions are robust across the set of structural models that satisfy the sign restrictions. However, this minimalist or agnostic approach comes at a cost. Sign restrictions usually deliver a set of structural parameters with very different implications for IRFs, elasticities, historical decomposition (HD) and forecast error variance decomposition (FEVD). On the one hand, this makes obtaining precise estimation, informative inference and meaningful economic results challenging (Uhlig, 2005; Paustian, 2007; Mountford, 2005; Rafiq and Mallick, 2008; Arias, Caldara, and Rubio-Ramirez, 2019; Antolín-Díaz and Rubio-Ramírez, 2018; Amir-Ahmadi and Drautzburg, 2018). On the other hand, some of the admissible structural models can contain implausible implications, which is even worse. Specifically, under sign restrictions, a contractionary monetary policy shock has no significant impact on real variables in the short-run (Uhlig, 2005; Mountford, 2005; Rafiq and Mallick, 2008) and does not necessarily lead to a decrease in real economic activity. Kilian and Murphy (2012) found that sign restrictions on IRFs of a SVAR for the oil market induce highly questionable implications for the price elasticity of the supply of oil to a demand shock. More recently, Arias, Caldara, and Rubio-Ramirez (2019) showed that sign restrictions in the work of Uhlig (2005) had a counter-intuitive impact on the systematic response of monetary policy; Antolín-Díaz and Rubio-Ramírez (2018) argued that sign restrictions on IRFs for the identification of oil and monetary policy shocks lead to implausible HD. Thus, the challenge for scholars and practitioners is to come up with a small number of additional uncontroversial restrictions that help shrink the set of admissible structural parameters, eliminate unreasonable implications and allow them to reach clear economic conclusions.

While sign restrictions typically impose inequality constraints on IRFs, this paper places (upper- and/or lower-) bounds on the FEVD as a way of sharpening identification, reducing the set of admissible structural parameters, increasing estimation precision and removing the

implausible implications of sign-restricted models. The benchmark in the literature is to treat the identifying constraints as if known with certainty (dogmatic restrictions); consistent with the spirit of Giacomini, Kitagawa, and Volpicella (2017), Baumeister and Hamilton (2018), and Baumeister and Hamilton (2019), the paper also introduces uncertainty about bounds on the FEVD (nondogmatic restrictions). This makes sure the identification is robust to doubts about the specific values used for bounding the FEVD.

In macroeconometrics, the FEVD is a very standard tool for evaluating whether, and to what extent, shocks of interest explain the unexpected fluctuations of the target variables. Put it another way, this paper bounds the average movements in the data, or unconditional expectations, and differs from some recent literature, where specific historical events are used to constrain the HD and identify shocks (Antolín-Díaz and Rubio-Ramírez, 2018; Ludvigson, Ma, and Ng, 2018, 2019).<sup>1</sup> The empirical application fully illustrates the difference in estimation and inference between restrictions on the FEVD and on the HD. On the other hand, the identification strategy in this work, although completely novel, reminds the spirit of Kilian and Murphy (2012), Baumeister and Hamilton (2018), and Baumeister and Hamilton (2019), who placed bounds on particular structural parameters. Specifically, this research makes a number of contributions to the literature on structural shock identification.

Firstly, in a bivariate and trivariate setting, I analytically prove that bounds on the FEVD deliver a strictly smaller set for IRFs relative to sign restrictions. Interestingly, this also applies to variables that are not subject to restrictions. For higher dimensional SVARs, I establish the necessary conditions in which the placing of bounds on the FEVD leads to a reduced identified set.

Secondly, the paper also addresses the trade-off between sharp identification and computation. In practice, it is unclear whether the identification is sharp enough so that the identified set has a small but positive measure, or whether the constraints are too tight and the set has a zero measure (empty set).<sup>2</sup> As long as restrictions get tighter and reduce the identified set, it can be hard to distinguish between small and empty sets. Thus, this paper establishes sufficient conditions to determine whether the identified set implied by the constraints on the FEVD has a positive measure; an algorithm provides a computationally-fast practical check of the conditions. While recent studies (Giacomini and Kitagawa, 2018; Amir-Ahmadi and Drautzburg, 2018; Gafarov, Meier, and Olea, 2018) establish conditions for non-emptiness under zero and sign restrictions, this paper advances the literature by investigating non-emptiness in the context of bounds on the FEVD.

---

<sup>1</sup>Chapter 4 of Kilian and Lütkepohl (2017) provides details about the difference between HD and FEVD.

<sup>2</sup>Uhlig (2017) summarized the trade-off as follows: “When a lot of draws are rejected, the identification is sharp”.

The current methodology for Bayesian estimation and inference of set-identified models relies on drawing reduced-form parameters and an orthonormal matrix that maps the former into structural parameters, IRFs and any other object of interest (Arias, Rubio-Ramirez, and Waggoner, 2018). Within this setting, the common approach is to impose a uniform distribution on the orthonormal matrix. However, it is well-known that (i) this choice does not imply a uniform distribution over the identified set of the structural parameters, and (ii) the posterior of structural parameters is proportional to the prior distribution, even asymptotically (Baumeister and Hamilton, 2015). Under a convexity criterion, this paper presents a robust-prior procedure through a numerical optimizer, where the identified set, which is constrained by bounds on the FEVD, is distribution-free and does not depend on a specific prior over the orthonormal matrix. This approach is in line with the proposals put forward by Giacomini and Kitagawa (2018), Gafarov, Meier, and Olea (2018) and Amir-Ahmadi and Drautzburg (2018) for sign and zero restrictions only.

Once it has been established that bounds on the FEVD help in a bi- and trivariate framework, it is necessary to find a way to choose a reasonable set of constraints in realistic settings. This creates the need to adapt the procedure used by Canova and Paustian (2011) and derive theory-driven bounds on the FEVD which are consistent with the implications of a variety of common, but different, theoretical frameworks. As illustrative example, popular DSGE models, with distinct real, nominal, and financial frictions, and with sufficiently wide ranges for their parameters, are considered. The procedure is fully generalized to incorporate uncertainty, or researchers' doubts, about the bounds.

A Monte-Carlo exercise verifies the effectiveness of both dogmatic and nondogmatic bounds as identifying restrictions in recovering the data-generating process (DGP) relative to sign restrictions.

While sign restrictions typically suggest that contractionary monetary policy shocks have no effects on real variables and are even likely to increase real activity, an empirical application shows that a few bounds on the FEVD tend to be highly informative, remove unreasonable effects of monetary shocks on real variables, increase precision of estimation and sharpen the inference of sign-restricted models. Remarkably, nondogmatic bounds on the FEVD identify structural parameters more successfully than sign restrictions and deliver very informative results. The paper shows the approach here is also more effective than alternative strategies of set-reduction, including standard equality restrictions on the FEVD, narrative sign restrictions (Antolín-Díaz and Rubio-Ramírez, 2018; Ludvigson, Ma, and Ng, 2018, 2019), constraints on the monetary policy equation (Arias, Caldara, and Rubio-Ramirez, 2019) and the ranking of IRFs (Amir-Ahmadi and Drautzburg, 2018).

As is amply clear, the aim of this work's approach is to reduce the size of the identified set

from a sign-restricted SVAR and remove implausible implications. This paper achieves this by complementing sign restrictions with a totally novel methodology, namely imposing constraints on the FEVD bounds. Although placing equality restrictions on the FEVD to identify shocks in SVARs is relatively common,<sup>3</sup> constraining the bounds of, or imposing inequality restrictions on, the FEVD is a novel strategy.<sup>4</sup> After earlier presentations of this paper, I became aware of manuscript by Lovcha and Pérez Laborda (2016), who employed a specific parametrization of a two-shock Real Business Cycle (RBC) framework to point-identify technology contributions in the frequency variance decomposition. However, my work is dramatically different and much more general because (i) the identification is based on the FEVD (time domain) rather than the frequency variance decomposition (frequency domain); (ii) the constraints bound (set-identify) the FEVD instead of point-identifying the frequency variance decomposition; (iii) restrictions, rather than deriving from small-scale RBC model, are consistent with a multiplicity of DSGE models with different nominal, real, and financial frictions; (iv) restrictions do not depend on a specific parametrization; (v) uncertainty about the constraints is fully taken into account.

This paper is organized as follows: Section 2 provides the econometric framework for set-identified SVARs; Section 3 introduces bounds on the FEVD, illustrates analytically the reduction of the identified set in a bivariate and trivariate setting, establishes conditions for non-emptiness and reduction for higher dimensional SVARs, and delivers estimation and inference under constraints on the FEVD; Section 4 shows how dogmatic and nondogmatic bounds on the FEVD can be derived; Section 5 presents a Monte-Carlo experiment to investigate the performance of the identification through bounds on the FEVD; Section 6 provides the monetary policy application; and finally, Section 7 provides the conclusion. An Appendix reports the results of robustness checks; a Technical Appendix as supplementary material provides proofs of the propositions in the main text.

## 2 The Econometric Framework

This section defines the SVAR. It then introduces the identification problem and the class of standard equality and sign restrictions.

---

<sup>3</sup>See Uhlig (2004a), Uhlig (2004b) and subsequent papers.

<sup>4</sup>The only partial exceptions are Dedola and Neri (2007). As a robustness check, amongst the set of structural impulse vectors that satisfy sign restrictions, they selected those that account for over 70 per cent of the FEV of labor productivity to a technology shock after 10 years. To my knowledge, I am the first to formalize the idea and develop the methodology.

## 2.1 The Model

Consider a SVAR(p) model

$$\mathbf{A}_0 \mathbf{y}_t = \mathbf{a} + \sum_{j=1}^p \mathbf{A}_j \mathbf{y}_{t-j} + \boldsymbol{\epsilon}_t \quad (2.1)$$

for  $t = 1, \dots, T$ , where  $\mathbf{y}_t$  is an  $n \times 1$  vector of endogenous variables,  $\boldsymbol{\epsilon}_t$  an  $n \times 1$  vector white noise process, normally distributed with mean zero and variance-covariance matrix  $\mathbf{I}_n$ ,  $\mathbf{A}_j$  for  $j = 0, \dots, p$  is an  $n \times n$  matrix of structural coefficient. As is usual in the literature, structural disturbances are assumed to be uncorrelated. The initial conditions  $\mathbf{y}_1, \dots, \mathbf{y}_p$  are given. Let  $\boldsymbol{\theta} = (\mathbf{A}_0, \mathbf{A}_+)$  collect the structural parameters, where  $\mathbf{A}_+ = (\mathbf{a}, \mathbf{A}_j)$  for  $j = 1, \dots, p$ . The reduced-form VAR is as follows:

$$\mathbf{y}_t = \mathbf{b} + \sum_{j=1}^p \mathbf{B}_j \mathbf{y}_{t-j} + \mathbf{u}_t, \quad (2.2)$$

where  $\mathbf{b} = \mathbf{A}_0^{-1} \mathbf{a}$  is an  $n \times 1$  vector of constants,  $\mathbf{B}_j = \mathbf{A}_0^{-1} \mathbf{A}_j$ ,  $\mathbf{u}_t = \mathbf{A}_0^{-1} \boldsymbol{\epsilon}_t$  denotes the  $n \times 1$  vector of reduced-form errors.  $\text{var}(\mathbf{u}_t) = E(\mathbf{u}_t \mathbf{u}_t') = \boldsymbol{\Sigma} = \mathbf{A}_0^{-1} (\mathbf{A}_0^{-1})'$  is the  $n \times n$  variance-covariance matrix of reduced-form errors. Let  $\boldsymbol{\phi} = (\mathbf{B}, \boldsymbol{\Sigma}) \in \boldsymbol{\Phi}$  collect the reduced-form parameters, where  $\mathbf{B} \equiv [\mathbf{b}, \mathbf{B}_1, \dots, \mathbf{B}_p]$ ,  $\boldsymbol{\Phi} \subset \mathcal{R}^{n+n^p} \times \boldsymbol{\Xi}$ , and  $\boldsymbol{\Xi}$  is the space of symmetric positive semidefinite matrices. Note that  $\boldsymbol{\Phi}$  is such that the VAR(p) is invertible into a VMA( $\infty$ ), i.e., the model is stationary. Thus, the VMA( $\infty$ ) representation of (2.2) is

$$\mathbf{y}_t = \mathbf{c} + \sum_{j=0}^{\infty} \mathbf{C}_j(\mathbf{B}) \mathbf{A}_0^{-1} \boldsymbol{\epsilon}_{t-j}, \quad (2.3)$$

where  $\mathbf{C}_j(\mathbf{B})$  is the  $j$ -th coefficient matrix of  $(\mathbf{I}_n - \sum_{j=1}^p \mathbf{B}_j L^j)^{-1}$ . Let the  $n \times n$  matrix

$$\mathbf{I}R^h = \mathbf{C}_h(\mathbf{B}) \mathbf{A}_0^{-1} \quad (2.4)$$

be the impulse response at  $h$ -th horizon for  $h = 0, 1, \dots$ , where its  $(i, j)$ -element denotes the effect on the  $i$ -th variable in  $\mathbf{y}_{t+h}$  of a unit shock to the  $j$ -th element of  $\boldsymbol{\epsilon}_t$ .

## 2.2 The Identification Problem

In the absence of any identifying restrictions, Uhlig (2005) showed that  $\{\mathbf{A}_0 = \mathbf{Q}' \boldsymbol{\Sigma}_{tr}^{-1} : \mathbf{Q} \in \boldsymbol{\Theta}(n)\}$  is the set of observationally equivalent  $\mathbf{A}_0$ 's consistent with reduced-form parameters, where  $\boldsymbol{\Sigma}$  relates to  $\mathbf{A}_0$  by  $\boldsymbol{\Sigma} = \mathbf{A}_0^{-1} (\mathbf{A}_0^{-1})'$ ,  $\boldsymbol{\Sigma}_{tr}$  denotes the lower triangular Cholesky matrix with non-negative diagonal coefficients of  $\boldsymbol{\Sigma}$ , and  $\mathbf{Q} \in \boldsymbol{\Theta}(n)$ , known as rotation matrix, is the

$n \times n$  orthonormal matrix belonging to the space of  $n \times n$  orthonormal matrices  $\Theta(n)$ . The likelihood function depends on  $\phi$  and does not contain any information about  $\mathbf{Q}$ , leading to ambiguity in decomposing  $\Sigma$ . Thus, there is a multiplicity of  $\mathbf{Q}$ 's which deliver  $\mathbf{A}_0$  given  $\phi$ . Similarly, the rest of structural parameters  $\mathbf{A}_+$  is a function of  $\mathbf{Q}$  and the Cholesky decomposition of reduced-form parameters. For simplicity, this section illustrates the identification problem that relies on  $\mathbf{A}_0$  only.

This paper focuses on set-identification, and therefore there will be fewer than  $n - j$  equality restrictions on the  $j$ -th structural shock;<sup>5</sup> thus, no matter how many sign restrictions are imposed, point-identification fails and there will only be set-identification. I have followed the example of Christiano, Eichenbaum, and Evans (1999) and assume that the diagonal elements of  $\mathbf{A}_0$  are non-negative, i.e., a structural shock is a one standard-deviation positive shock to the related variable. As a result, the set of observationally equivalent  $\mathbf{A}_0$ 's becomes  $\{\mathbf{A}_0 = \mathbf{Q}'\Sigma_{tr}^{-1} : \mathbf{Q} \in \Theta(n), \text{diag}(\mathbf{Q}'\Sigma_{tr}^{-1}) \geq \mathbf{0}\}$ , where  $\text{diag}(\bullet) \geq \mathbf{0}$  implies that all diagonal elements of  $\bullet$  are non-negative. Thus, in the absence of any identifying restrictions, there is a multiplicity of  $\mathbf{Q}$ 's consistent with  $\mathbf{A}_0$ , given the reduced-form parameters:

$$\mathcal{Q}(\phi) = \{\mathbf{Q} \in \Theta(n) : \text{diag}(\mathbf{Q}'\Sigma_{tr}^{-1}) \geq \mathbf{0}\}.$$

Without loss of generality, suppose that one is interested in a specific (structural) impulse response; for instance, the  $(i, j)$ -th element of  $\mathbf{IR}^h$ :

$$g_{ij}^h(\phi, \mathbf{Q}) \equiv \mathbf{e}'_i \mathbf{C}_h(\mathbf{B})\Sigma_{tr}\mathbf{Q}\mathbf{e}_j \equiv \mathbf{c}'_{ih}(\phi)\mathbf{q}_j,$$

where  $g_{ij}^h(\phi, \mathbf{Q}) \in \mathcal{R}$ ,  $\mathbf{e}_i$  is the  $i$ -th column vector of  $\mathbf{I}_n$ ,  $\mathbf{q}_j$  is the  $j$ -th column of  $\mathbf{Q}$  and  $\mathbf{c}'_{ih}(\phi)$  represents the  $i$ -th row vector of  $\mathbf{C}_h(\mathbf{B})\Sigma_{tr}$ . Since  $\mathbf{Q}$  is orthonormal,  $\mathbf{q}'_j\mathbf{q}_i = 0$  for  $j \neq i$ . However, this orthogonality condition matters if and only if a multiplicity of shocks is restricted; in fact, given an unrestricted shock  $j^*$ , in the Nullspace of the constrained shocks a vector  $\mathbf{q}$  such that  $\mathbf{q}'_{j^*}\mathbf{q} = 0$  can always be constructed. Note that the analysis for the impulse responses can be easily extended to the structural parameters  $\mathbf{A}_0$  and  $\mathbf{A}_+$ , since each structural parameter can be expressed by the inner product of a vector, depending on  $\phi$ , and a column vector of  $\mathbf{Q}$ .

---

<sup>5</sup>The set of  $\mathbf{A}_0$  and  $\mathbf{A}_+$  collapses to a singleton as long as identifying assumptions are able to deliver a unique  $\mathbf{Q}$  that recovers structural parameter  $\mathbf{A}_0$  and  $\mathbf{A}_+$ , i.e., point-identification. Rothenberg (1971) proved that the necessary conditions for point-identification require that the number of equality restrictions is greater than or equal to  $n(n - 1)/2$ . Rubio-Ramirez, Waggoner, and Zha (2010) established sufficient conditions for point-identification: there must be at least  $n - j$  equality restrictions on the  $j$ -th structural shock, for  $1 \leq j \leq n$ , and sign normalizations on the impulse responses to each structural shock.

### 2.2.1 Equality Restrictions

Typical equality restrictions include zero restrictions on the off-diagonal elements of  $\mathbf{A}_0$ , which correspond to a subset of the restrictions imposed by the classical recursive identification scheme that sets the upper-triangular elements of  $\mathbf{A}_0$  to zero, and on contemporaneous impulse responses  $\mathbf{IR}^0 = \mathbf{A}_0^{-1}$ . The econometric framework here also allows one to place zero restrictions on the lagged coefficients  $\mathbf{A}_l : l = 1, \dots, p$  and restrictions on the long-run impulse responses  $\mathbf{IR}^\infty = (\mathbf{I}_n - \sum_{j=1}^p \mathbf{B}_j)^{-1} \Sigma_{tr} \mathbf{Q}$ . For simplicity and without loss of generality, this paper reduces the set of equality restrictions to zero restrictions only (in the short- or long-run). They can be written as linear constraints on the columns of  $\mathbf{Q}$  with coefficients depending on the reduced-form parameters  $\phi$ .<sup>6</sup> As a result, zero restrictions can be represented as follows:

$$\mathbf{F}(\phi, \mathbf{Q}) \equiv \begin{pmatrix} \mathbf{F}_1(\phi) \mathbf{q}_1 \\ \vdots \\ \mathbf{F}_n(\phi) \mathbf{q}_n \end{pmatrix} = \mathbf{0}, \quad \mathbf{F}_i(\phi): f_i \times n, \quad (2.5)$$

where  $f_i \times n$  matrix  $\mathbf{F}_i(\phi)$  depends on  $\phi$ . Each row vector in  $\mathbf{F}_i(\phi)$  is the coefficient vector of a zero restriction that constrains the correspondent column of  $\mathbf{Q}$ . More generally,  $\mathbf{F}_i(\phi)$  collects all the coefficient vectors that multiply  $\mathbf{q}_i$  into a matrix and  $f_i$  denotes number of zero restrictions constraining  $\mathbf{q}_i$ .

### 2.2.2 Sign Restrictions

Assume that the researcher is interested in imposing some sign restrictions on the impulse response vector to the  $j$ -th structural shock, and let  $s_{hj}$  denote the number of sign restrictions on impulse responses at horizon  $h$ . In this case, the impulse response is given by the  $j$ -th column vector of  $\mathbf{IR}^h = \mathbf{C}_h(\mathbf{B}) \Sigma_{tr} \mathbf{Q}$ , and the sign restrictions are

$$\mathbf{S}_{hj}(\phi) \mathbf{q}_j \geq \mathbf{0},$$

where  $\mathbf{S}_{hj}(\phi) \equiv \mathbf{D}_{hj} \mathbf{C}_h(\mathbf{B}) \Sigma_{tr}$  is a  $s_{hj} \times n$  matrix and  $\mathbf{D}_{hj}$  is the  $s_{hj} \times n$  selection matrix that selects the sign-restricted responses from the  $n \times 1$  response vector  $\mathbf{C}_h(\mathbf{B}) \Sigma_{tr} \mathbf{q}_j$ . The nonzero elements of  $\mathbf{D}_{hj}$  can be equal to 1 or to -1 depending on the sign of the restriction on the impulse response of interest. By considering multiple horizons, the whole set of sign restrictions placed on the  $j$ -th shock is

$$\mathbf{S}_j(\phi) \mathbf{q}_j \geq \mathbf{0}. \quad (2.6)$$

---

<sup>6</sup>For instance, zero restrictions on  $\mathbf{A}_0$  are:  $(i, j)$ -th element of  $\mathbf{A}_0 = 0 \Leftrightarrow (\Sigma_{tr}^{-1} \mathbf{e}_j)' \mathbf{q}_i = 0$ .

Specifically,  $\mathbf{S}_j$  is a  $\left(\sum_{h=0}^{\tilde{h}_j} s_{hj}\right) \times n$  matrix defined by  $\mathbf{S}_j(\phi) = \left[\mathbf{S}'_{0j}(\phi), \dots, \mathbf{S}'_{\tilde{h}_j j}(\phi)\right]'$ . Let  $\mathcal{I}_S \subset \{1, 2, \dots, n\}$  be the set of indices such that  $j \in \mathcal{I}_S$  if some of the impulse responses to the  $j$ -th structural shock are sign-constrained. Thus, the set of all sign restrictions is

$$\mathbf{S}_j(\phi)\mathbf{q}_j \geq \mathbf{0}, \text{ for } j \in \mathcal{I}_S. \quad (2.7)$$

With abuse of notation, let  $\mathbf{S}(\phi, \mathbf{Q}) \geq \mathbf{0}$  collect all sign restrictions  $\mathbf{S}_j(\phi)\mathbf{q}_j \geq \mathbf{0}$  for any  $j \in \mathcal{I}_S$ .<sup>7</sup>

The sign restrictions above can be easily added to the zero restrictions; let  $\mathcal{Q}(\phi|\mathbf{F}, \mathbf{S})$  be the set of  $\mathbf{Q}$ 's that satisfy sign normalizations, zero and sign restrictions, given  $\phi$ :

$$\mathcal{Q}(\phi|\mathbf{F}, \mathbf{S}) = \{\mathbf{Q} \in \Theta(n) : \mathbf{F}(\phi, \mathbf{Q}) = \mathbf{0}, \mathbf{S}(\phi, \mathbf{Q}) \geq \mathbf{0}, \text{diag}(\mathbf{Q}'\Sigma_{tr}^{-1}) \geq \mathbf{0}\}.$$

The identified set for the object of interest is a set-valued map from  $\phi$  to a subset in  $\mathcal{R}$  that delivers the range of  $g_{ij}^h(\phi, \mathbf{Q})$  when  $\mathbf{Q}$  varies over  $\mathcal{Q}(\phi|\mathbf{F}, \mathbf{S})$ :

$$IS_g(\phi|\mathbf{F}, \mathbf{S}) = \{g_{ij}^h(\phi, \mathbf{Q}) : \mathbf{Q} \in \mathcal{Q}(\phi|\mathbf{F}, \mathbf{S})\}. \quad (2.8)$$

### 3 Bounds on the Forecast Error Variance Decomposition

While zero and sign restrictions are well-established tools for identifying shocks, this section introduces constraints on the bounds of the FEVD. Firstly, it explains how bounds on the FEVD shape the identified set. Secondly, it illustrates analytically the reduction in the identified set induced by bounds on the FEVD in static bivariate and trivariate models; interestingly, the identified set gets smaller also for structural objects that are not subject to the restrictions. Thirdly, for higher-dimensional SVARs, it provides conditions for non-emptiness and reduction. Fourthly, it presents a robust-prior procedure for estimation and inference.

#### 3.1 The Forecast Error Variance

The  $\tilde{h}$ -step ahead Forecast Error (FE) for a SVAR, as in equation (2.1), given all the data up to  $t-1$ , is  $\mathbf{FE}(\tilde{h}) \equiv \mathbf{y}_{t+\tilde{h}} - \mathbf{y}_{t+\tilde{h}|t-1} = \sum_{h=0}^{\tilde{h}} \mathbf{IR}^h \boldsymbol{\epsilon}_{t+\tilde{h}-h}$ . Thus, the FEV at horizon  $\tilde{h}$  is

$$\mathbf{FEV}(\tilde{h}) \equiv E \left[ (\mathbf{y}_{t+\tilde{h}} - \mathbf{y}_{t+\tilde{h}|t-1})(\mathbf{y}_{t+\tilde{h}} - \mathbf{y}_{t+\tilde{h}|t-1})' \right] = \sum_{h=0}^{\tilde{h}} \mathbf{IR}^h \mathbf{IR}^{h'}.$$

---

<sup>7</sup>Given the  $j$ -th shock, sign restrictions on  $\mathbf{A}_0$  and  $\mathbf{A}_+$  can be appended to equation (2.6), since they can be expressed as linear inequalities on  $\mathbf{q}_j$ .

As a result, the contribution of shock  $j$  to the FEV of variable  $z$  at horizon  $\tilde{h}$  is

$$CFEV_j^z(\tilde{h}) \equiv \frac{FEV_j^z(\tilde{h})}{FEV^z(\tilde{h})} = \frac{\sum_{h=0}^{\tilde{h}} (\mathbf{IR}_{z,j}^h)^2}{\sum_{j=1}^n \sum_{h=0}^{\tilde{h}} (\mathbf{IR}_{z,j}^h)^2}, \quad (3.1)$$

where  $FEV_j^z(\tilde{h}) = \sum_{h=0}^{\tilde{h}} (\mathbf{IR}_{z,j}^h)^2$  is the FEV of variable  $z$  due to shock  $j$  at horizon  $\tilde{h}$ ,  $FEV^z(\tilde{h}) = \sum_{j=1}^n \sum_{h=0}^{\tilde{h}} (\mathbf{IR}_{z,j}^h)^2$  denotes the total FEV of variable  $z$  at horizon  $\tilde{h}$ ,  $\mathbf{IR}_{z,j}^h$  represents the  $(z, j)$ -th element of  $\mathbf{IR}^h$ , and  $0 \leq CFEV_j^z(\tilde{h}) \leq 1$  by definition. Uhlig (2004b) showed that equation (3.1) can be written as

$$CFEV_j^z(\tilde{h}) = \mathbf{q}'_j \mathbf{\Upsilon}^z(\phi) \mathbf{q}_j, \quad (3.2)$$

where  $\mathbf{\Upsilon}^z(\phi) = \frac{\sum_{h=0}^{\tilde{h}} \mathbf{c}_{zh}(\phi) \mathbf{c}'_{zh}(\phi)}{\sum_{h=0}^{\tilde{h}} \mathbf{c}'_{zh}(\phi) \mathbf{c}_{zh}(\phi)}$  is a positive semidefinite  $n \times n$  real matrix. Note that  $\mathbf{\Upsilon}^z(\phi)$  also depends on  $\tilde{h}$ ; in order to avoid heavy notation,  $\tilde{h}$  is omitted.

The quantity in equation (3.2) is commonly used to evaluate whether, and at what degree, a shock of interest  $j$  drives the unexpected fluctuations of a target variable  $z$  at horizon  $\tilde{h}$ . This is typically employed to illustrate the sources of variables fluctuation in the short-, medium-, and long-run.

Suppose that a researcher believes that the contribution of shock  $j$  to FEV of variable  $z$  at horizon  $\tilde{h}$  is bounded between  $\underline{k}_j^z$  and  $\bar{k}_j^z$ , where  $0 \leq \underline{k}_j^z \leq \bar{k}_j^z \leq 1$  and for simplicity  $\tilde{h}$  is omitted from  $\underline{k}_j^z$  and  $\bar{k}_j^z$ . This implies that

$$\underline{k}_j^z \leq \mathbf{q}'_j \mathbf{\Upsilon}^z(\phi) \mathbf{q}_j \leq \bar{k}_j^z. \quad (3.3)$$

Let  $\mathcal{I}_{FEV}$  be a set of indices such that  $j \in \mathcal{I}_{FEV}$  if shock  $j$  is restricted as in (3.3); let  $\Lambda_j$  be a set of indices such that  $z \in \Lambda_j$ , where  $j \in \mathcal{I}_{FEV}$ , if the FEV of variable  $z \in \{1, \dots, n\}$  to shock  $j$  is bounded as in (3.3). Thus, the set of all the bounds on the FEVD can be accordingly expressed by

$$\underline{k}_j^z \leq \mathbf{q}'_j \mathbf{\Upsilon}^z(\phi) \mathbf{q}_j \leq \bar{k}_j^z, \text{ for } j \in \mathcal{I}_{FEV} \text{ and } z \in \Lambda_j. \quad (3.4)$$

As a shorthand notation, let  $\underline{\mathbf{k}} \leq \mathbf{\Gamma}(\phi, \mathbf{Q}) \leq \bar{\mathbf{k}}$  be the whole set of bounds on the FEVD represented by (3.4), where  $\mathbf{\Gamma}(\phi, \mathbf{Q})$  collects  $\mathbf{q}'_j \mathbf{\Upsilon}^z(\phi) \mathbf{q}_j$  for  $j \in \mathcal{I}_{FEV}$  and  $z \in \Lambda_j$ . Note that sign restrictions impose linear constraints on the columns of  $\mathbf{Q}$ ; on the other hand, bounds on the FEVD place quadratic inequalities.

Thus, the set of  $\mathbf{Q}$ 's that satisfy sign normalizations, zero restrictions, sign restrictions and restrictions on the FEVD is

$$\mathcal{Q}(\phi | \mathbf{F}, \mathbf{S}, \mathbf{\Gamma}) = \{\mathbf{Q} \in \Theta(n) : \mathbf{F}(\phi, \mathbf{Q}) = \mathbf{0}, \mathbf{S}(\phi, \mathbf{Q}) \geq \mathbf{0}, \underline{\mathbf{k}} \leq \mathbf{\Gamma}(\phi, \mathbf{Q}) \leq \bar{\mathbf{k}}, \text{diag}(\mathbf{Q}' \mathbf{\Sigma}_{tr}^{-1}) \geq \mathbf{0}\}.$$

The identified set for the object of interest is:

$$IS_g(\phi|\mathbf{F}, \mathbf{S}, \mathbf{\Gamma}) = \{g_{ij}^h(\phi, \mathbf{Q}) : \mathbf{Q} \in \mathcal{Q}(\phi|\mathbf{F}, \mathbf{S}, \mathbf{\Gamma})\}. \quad (3.5)$$

Note that the identified set induced by inequality constraints on the FEVD and/or sign restrictions can be empty, as opposed to the case with zero restrictions only (Giacomini and Kitagawa, 2018). Section 3.3 establishes conditions to deliver non-empty sets.

## 3.2 Small-Scale Framework

This section illustrates analytically the reduction in the identified set induced by bounds on the FEVD in static bivariate and trivariate models; interestingly, the identified set gets smaller also for structural objects that are not subject to the restrictions. Technical Appendix provides the proofs.

### 3.2.1 Bivariate Setting

The structural framework is the following:

$$\mathbf{A}_0 \begin{pmatrix} y_{1t} \\ y_{2t} \end{pmatrix} = \begin{pmatrix} \epsilon_{1t} \\ \epsilon_{2t} \end{pmatrix}, \quad \mathbf{A}_0 = \begin{pmatrix} a_{11} & a_{12} \\ a_{21} & a_{22} \end{pmatrix}, \quad t=1, \dots, T, \quad (3.6)$$

where  $(y_{1t}, y_{2t})$  are two endogenous variables, respectively.  $(\epsilon_{1t}, \epsilon_{2t})$  denotes an i.i.d. normally distributed vector of structural shocks with variance-covariance the identity matrix.  $\boldsymbol{\theta} = \mathbf{A}_0$  collects the structural parameters, and the contemporaneous impulse responses are elements of  $\mathbf{A}_0^{-1}$ . The reduced-form model is indexed by  $\boldsymbol{\Sigma}$  (the variance-covariance matrix of the endogenous variables), which satisfies  $\boldsymbol{\Sigma} = \mathbf{A}_0^{-1}(\mathbf{A}_0^{-1})'$ . Let  $\boldsymbol{\Sigma}_{tr} = \begin{pmatrix} \sigma_{11} & 0 \\ \sigma_{21} & \sigma_{22} \end{pmatrix}$  denote its lower triangular Cholesky decomposition, where  $\sigma_{11} \geq 0$  and  $\sigma_{22} \geq 0$ . Thus,  $\boldsymbol{\phi} = (\sigma_{11}, \sigma_{21}, \sigma_{22}) \in \boldsymbol{\Phi} = \mathbb{R}_+ \times \mathbb{R} \times \mathbb{R}_+$  collects the reduced-form parameters. Following the example of Uhlig (2005),  $\mathbf{A}_0$  can be parametrized via the Cholesky matrix  $\boldsymbol{\Sigma}_{tr}$  and a rotation matrix  $\mathbf{Q} = \begin{pmatrix} \cos \rho & -\sin \rho \\ \sin \rho & \cos \rho \end{pmatrix}$  with spherical coordinate  $\rho \in [0, 2\pi]$ . The structural matrix of impact responses can be written as

$$\mathbf{IR}^0 = \mathbf{A}_0^{-1} = \boldsymbol{\Sigma}_{tr} \mathbf{Q} = \begin{pmatrix} \sigma_{11} \cos \rho & -\sigma_{11} \sin \rho \\ \sigma_{21} \cos \rho + \sigma_{22} \sin \rho & -\sigma_{21} \sin \rho + \sigma_{22} \cos \rho \end{pmatrix}.$$

Without loss of generality, let the structural object of interest  $\alpha$  be the response of  $y_1$  to a unit shock  $\epsilon_1$ ,  $\alpha \equiv \sigma_{11} \cos \rho$ .

Two standard sign restrictions (*SR*) are imposed on IRFs:

- *SR1*

On impact, positive shock  $\epsilon_2$  does not increase variable  $y_1$ :  $\sigma_{11} \sin \rho \geq 0$ .

- *SR2*

Positive shock  $\epsilon_1$  does not reduce variable  $y_2$ :  $-\sigma_{22} \sin \rho - \sigma_{21} \cos \rho \leq 0$ .

Note that standard sign restrictions impose linear inequalities on  $\rho$ . Technical Appendix proves that the identified set for  $\alpha$  is

$$IS_\alpha(\phi) \equiv \begin{cases} \left[ \sigma_{11} \cos \left( \arctan \left( \frac{\sigma_{22}}{\sigma_{21}} \right) \right), \sigma_{11} \right], & \text{for } \sigma_{21} > 0, \\ \left[ 0, \sigma_{11} \cos \left( \arctan \left( -\frac{\sigma_{21}}{\sigma_{22}} \right) \right) \right], & \text{for } \sigma_{21} \leq 0. \end{cases} \quad (3.7)$$

- *FEVR*

Assume that the contribution of shock  $\epsilon_2$  to the total error variance of  $y_1$  is bounded between  $\underline{k}$  and  $\bar{k}$ ; this constrains the FEVD. Following the notation introduced in Section 3, this restriction can be written as  $\underline{k} \leq CFEV_{\epsilon_2}^{y_1}(0) \leq \bar{k}$ , where  $0 \leq \underline{k} < \bar{k} \leq 1$ .

*SR1*, *SR2* and *FEVR* deliver the following identified set for  $\alpha$ :

$$IS_\alpha(\phi) \equiv \begin{cases} \left[ \sigma_{11} \cos(\arcsin \sqrt{\bar{k}}), \sigma_{11} \cos(\arcsin \sqrt{\underline{k}}) \right], \\ \text{for } \{ \sigma_{21} > 0, \bar{k} < \bar{k}^*(\phi) \} \cup \{ \sigma_{21} \leq 0, \underline{k} > \underline{k}^*(\phi) \}, \\ \left[ \sigma_{11} \cos \left( \arctan \left( \frac{\sigma_{22}}{\sigma_{21}} \right) \right), \sigma_{11} \cos(\arcsin \sqrt{\underline{k}}) \right], \\ \text{for } \sigma_{21} > 0, \bar{k} \geq \bar{k}^*(\phi), \\ \left[ \sigma_{11} \cos(\arcsin \sqrt{\bar{k}}), \sigma_{11} \cos \left( \arctan \left( -\frac{\sigma_{21}}{\sigma_{22}} \right) \right) \right], \\ \text{for } \sigma_{21} \leq 0, \underline{k} \leq \underline{k}^*(\phi), \end{cases} \quad (3.8)$$

where  $\bar{k}^*(\phi) = \sin^2 \left( \arctan \left( \frac{\sigma_{22}}{\sigma_{21}} \right) \right)$  and  $\underline{k}^*(\phi) = \sin^2 \left( \arctan \left( -\frac{\sigma_{21}}{\sigma_{22}} \right) \right)$ . The following proposition formally compares the identified set induced by sign restrictions only with that in (3.8).

**Proposition 3.1** *The identified set for the structural impulse response  $\alpha$  in (3.8) is strictly smaller than in (3.7) unless  $\underline{k} = 0$ ,  $\bar{k} \geq \bar{k}^*(\phi)$ ,  $\sigma_{21} > 0$  or  $\bar{k} = 1$ ,  $\underline{k} \leq \underline{k}^*(\phi)$ ,  $\sigma_{21} \leq 0$ , where the identified sets are equivalent.*

The proposition above provides some interesting insights. Firstly, if both lower and upper bounds are imposed, i.e.,  $\underline{k} \neq 0$ ,  $\bar{k} \neq 1$ , then such restrictions always shrink the identified set of  $\alpha$  with respect to the set induced by *SR1* and *SR2* for any  $\phi = (\sigma_{11}, \sigma_{21}, \sigma_{22}) \in \Phi = \mathbb{R}_+ \times \mathbb{R} \times \mathbb{R}_+$ . Secondly, suppose that  $CFEV_{\epsilon_2}^{y_1}(0)$  is unbounded from below ( $\underline{k} = 0$ ); shrinkage

then occurs for any  $\sigma_{21} \leq 0$  or if  $\bar{k} < \bar{k}^*(\phi)$ . In other words, if there is no lower bound and the unconditional covariance is positive, the upper bound must be low enough to deliver a restriction of the identified set. Thirdly, assume that  $CFEV_{\epsilon_2}^{y_1}(0)$  is unbounded from above ( $\bar{k} = 1$ ); then there is shrinkage for any  $\sigma_{21} > 0$  or if  $\underline{k} > \underline{k}^*(\phi)$ . This implies that if there is no upper bound and the unconditional covariance is non-positive, the lower bound must be high enough to deliver a restriction of the identified set.

Note that *FEVR* is restricting the FEVD of the variable of interest, namely  $y_1$ . However, conditions similar to those in Proposition 3.1 can be easily found for bounds on the FEVD of variables other than  $y_1$ .

- *FEVR2*

Suppose that the contribution of shock  $\epsilon_1$  to the total error variance of  $y_2$  is bounded as follows:  $\underline{k} \leq CFEV_{\epsilon_1}^{y_2}(0) \leq \bar{k}$ , where  $0 \leq \underline{k} < \bar{k} \leq 1$ .

Technical Appendix provides the details of the following proposition, in which  $\bar{k}^{**}(\phi)$  and  $\underline{k}^{**}(\phi)$  denote functions of reduced-form parameters.

**Proposition 3.2** *The identified set for the structural impulse response  $\alpha$  induced by SR1, SR2 and FEVR2 is strictly smaller than in (3.7) unless  $\underline{k} = 0$ ,  $\bar{k} \geq \bar{k}^{**}(\phi)$ ,  $\sigma_{21} \leq 0$  or  $\bar{k} = 1$ ,  $\underline{k} \leq \underline{k}^{**}(\phi)$ ,  $\sigma_{21} > 0$ , where the identified sets are equivalent.*

### 3.2.2 Trivariate Setting

The bivariate illustration shows that bounds on the FEVD shrink the set induced by sign restrictions. Higher dimensional cases are more complex. However, while Proposition 3.1 and 3.2 are easily replicable in a trivariate framework, this is useful to show the effect of bounds on the FEVD of variables and shocks other than those in the object of interest.

The structural framework is the following:

$$\mathbf{A}_0 \begin{pmatrix} y_{1t} \\ y_{2t} \\ y_{3t} \end{pmatrix} = \begin{pmatrix} \epsilon_{1t} \\ \epsilon_{2t} \\ \epsilon_{3t} \end{pmatrix}. \quad (3.9)$$

The reduced-form model is indexed by  $\Sigma$  (the variance-covariance matrix of the endogenous variables), which satisfies  $\Sigma = \mathbf{A}_0^{-1}(\mathbf{A}_0^{-1})'$ . Let  $\Sigma_{tr} = \begin{pmatrix} \sigma_{11} & 0 & 0 \\ \sigma_{21} & \sigma_{22} & 0 \\ \sigma_{31} & \sigma_{32} & \sigma_{33} \end{pmatrix}$  denote its lower triangular Cholesky decomposition, where  $\sigma_{11} \geq 0$ ,  $\sigma_{22} \geq 0$  and  $\sigma_{33} \geq 0$ .  $\phi =$

$(\sigma_{11}, \sigma_{21}, \sigma_{22}, \sigma_{31}, \sigma_{32}, \sigma_{33})$  collects the reduced-form parameters. Let the structural object of interest  $\alpha$  be the response of  $y_1$  to a unit positive shock  $\epsilon_1$ ,  $\alpha \equiv \sigma_{11} \cos \rho$ , where  $\rho \in [0, 2\pi]$ .

Three standard sign restrictions (*SR*) are imposed:

- *SR1*

On impact, positive shock  $\epsilon_3$  does not increase variable  $y_1$ :  $\sigma_{11} \sin \rho \geq 0$ .

- *SR2*

Positive shock  $\epsilon_1$  does not reduce variable  $y_2$  on impact:  $\sigma_{21} \cos \rho \geq 0$ .

- *SR3*

Positive shock  $\epsilon_1$  does not decrease variable  $y_3$  on impact:  $\sigma_{31} \cos \rho + \sigma_{33} \sin \rho \geq 0$ .

The implied identified set for  $\alpha$  is

$$IS_\alpha(\phi) \equiv \begin{cases} \left[ \sigma_{11} \cos \left( \arctan \left( \frac{\sigma_{33}}{\sigma_{31}} \right) \right), \sigma_{11} \right], & \text{for } \sigma_{31} > 0, \\ \left[ 0, \sigma_{11} \cos \left( \arctan \left( -\frac{\sigma_{31}}{\sigma_{33}} \right) \right) \right], & \text{for } \sigma_{31} \leq 0, \end{cases} \quad (3.10)$$

where sign restrictions are defined only over  $\sigma_{21} \geq 0$ .

- *FEVR3*

Suppose that the contribution of shock  $\epsilon_3$  to the total error variance of  $y_2$  is bounded as follows:  $\underline{k} \leq CFEV_{\epsilon_3}^{y_2}(0) \leq \bar{k}$ , where  $0 \leq \underline{k} < \bar{k} \leq 1$ .

The identified set induced by *SR1*, *SR2*, *SR3*, and *FEVR3* is

$$IS_\alpha(\phi) \equiv \begin{cases} \left[ \sigma_{11} \cos \left( \arcsin \left( \frac{\sqrt{\bar{k}(\sigma_{21}^2 + \sigma_{22}^2)}}{\sigma_{21}} \right) \right), \sigma_{11} \cos \left( \arcsin \left( \frac{\sqrt{\underline{k}(\sigma_{21}^2 + \sigma_{22}^2)}}{\sigma_{21}} \right) \right) \right], \\ \text{for } \{ \sigma_{31} > 0, \bar{k} < \bar{k}^*(\phi) \} \cup \{ \sigma_{31} \leq 0, \underline{k} > \underline{k}^*(\phi) \}, \\ \left[ \sigma_{11} \cos \left( \arctan \left( \frac{\sigma_{33}}{\sigma_{31}} \right) \right), \sigma_{11} \cos \left( \arcsin \left( \frac{\sqrt{\underline{k}(\sigma_{21}^2 + \sigma_{22}^2)}}{\sigma_{21}} \right) \right) \right], \\ \text{for } \sigma_{31} > 0, \bar{k} \geq \bar{k}^*(\phi), \\ \left[ \sigma_{11} \cos \left( \arcsin \left( \frac{\sqrt{\bar{k}(\sigma_{21}^2 + \sigma_{22}^2)}}{\sigma_{21}} \right) \right), \sigma_{11} \cos \left( \arctan \left( -\frac{\sigma_{31}}{\sigma_{33}} \right) \right) \right], \\ \text{for } \sigma_{31} \leq 0, \underline{k} \leq \underline{k}^*(\phi), \end{cases} \quad (3.11)$$

where  $\underline{k}^*(\phi) = \frac{\sigma_{21}^2}{\sigma_{21}^2 + \sigma_{22}^2} \sin^2 \left( \arctan \left( -\frac{\sigma_{31}}{\sigma_{33}} \right) \right)$ ,  $\bar{k}^*(\phi) = \frac{\sigma_{21}^2}{\sigma_{21}^2 + \sigma_{22}^2} \sin^2 \left( \arctan \left( \frac{\sigma_{33}}{\sigma_{31}} \right) \right)$ , and  $\sigma_{21} \geq 0$ . A comparison between (3.10) and (3.11) leads to the following proposition:

**Proposition 3.3** *The identified set for the structural impulse response  $\alpha$  in (3.11) is strictly smaller than in (3.10) unless  $\underline{k} = 0$ ,  $\bar{k} \geq \bar{k}^*(\phi)$ ,  $\sigma_{31} > 0$  or  $\bar{k} = 1$ ,  $\underline{k} \leq \underline{k}^*(\phi)$ ,  $\sigma_{31} \leq 0$ , where the identified sets are equivalent.*

### 3.3 Non-Emptiness and Reduction of the Identified Set

The previous section showed that bounds on the FEVD reduce the identified set for small-scale models. However, there is a well-known trade-off between sharp identification and computation (Uhlig, 2017; Amir-Ahmadi and Drautzburg, 2018; Giacomini and Kitagawa, 2018; Gafarov, Meier, and Olea, 2018). In fact, tight restrictions can potentially lead to sets with zero measure, or empty sets; thus, it is crucial to distinguish when the identification is sharp because the identified set has a reduced but positive measure, and when constraints are too tight and lead to empty sets. Therefore, this section addresses this trade-off and (i) provides sufficient conditions for assessing whether bounds on the FEVD deliver a non-empty set, (ii) establishes necessary conditions for the reduction of the set in the context of bounds on the FEVD for any-scale SVARs, especially useful when closed-form characterization of the identified set is hard.

In order to elucidate the results in this section, it is helpful to introduce some more notation. Let  $\mathbf{\Upsilon}_S^z(\phi) = \frac{\mathbf{\Upsilon}^z(\phi) + (\mathbf{\Upsilon}^z(\phi))'}{2}$  denote the symmetric part of  $\mathbf{\Upsilon}^z(\phi)$ , where  $z \in \Lambda_j$ ;  $\lambda_{l,j}^z$  for  $l = \{1, \dots, n\}$  are the  $n$  real eigenvalues of  $\mathbf{\Upsilon}_S^z(\phi)$ . Note that  $\lambda_{max,j}^z = \max\{\lambda_{1,j}^z, \dots, \lambda_{n,j}^z\}$  and  $\lambda_{min,j}^z = \min\{\lambda_{1,j}^z, \dots, \lambda_{n,j}^z\}$ . Finally, let  $\tilde{\mathbf{q}}$  be the eigenvector associated with  $\lambda_{l,j}^z$ , namely  $\mathbf{\Upsilon}_S^z(\phi)\tilde{\mathbf{q}} = \lambda_{l,j}^z\tilde{\mathbf{q}}$ .

Proposition 3.4 establishes conditions for the non-emptiness of  $IS_g(\phi|\mathbf{F}, \mathbf{S}, \mathbf{\Gamma})$ .

**Proposition 3.4** *(Non-emptiness) Let  $\{g_{ij}^h(\phi, \mathbf{Q}) = \mathbf{c}'_{ih}(\phi)\mathbf{q}_{j^*} : i = 1, \dots, n, h = 0, 1, \dots\}$  denote the impulse responses to the  $j^*$ -th shock. Assume that identifying restrictions are placed on the  $j^*$ -th structural shock only, i.e.,  $f_i = 0$  for  $i \neq j^*$ ,  $\mathcal{I}_S = \mathcal{I}_{\mathcal{F}\mathcal{E}\mathcal{V}} = \{j^*\}$ , and let  $z, z^* \in \{1, \dots, n\}$ . If the following conditions hold*

- (a)  $\exists z \in \Lambda_{j^*} \mid \underline{k}_{j^*}^z \leq \lambda_{l,j^*}^z \leq \bar{k}_{j^*}^z, \mathbf{\Upsilon}_S^z(\phi)\tilde{\mathbf{q}} = \lambda_{l,j^*}^z\tilde{\mathbf{q}}$  for some  $l = \{1, \dots, n\}$ ,
- (b)  $\underline{k}_{j^*}^{z^*} \leq \tilde{\mathbf{q}}'\mathbf{\Upsilon}^{z^*}(\phi)\tilde{\mathbf{q}} \leq \bar{k}_{j^*}^{z^*} \forall z^* \neq z \in \Lambda_{j^*}, \mathbf{S}_{j^*}(\phi)\tilde{\mathbf{q}} \geq \mathbf{0}, \mathbf{F}_{j^*}(\phi)\tilde{\mathbf{q}} = \mathbf{0}$ ,

*then the identified set  $IS_g(\phi|\mathbf{F}, \mathbf{S}, \mathbf{\Gamma})$  is non-empty and bounded.*

The main assumption is that restrictions constrain a single shock; however, in the empirical literature this is relatively common (Uhlig, 2005; Dedola and Neri, 2007; Vargas-Silva, 2008; Scholl and Uhlig, 2008; Rafiq and Mallick, 2008; Fujita, 2011; Dedola, Rivolta, and Stracca, 2017). If there is a  $z \in \Lambda_{j^*}$  satisfying condition (a), constraint  $\underline{k}_{j^*}^z \leq \mathbf{q}'_{j^*}\mathbf{\Upsilon}^z(\phi)\mathbf{q}_{j^*} \leq \bar{k}_{j^*}^z$  is

fulfilled for  $\mathbf{q}_{j^*} = \tilde{\mathbf{q}}$ , where  $\tilde{\mathbf{q}}$  is the eigenvector associated with  $\lambda_{l,j^*}^z$  and is as such analytically available. If  $\tilde{\mathbf{q}}$  satisfies the remaining restrictions (condition b), then the set is non-empty. If one wanted to verify whether a specific restriction on the FEVD induces a non-empty set, she/he would need to apply conditions (a) and (b) to that constraint.

The following algorithm implements Proposition 3.4:

**Algorithm 3.1**

*Step 1: Draw  $\phi$  from posterior distribution of the reduced-form VAR.*

*Step 2: For a variable  $z \in \Lambda_{j^*}$ , compute the correspondent eigenvalues  $\lambda_{l,j^*}^z$  of  $\Upsilon_{\mathcal{S}}^z(\phi)$  for  $l = \{1, \dots, n\}$ .*

*Step 3: Store  $\forall \lambda_{l,j^*}^z \mid \underline{k}_{j^*}^z \leq \lambda_{l,j^*}^z \leq \bar{k}_{j^*}^z$ ; otherwise, i.e.,  $\nexists \lambda_{l,j^*}^z \mid \underline{k}_{j^*}^z \leq \lambda_{l,j^*}^z \leq \bar{k}_{j^*}^z$ ,  $IS_g(\phi|\mathbf{F}, \mathbf{S}, \mathbf{\Gamma})$  is empty.*

*Step 4: If  $\exists \lambda_{l,j^*}^z$  such that the associated eigenvector  $\tilde{\mathbf{q}}$  satisfies the remaining restrictions, then  $IS_g(\phi|\mathbf{F}, \mathbf{S}, \mathbf{\Gamma})$  is non-empty. Otherwise, go back to Step 2 and select  $z^* \neq z \in \Lambda_{j^*}$ .*

Proposition 3.4 is potentially characterized by a gray area, where sufficient conditions do not hold. However, in the empirical application sufficient conditions are satisfied in more than 75 per cent of the draws. If these conditions fail, a numerical procedure described in Section 3.4 is used to detect non-emptiness. Note that under some conditions specified in Section 3.4 emptiness detection methods in Gafarov, Meier, and Olea (2018) and Amir-Ahmadi and Drautzburg (2018) can be also applied.

The following proposition builds on the non-emptiness to derive necessary conditions for the reduction of the identified set; this is useful when an analytical characterization of the identified set, e.g., the 2- and 3-variable model in Section 3.2, is not feasible.

**Proposition 3.5 (Shrinkage)** *Let  $\{g_{ij^*}^h(\phi, \mathbf{Q}) = \mathbf{c}'_{ih}(\phi)\mathbf{q}_{j^*} : i = 1, \dots, n, h = 0, 1, \dots\}$  denote the impulse responses to the  $j^*$ -th shock. Assume that (i) identifying restrictions are placed on the  $j^*$ -th structural shock only, i.e.,  $f_i = 0$  for  $i \neq j^*$ ,  $\mathcal{I}_{\mathcal{S}} = \mathcal{I}_{\mathcal{F}\mathcal{E}\mathcal{V}} = \{j^*\}$  and (ii)  $IS_g(\phi|\mathbf{F}, \mathbf{S}, \mathbf{\Gamma})$  is non-empty. Let  $z \in \{1, \dots, n\}$ . If  $IS_g(\phi|\mathbf{F}, \mathbf{S}, \mathbf{\Gamma}) \subset IS_g(\phi|\mathbf{F}, \mathbf{S})$ , then  $\exists z \in \Lambda_{j^*} \mid \lambda_{min,j^*}^z < \underline{k}_{j^*}^z$  or  $\lambda_{max,j^*}^z > \bar{k}_{j^*}^z$ .*

Note that conditions for the reduction relate to the eigenvalues of  $\Upsilon_{\mathcal{S}}^z(\phi)$ , which only depends on the reduced-form, and are as such easy-to-check.

### 3.4 Estimation and Inference

For set-identified SVARs, estimation and inference are not straightforward. The posterior distribution of structural parameters and IRFs reflects uncertainty about the reduced-form parameters  $\phi$  and the rotation matrix  $\mathbf{Q}$ . The common approach is to impose a uniform distribution on  $\mathbf{Q}$  in the space of orthonormal matrices. However, Baumeister and Hamilton (2015) showed that this choice does not imply a uniform distribution over the identified set of the structural parameters, because the latter are a function of reduced-form parameters and rotation matrix. Additionally, since  $\mathbf{Q}$  cannot get updated by data, as opposed to reduced-form parameters, Baumeister and Hamilton (2015) stressed that, even asymptotically, the posterior of structural parameters is proportional to the prior distribution. Furthermore, Arias, Rubio-Ramirez, and Waggoner (2018) pointed out that practitioners are likely to combine sign and zero restrictions by introducing unintended prior information.

This paper addresses the above criticisms by Baumeister and Hamilton (2015) and Arias, Rubio-Ramirez, and Waggoner (2018) by computing, under a convexity criterion, the infimum and supremum over all admissible rotation matrices. This implies that the identified set is distribution-free, i.e., it does not depend on a specific prior over  $\mathbf{Q}$ . Specifically, the set is conditional on reduced-form parameters  $\phi$ , and as such reflects the reduced-form parameter uncertainty. For sign and zero restrictions only, a similar solution was proposed by Giacomini and Kitagawa (2018), Gafarov, Meier, and Olea (2018), and Amir-Ahmadi and Drautzburg (2018); this paper suggests a distribution-free identified set that is subject to bounds on the FEVD and generalizes the optimization problem in Amir-Ahmadi and Drautzburg (2018) to include quadratic inequality constraints. As is common in the literature (Giacomini and Kitagawa, 2018; Gafarov, Meier, and Olea, 2018), characterization of the set is defined for models that place restrictions on a single shock.<sup>8</sup>

Specifically, Algorithm 3.2 describes the steps for estimating the identified set of  $g_{ij^*}^h(\phi, \mathbf{Q}) = \mathbf{c}'_{ih}(\phi)\mathbf{q}_{j^*}$  for some  $i = \{1, \dots, n\}$ ,  $h = 0, 1, \dots$ , and a shock of interest  $j^* \in \{1, \dots, n\}$ .

#### Algorithm 3.2

*Step 1: Draw  $\phi$  from posterior distribution of the reduced-form VAR.*

*Step 2: If  $IS_g(\phi|\mathbf{S}, \mathbf{\Gamma})$  is non-empty, go to Step 3. Otherwise, go back to Step 1.*

---

<sup>8</sup>Amir-Ahmadi and Drautzburg (2018) generalize to multiple shocks at cost of challenging and burdensome practical implementation.

Step 3: Compute the bounds of the set of  $g_{ij}^h(\phi, \mathbf{Q})$ :

$$\begin{aligned} & \min_{\mathbf{q}_{j^*}} \text{ and } \max_{\mathbf{q}_{j^*}} \mathbf{c}'_{ih}(\phi) \mathbf{q}_{j^*} \\ \text{s.t. } & \mathbf{S}_{j^*}(\phi) \mathbf{q}_{j^*} \geq \mathbf{0}, \underline{k}_{j^*}^z \leq \mathbf{q}'_{j^*} \mathbf{\Upsilon}^z(\phi) \mathbf{q}_{j^*} \leq \bar{k}_{j^*}^z \text{ for any } z \in \Lambda_{j^*}, \|\mathbf{q}_{j^*}\| = 1. \end{aligned}$$

Step 4: Repeat Step 1-3  $L$  times.<sup>9</sup>

In the views of Giacomini and Kitagawa (2018) and Amir-Ahmadi and Drautzburg (2018), Algorithm 3.2 delivers prior-robust estimation and inference because it is not dependent on a specific prior over  $\mathbf{Q}$ . Thus, according to DiTraglia and García-Jimeno (2016), it is also frequentist friendly and fully complies with the principle of transparent parametrization invoked by Schorfheide (2017). The algorithm relies jointly on a standard sampling from the posterior of reduced-form parameters (Step 1), the detection of emptiness (Step 2) and a numerical optimization to derive bounds of the set (Step 3), i.e., solving a constrained optimization problem. The latter consists of a linear objective function with linear inequality, quadratic inequality and equality constraints. Put another way, for medium- and high-scale models Algorithm 3.2 mirrors the analytical characterization of the identified set in the 2- and 3-variable framework in Section 3.2. In order to work, optimization problem in Step 3 needs to be convex. The following proposition establishes the conditions for convexity:

**Proposition 3.6** (*Convexity*) Let  $\{g_{ij}^h(\phi, \mathbf{Q}) = \mathbf{c}'_{ih}(\phi) \mathbf{q}_{j^*} : i = 1, \dots, n, h = 0, 1, \dots\}$  denote the impulse responses to the  $j^*$ -th shock. Assume that identifying restrictions are placed on the  $j^*$ -th structural shock only, i.e.,  $\mathcal{I}_{\mathcal{S}} = \mathcal{I}_{\mathcal{F}\mathcal{E}\mathcal{V}} = \{j^*\}$ , and that there are no zero restrictions, and let  $z \in \{1, \dots, n\}$ . For  $z \in \Lambda_{j^*}$ , if one of the following conditions hold

(a)  $\underline{k}_{j^*}^z = 0$ ,

(b)  $z$  subject to bounds on the FEVD up to horizon  $\tilde{h}$  and responses  $g_{zj^*}^h(\phi, \mathbf{Q})$  are sign-restricted for  $h = 0, \dots, \tilde{h}$ ,

then  $\{\mathbf{q}_{j^*} \in \mathcal{R}^n | \mathbf{S}_{j^*}(\phi) \mathbf{q}_{j^*} \geq \mathbf{0}, \underline{k}_{j^*}^z \leq \mathbf{q}'_{j^*} \mathbf{\Upsilon}^z(\phi) \mathbf{q}_{j^*} \leq \bar{k}_{j^*}^z \ \forall z \in \Lambda_{j^*}, \|\mathbf{q}_{j^*}\| = 1\}$  and  $IS_g(\phi | \mathbf{S}, \mathbf{\Gamma})$  are convex.

Technical Appendix provides the proof. The intuition is that, under condition (a), the space defined by quadratic constraints on  $\mathbf{q}_{j^*}$  due to the bounds on the FEVD is always convex. On the other hand, condition (b) linearizes the restrictions on the FEVD, i.e., it reduces the constraints on the FEVD to linear inequalities on  $\mathbf{q}_{j^*}$ ; in a nutshell, under condition (b) the

---

<sup>9</sup>In the empirical application,  $L = 1000$ .

identifying restrictions are a set of linear inequality constraints on  $\mathbf{q}_{j^*}$ . Thus, this offers great flexibility because distribution-free algorithms in the works of Giacomini and Kitagawa (2018), Gafarov, Meier, and Olea (2018), and Amir-Ahmadi and Drautzburg (2018) and emptiness detection methods in Gafarov, Meier, and Olea (2018) and Amir-Ahmadi and Drautzburg (2018) can be also applied as long as (b) holds  $\forall z \in \Lambda_{j^*}$ . If the problem is not convex, the common procedure of imposing a uniform specification on  $\mathbf{Q}$  can be still used for estimation and inference. Note that the Monte-Carlo exercise and the empirical application will (i) show that convexity conditions are easy to satisfy and (ii) present results by both employing distribution-free and standard approach.

Compared to the influential paper by Giacomini and Kitagawa (2018), there are three main differences. Firstly, in order to compute bounds of the identified set, numerical optimization is used rather than Monte Carlo integration. The latter may be very complicated and impractical, especially for medium- and large-size SVARs, and tends to underestimate the set. Secondly, there is an analytical criterion for checking for non-emptiness, while Giacomini and Kitagawa (2018) relied on simulation to detect emptiness. Furthermore, the optimization problem contains quadratic constraints on  $\mathbf{q}_{j^*}$ , that are induced by bounds on the FEVD. This is also the main departure from the works of Gafarov, Meier, and Olea (2018), and Amir-Ahmadi and Drautzburg (2018).

Finally, when conditions in Proposition 3.4 fail, this paper considers the identified set empty if the Step 3 in Algorithm 3.2 cannot find an interior solution for a multiplicity of starting points. Alternatively, one can follow the standard literature and treat the set as empty whether, for a number of draws from the orthonormal space, an admissible rotation matrix  $\mathbf{Q}$  cannot be found.

## 4 How to derive restrictions

The previous section showed that bounds on the FEVD can help in bi- and trivariate settings. However, we still need to find a way to choose a reasonable set of constraints in realistic SVAR frameworks. Specifically, the baseline case in this paper considers the following seven key macroeconomic variables: real output, consumption, investment, wage, and hours worked, inflation, and interest rates. The seven indicators are typically those covered in the commonly used DSGE model of Smets and Wouters (2007), in several related analyses, such as Justiniano, Primiceri, and Tambalotti (2011), and in the growing literature about identification of uncertainty shocks (Jurado, Ludvigson, and Ng, 2015; Carriero, Clark, and Marcellino, 2018).

This section presents a methodology to derive dogmatic and nondogmatic bounds on the FEV. The former are identifying restrictions treated as if known with certainty, which is the

standard approach in the literature; the latter introduce doubts, or uncertainty, about the identifying assumptions.

## 4.1 Dogmatic Bounds

The current section presents a methodology to derive dogmatic theory-driven bounds on the FEVD. To do so, I adapt to the FEVD the approach that Canova and Paustian (2011) used to obtain sign restrictions from DSGE models for the IRFs.<sup>10</sup> Generally, embodying theory-driven implications of DSGE frameworks into SVARs as identifying restrictions is increasingly common.<sup>11</sup> The analysis starts from a framework with an approximate state space representation. I investigate the FEVD of the endogenous variables in response to the disturbances for competing parametrizations. In doing so, I assume that all DSGE parameters are uniformly and independently distributed over reasonable ranges derived from the literature. This allows me to establish bounds on the FEVD that are robust towards parameter uncertainty and without favoring any specific parametrization. Note that identification restrictions are explicitly inferred and only robust restrictions are admitted. Thus, the methodology depends on generic conditional dynamics and does not rely on a particular parametrization. However, the bounds on the FEVD so obtained are still dependent on the specific state space representation; thus, they are kept and used as identifying constraints if and only if less (or equally) restrictive than those implied by alternative state space representations. The procedure can be summarized as follows:

1. select a state space representation (Section 4.1.1);
2. adapt the methodology in Canova and Paustian (2011) to assure that bounds on the FEVD are robust across parametrizations within the chosen state space framework (Section 4.1.2);
3. verify whether those bounds on the FEVD are less (or equally) restrictive than those induced by alternative state space models (Section 4.1.3).

It is of utmost importance to stress that there are alternative ways of deriving the bounds on the FEVD. For instance, if the researcher was particularly confident of a specific state

---

<sup>10</sup>Among others, this methodology has been used by Dedola and Neri (2007), Pappa (2009), Peersman and Straub (2009), and Lippi and Nobili (2012).

<sup>11</sup>See Canova and Paustian (2011) for details about the proper procedure to do so and how SVARs can be employed for validation and selection amongst competing theoretical frameworks. On the other hand, Del Negro and Schorfheide (2004) propose to (i) infer the prior of reduced-form VAR from the DSGE posterior and (ii) draw the rotation matrix needed for point-identifying the SVAR from the posterior distribution of a DSGE model. While (i) can be easily incorporated in this paper, (ii) represents an alternative (point-)identification strategy.

space representation, Step 3 would be pointless. Similarly, posterior estimation of a specific theoretical framework could fully replace the uniform support in Step 2 and the whole Step 3. However, the choice of placing uniform specifications (Step 2) and then checking for alternative state space forms (Step 3) guarantees additional robustness and delivers less restrictive, more general bounds on the FEVD.

On the other hand, bounds on the FEVD can be descended from alternative sources, such as researcher's beliefs. For instance, Dedola and Neri (2007) argued that technology shocks need to explain at least the 70 per cent of the FEV of the labor productivity in the medium-run. In fact, this is a lower bound on the FEVD of the labor productivity to technology shock and can be used as identifying assumption. The machinery in this section is therefore of separate interest with respect to the rest of the paper and is not the only available option to get bounds on the FEVD.

#### **4.1.1 A Benchmark Model with Real and Nominal Frictions**

To illustrate the fundamental restrictions that a theoretical structure imposes on the FEVD to monetary policy shock in a setting with the macroeconomic variables listed above, the medium-size New-Keynesian framework has been considered. However, it is vital to point out that the medium-scale New-Keynesian framework here has an illustrative purpose only and it has been selected because of its overwhelming diffusion after the seminal works by Smets and Wouters (2005) and Smets and Wouters (2007). In fact, the methodology can be applied to any other theoretical framework researcher believes in.

This section introduces the model; however, since the framework is currently well-established and -known, to save on space, this paper refers to Smets and Wouters (2005) and Smets and Wouters (2007) for the details about the micro-foundation of the model and its equilibrium conditions. Table in Technical Appendix 2 provides details about the DSGE parameters and their support; this is constructed to include commonly estimated values for the US.

The model contains many shocks and frictions. Specifically, it features sticky nominal price and wage settings that allow for backward indexation, habit formation in consumption and investment adjustment costs that create hump-shaped responses of aggregate demand, and variable capital utilization and fixed costs in production. The stochastic dynamics is driven by many structural shocks, including the total factor productivity shock, shocks that affect the intertemporal margin, shocks that affect the intratemporal margin, and policy shocks (exogenous spending and monetary policy shocks).

Households maximize a non-separable utility function with the consumption of goods and their labor effort as arguments over an infinite horizon. An external habit variable appears in

the utility function. Labor is characterized by the existence of a union, leading to a certain level of monopoly power in relation to wages and an explicit wage equation, which allows for different degrees of sticky nominal wages (Calvo model). Households rent capital services to firms and establish how much capital to collect, subject to the capital adjustment costs. As the capital rental price moves, the utilization of the capital stock can be amended at increasing cost. Firms produce differentiated goods, settle upon labor and capital inputs, and set prices (Calvo model). As an adjunct to the Calvo setting, both prices and wages can be (fully or partially) indexed. Thus, prices are a function of current marginal costs, but are also affected by the past and expected inflation rate. The marginal costs depend on wages, the rental rate of capital, and productivity process. Similarly, wages are also determined by past and expected future wages and past, current and expected inflation. The central bank follows the Taylor rule by adjusting the policy interest rate to inflation and the output gap, namely the difference between actual and potential output.<sup>12</sup> A short-run effect from the current changes in the output gap and inflation is also taken into account. The model features two monetary shocks: a temporary i.i.d. interest rate shock, namely a standard monetary policy shock; a permanent shock to the inflation objective.<sup>13</sup>

#### 4.1.2 Deducing Robust Restrictions on the FEVD

I have drawn 10,000 parameter vectors from the uniform distributions of the DSGE parameters. The support of the standard deviation of the shocks is consistent with the estimates in literature, follows Table 1b in Smets and Wouters (2007), and is omitted to save on space. Specifically, the upper bound for the monetary shock is 55 basis points. However, as further check, increasing the size to 75 and 100 basis point does not affect the results. Restrictions are therefore robust to variation in the shocks size.

For each draw, I have computed the impulse responses and the FEVD to 1 standard deviation positive (contractionary) monetary policy shock for output ( $y_t$ ), consumption ( $c_t$ ), investment ( $I_t$ ), real wages ( $w_t$ ), hours worked ( $l_t$ ), inflation rate ( $\pi_t$ ), and interest rates ( $i_t$ ). Table 1 shows the signs of the impact impulse responses<sup>14</sup> and the FEVD at horizon  $h = 0$ . Specifically,  $+$ ( $-$ ) indicates that all the draws find that a certain variable has a positive (negative) response upon impact; ? indicates that the sign of the response cannot be uniquely pinned down; the bounds of the FEVD are computed as the maximum and minimum value of the FEVD across

---

<sup>12</sup>The potential output is the level of output under flexible wages and prices, and without mark-up shocks.

<sup>13</sup>Error variance decomposition to standard monetary policy shock shown in the next section is robust to shutting down the permanent shock.

<sup>14</sup>These signs are sufficient to disentangle monetary policy shocks from other disturbances.

the 10,000 draws.<sup>15</sup>

The first row in Table 1 shows that upon the impact sign of the impulse responses to a monetary policy shock is uniquely pinned down, with the significant exception of real wages.

Given the variety of parametrizations embodied, the FEVD in Table 1 shows relatively large intervals; with the notable exception of interest rates, the lower bound is zero for most of the variables. However, the upper bounds are well-below one for all the variables. According to Table 1, in the short-run a monetary policy shock can explain a large share of the FEV of interest rates, whereas the impact on the real variables and inflation rate, although well below the 50 per cent, is more ambiguous, going from being negligible to being significant. This reflects the parametrization uncertainty.

As discussed, a fully viable alternative is estimating a specific model and drawing from its posterior distribution. For instance, the bounds on the FEVD from Smets and Wouters (2007) are, as expected, much more restrictive than those reported in Table 1; posterior estimation can be therefore viewed as a specific case of the general procedure presented in this section.

**Table 1**

|               | $y_t$        | $c_t$        | $I_t$        | $w_t$        | $l_t$        | $\pi_t$      | $i_t$        |
|---------------|--------------|--------------|--------------|--------------|--------------|--------------|--------------|
| IRFs, $h = 0$ | -            | -            | -            | ?            | -            | -            | +            |
| FEV, $h = 0$  | [0.00, 0.25] | [0.00, 0.20] | [0.00, 0.19] | [0.00, 0.10] | [0.00, 0.12] | [0.00, 0.38] | [0.30, 0.77] |

Sign of impact responses and FEV at horizon  $h = 0$  to contractionary monetary policy shock.  $+(-)$  indicates that all the draws find that a certain variable has a positive (negative) response upon impact;  $?$  indicates that the sign of the response cannot be uniquely pinned down; the bounds of the FEVD are computed as the maximum and minimum value of the FEVD across the 10,000 draws.

### 4.1.3 Alternative State Space Forms

Although the framework illustrated in Section 4.1.1 contains several real and nominal frictions, financial ones are absent. Thus, in order to evaluate further the robustness of the bounds in Table 1, the models in Gertler and Karadi (2011), Christiano, Motto, and Rostagno (2014), and Curdia and Woodford (2010) are considered. Note that the paper is focusing on medium-size frameworks because they are increasingly common and more realistic than small-scale representations. A wide spectrum of financial frictions and shocks is therefore added to the baseline state space form and reduce the probability that the bounds on the FEVD are model specific. Since the models employ different variables, I focus on the real output, inflation and interest rate, which are common to the different specifications. I find that the FEVD of those

---

<sup>15</sup>An alternative is extracting 90 per cent intervals. This trades-off two elements: robustness, which would lead to a selection of large intervals, and potential misspecification, whereby no restrictions would hold with a probability of one. However, the results are identical to what presented in the main text.

variables to (conventional) monetary policy shock as reported in Table 1 delivers larger bounds than those in Gertler and Karadi (2011), Christiano, Motto, and Rostagno (2014), and Curdia and Woodford (2010); this puts some additional evidence on the robustness of the results. Amongst the alternative models considered here, Gertler and Karadi (2011) have the most similar set of endogenous variables to that in the baseline specification of seven macroeconomic variables. For instance, they include consumption and investment; it is therefore encouraging that in Table 1 also the bounds on the FEVD of such variables are larger than those implied by Gertler and Karadi (2011).

## 4.2 NonDogmatic Bounds

This section introduces uncertainty over the bounds on the FEVD, or nondogmatic identifying assumptions. This is consistent with very recent and growing literature, including Baumeister and Hamilton (2019), Baumeister and Hamilton (2018), and Giacomini, Kitagawa, and Volpicella (2017), arguing that researchers treat identifying assumptions as if known with certainty, while they need to acknowledge explicitly that there are substantial doubts about the restrictions that are typically employed as identifying constraints. In other words, standard imposition of identifying restrictions relies on an all-or-nothing approach. For instance, in Table 1 dogmatic bounds on inflation and interest rates imply

$$0.30 \leq CFEV_i^i(0) \leq 0.77, \quad (4.1)$$

$$CFEV_i^\pi(0) \leq 0.38. \quad (4.2)$$

In other words, according to Table 1,  $CFEV_i^i(0) = 0.30$  is fully plausible, whereas  $CFEV_i^i(0) = 0.29$  is a violation of the identifying assumptions. This all-or-nothing approach is common to any identifying constraints, including zero and sign restrictions, and is not therefore a specific feature of the constraints on the FEVD; in fact, it is the benchmark in the literature.

The methodology proposed below exemplifies how to incorporate uncertainty, or doubts, about the constraints on the FEVD. As illustrative example, consider inflation and interest rates. Instead of looking upon bounds on  $CFEV_i^i(0)$  and  $CFEV_i^\pi(0)$  as fixed (or dogmatic) values, assume that

$$\underline{k}_i^i \leq CFEV_i^i(0), \quad (4.3)$$

$$CFEV_i^\pi(0) \leq \bar{k}_i^\pi, \quad (4.4)$$

where  $\underline{k}_i^i \sim Beta(\alpha_i, \beta_i)$  and  $\bar{k}_i^\pi \sim Beta(\alpha_\pi, \beta_\pi)$ . Nondogmatic bounds are random variables following Beta distributions; note that the upper bound on  $CFEV_i^i(0)$  is left unrestricted, as opposed to dogmatic bounds in (4.1). Parameters  $\alpha_i, \beta_i, \alpha_\pi, \beta_\pi$  are set such that  $CFEV_i^i(0)$

and  $CFEV_i^\pi(0)$  vary across most of the values found in the literature. Specifically, (i) the distributions are still centred at the values found in Section 4, namely  $E(k_i^i) = 0.30$  and  $E(\bar{k}_i^\pi) = 0.38$  and (ii) with 95 per cent probability,  $k_i^i \geq 0.06$  and  $\bar{k}_i^\pi \leq 0.78$ . To my knowledge, theoretical frameworks suggesting that, with significant probability, the effect of a monetary shock explains more than 78 per cent of the unexpected fluctuations of inflation rates upon impact are uncommon; a similar analysis of the literature has been carried out for  $k_i^i$ . As a result, the nondogmatic bounds give a small, but non-zero, probability to extreme values of the FEVD.

In addition to the introduction of uncertainty about the identifying assumptions, nondogmatic bounds i) augment the dogmatic ones by analysing the literature and ii) make sure the identification, estimation, and inference do not strictly depend on a specific value given to the bounds of the FEVD. The Monte-Carlo simulation and empirical application fully illustrates (ii). Computationally, the implementation of nondogmatic bounds requires to extract  $k_{j*}^z$  and  $\bar{k}_{j*}^z$  in Step 3 of Algorithm 3.2 from a stochastic process.

The next section describes how dogmatic bounds in Table 1 and nondogmatic bounds can be used as identifying restrictions, and evaluates them through a Monte-Carlo exercise. Since the literature typically considered dogmatic restrictions as the only source of identifying constraints, from now on the terms “bounds” and “dogmatic bounds” will be used interchangeably.

## 5 A Monte-Carlo Experiment

The Monte-Carlo experiment in this section makes a comparison between the performance of identification schemes based on restrictions on the FEVD and sign restrictions. The DGP is the model in Smets and Wouters (2007), calibrated at its posterior means; the reduced-form VAR includes the variables listed above in the first difference, with the exception of inflation and interest rates, and has a lag length of five. Without loss of generality, I want to evaluate the ability of theory-driven restrictions on the FEVD to replicate and identify the DGP output response to monetary policy shock, as opposed to sign restrictions, where the shock size is common across the competing models. Specifically, I have evaluated the following structural models:<sup>16</sup>

- *Sign Restrictions*

This model identifies an interest rate shock through sign restrictions on impact responses. Specifically, it employs the sign restrictions in Table 1. A contractionary interest rate shock reduces inflation, consumption, investment and hours worked, and increases interest

---

<sup>16</sup>For those models the optimization problem illustrated in Algorithm 3.2 is convex.

rates:  $IR_{ci}^0 \leq 0$ ,  $IR_{Ii}^0 \leq 0$ ,  $IR_{li}^0 \leq 0$ ,  $IR_{\pi i}^0 \leq 0$ ,  $IR_{ii}^0 \geq 0$ . The object of interest  $IR_{yi}$ , i.e., the output response, is left unrestricted.

- *Bounds on the FEVD*

In addition to the sign restrictions, the FEVD of nominal variables is bounded as in Table 1:  $0.30 \leq CFEV_i^i(0) \leq 0.77$  and  $CFEV_i^\pi(0) \leq 0.38$ . Since the object of interest is the real output response, the FEVD of real variables is not directly bounded. The model therefore assumes that the monetary disturbance is free to potentially explain a large share of the short-run unexpected movements in the interest rates, whereas its contribution to the fluctuations of  $\pi$  may be large, but also unbounded from below.

- *NonDogmatic Bounds on the FEVD*

In addition to the sign restrictions, the FEVD of nominal variables is bounded as in Section 4.2.

## 5.1 Analysis without Estimation Uncertainty

Firstly, I have considered the analysis without sample bias or estimation uncertainty, i.e., population analysis. Suppose that there is an infinite amount of data on observables; that implies that the reduced-form VAR is estimated without error and is fixed at values implied by the DGP. As a result, the only unknown object is the matrix  $\mathbf{A}_0$  in equation (3.1). In order to recover  $\mathbf{A}_0$ , I have used the true covariance matrix  $\Sigma$  and identifying restrictions. The setting of this Monte-Carlo experiment isolates the identification uncertainty and excludes sample bias by construction. For each model, Figure 1 reports the DGP output response to a (contractionary) monetary policy shock and the identified set of output response computed with Algorithm 3.2, where in Step 1 the reduced-form is fixed by the DGP. As long as there is no estimation of the reduced-form VAR, such a set captures the identification uncertainty implied by identifying restrictions. Additionally, the black solid line represents the median induced by a uniform distribution on  $\mathbf{Q}$ , i.e., the standard approach. Impulse responses are non-cumulative.

While sign restrictions are unlikely to identify the theoretical response (panel c), dogmatic and nondogmatic restrictions on the FEVD (panel a and b, respectively) shrink the identified set, are able to pin down the sign of output response and deliver precise estimation. Furthermore, under a uniform prior for  $\mathbf{Q}$  the median replicates the DGP response well, as opposed to sign restrictions.<sup>17</sup> Remarkably, the results are very robust to the introduction of uncertainty

---

<sup>17</sup>There is huge debate over which measure of central tendency should be used for set-identified SVARs. The common measure is the median, but Fry and Pagan (2011) and Inoue and Kilian (2013) proposed alternative

over the bounds on the FEVD: panel b shows that nondogmatic bounds on the FEVD identify the DGP response and deliver a dramatic reduction of the response set implied by sign restrictions. As a result, the identification ability of the constraints on the FEVD does not strictly depend on a specific value given to the bounds of the FEVD. In other words, the identification is robust to doubts about the specific values used for bounding the FEVD.

---

measures. I have employed the median as a measure of central tendency because it is widely used in empirical works and makes a comparison with the literature simpler. However, note that using the alternative measures leaves the results unchanged; the same applies to the empirical application in Section 6.

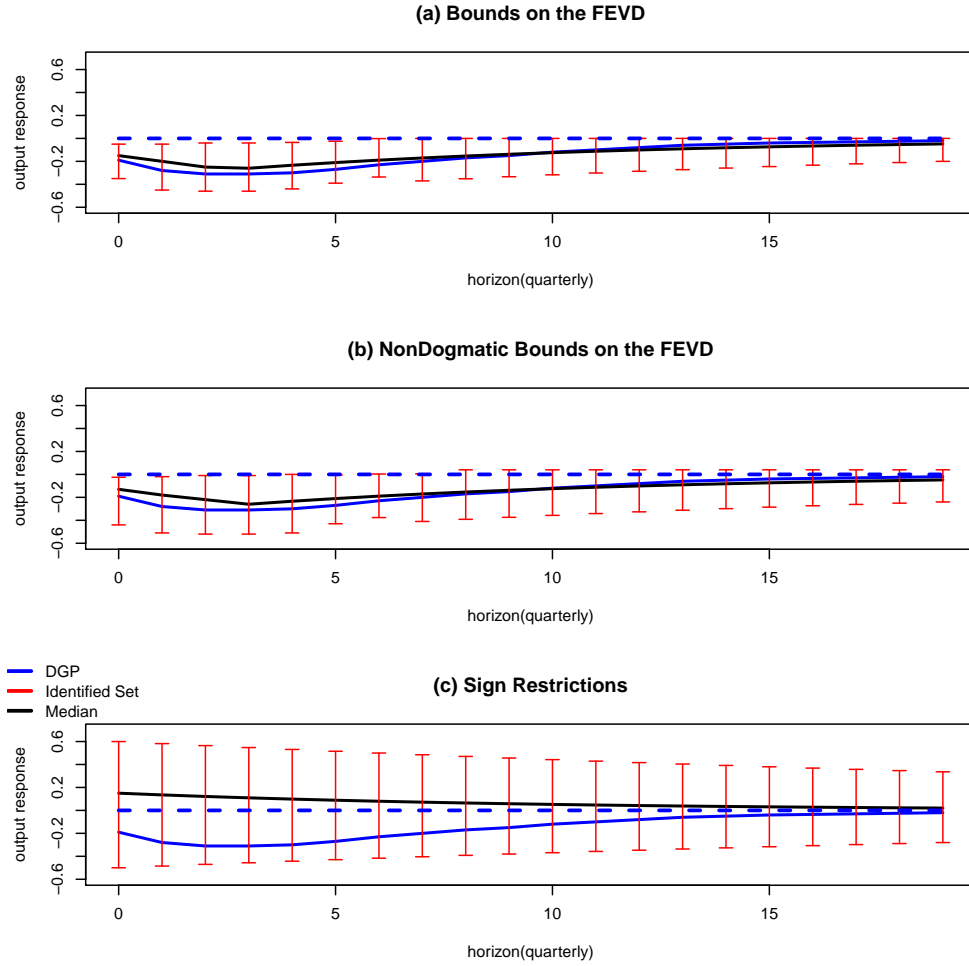


**Figure 1: Population Analysis, Monte-Carlo Simulation**

Figure 1 reports the theoretical DGP output response (blue line) to contractionary monetary policy shock, the output response identified set (red vertical bars) as per Algorithm 3.2 and the median induced by a uniform distribution on  $Q$  (black line). See Section 5 for details. The shock size is set to one standard deviation and is common to all the three specifications. The response is measured in percentage.

## 5.2 Estimation Uncertainty

The previous exercise focused on the uncertainty arising from the ability of identifying assumptions to recover the DGP response. There, the VAR coefficient matrices were held fixed at the values implied by the DGP. However, in empirical works these matrices must be estimated from finite samples. Thus, sampling, or estimation, uncertainty is an additional issue to take into account. In order to assess the impact of estimation uncertainty, this section generates 1,000 datasets and sets the length of time series to 1,000, where the first 800 observations are discarded in order to remove the impact of initial conditions, so that  $T^* = 200$  is the artificial sample size with quarterly frequency. At each replication, artificial data are used to estimate the reduced-form VAR from a flat Normal Inverse Wishart distribution.

Figure 2 introduces the estimation uncertainty. Specifically, the red vertical bars depict the 90 per cent Bayesian region across the replications of the identified set computed with the distribution-free approach; the black line reports the median across the replications when a uniform prior is imposed on  $\mathbf{Q}$ . Sample bias does not affect the results, in which only the dogmatic and nondogmatic bounds on the FEVD are able to recover and identify the sign of the DGP response.

The mechanism behind the dramatic change in estimation and inference is extensively discussed in Section 6.3. Here it is worthy of mention that bounds on the FEVD of inflation and interest rate are sufficient, but not necessary, to obtain the meaningful results in Figure 1 and 2. For instance, bounds on the FEVD of  $c_t$ ,  $I_t$ ,  $w_t$ , and  $l_t$  deliver a similar informative outcome on their own; a full analysis of the issue is postponed to Section 6.3. The effect of misspecification between the theoretical framework and the estimated model is studied in Section 6.5.

In a controlled experiment, Paustian (2007) argued that a monetary policy shock that is much larger (up to ten times) than the values implied by standard DSGE models helps (but is not sufficient for) sign restrictions to identify the DGP. Specifically, he found that monetary shocks that explain a large share (much more than what theory suggests) of the FEV of real variables in the long-run are more likely to identify structural parameters if combined with sign restrictions. The approach in this paper is radically different because I employ a multiplicity of different standard DSGE models and investigate the literature to construct bounds on the contribution of a monetary policy shock. Specifically, here i) the shock size is normalized to be common across all the models; ii) the monetary shock does not dominate the FEV of endogenous variables (most of them are left unrestricted, and bounds on the FEV of the inflation and interest rate derive from a theory- and literature-driven methodology that prevents the imposition of an artificially/unrealistically high contribution from the monetary

disturbance). As a further check, in the model in which constraints on the FEVD are imposed the contribution of monetary shocks to the FEVD of real variables and interest rates approaches zero at long horizons, as opposed to Paustian (2007).

This Monte-Carlo exercise shows that dogmatic and nondogmatic constraints on the FEVD shrink the identified set of the output response, yield precise estimation, and fully identify the sign and magnitude of the DGP response, as opposed to sign restrictions, regardless the approach over the rotation matrix. The next section evaluates the identification schemes in the data and investigates the mechanisms and channels through which dogmatic and nondogmatic bounds on the FEVD deliver a reduced and more plausible set.

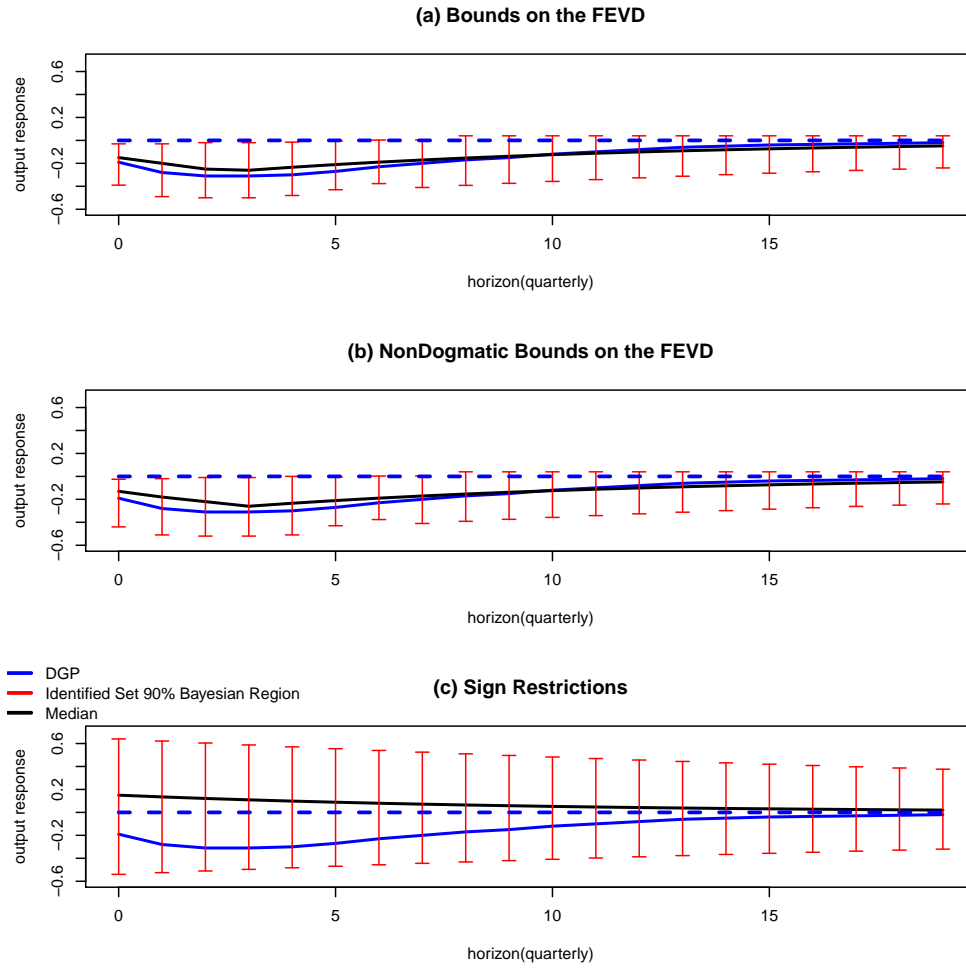


**Figure 2: Sample Analysis, Monte-Carlo Simulation**

Figure 1 reports the theoretical DGP output response (blue line) to contractionary monetary policy shock, the 90% Bayesian credibility region of the output response identified set across replications (red vertical bars) as per Algorithm 3.2 and the median across replications induced by a uniform distribution on  $Q$  (black line). See Section 5 for details. The shock size is set to one standard deviation and is common to all the three specifications. The response is measured in percentage.

## 6 Empirical Application: Monetary Policy Shocks

A considerable body of literature has studied the impact of monetary policy shocks on output using SVARs, identified with zero restrictions (Christiano, Eichenbaum, and Evans, 1999; Bernanke and Mihov, 1998), sign restrictions (Uhlig, 2005) and both (Arias, Caldara, and Rubio-Ramirez, 2019). SVARs identified using zero restrictions have consistently found that a contractionary monetary policy shock implies a significant reduction in short-run real economic activity. This consensus view has been challenged by Uhlig (2005), who has argued against imposing a controversial zero restriction on the IRF of output to a monetary policy shock upon impact. Specifically, he identified a monetary policy shock by imposing sign restrictions only on the IRFs of variables other than the output, that was therefore left unrestricted. The lack of restrictions on output makes this approach appealing and explains why it has been used extensively in empirical studies. Under this identification scheme, a contractionary monetary policy shock has no significant impact on real variables in the short-run (Uhlig, 2005; Mountford, 2005; Rafiq and Mallick, 2008), does not necessarily lead to a decrease in real activity and the inference is largely uninformative; this outcome is robust to the choice of variables in the SVAR, lag selection, prior specification and sample periods. Furthermore, Arias, Caldara, and Rubio-Ramirez (2019) showed that sign restrictions on IRFs have counter-intuitive consequences on the systematic response of monetary policy to real output; Antolín-Díaz and Rubio-Ramírez (2018) argued that sign-restricted IRFs yield implausible implications for HD.

Firstly, this section illustrates that dogmatic and nondogmatic bounds on the FEVD are highly informative, deliver precise estimation, and tend to exclude implausible implications by recovering significant effects of monetary policy shocks on real variables (Section 6.1). Both the distribution-free approach in Algorithm 3.2 and placing a uniform distribution on  $\mathbf{Q}$  (Arias, Rubio-Ramirez, and Waggoner, 2018) have been used. Secondly, I have compared the results with those induced by the most relevant and recent approaches to enrich sign restrictions, including narrative sign restrictions (Antolín-Díaz and Rubio-Ramírez, 2018), the ranking of IRFs (Amir-Ahmadi and Drautzburg, 2018), and constraints on the systematic response of the monetary policy equation (Arias, Caldara, and Rubio-Ramirez, 2019) (Section 6.2). I have then investigated the mechanism behind the change in estimation and inference implied by bounds on the FEVD (Section 6.3) and run a sensitivity analysis (Section 6.4). Finally, Section 6.5 analyses the effect of misspecification between the theoretical framework and the estimated model.

## 6.1 Seven-Variable SVAR

This section estimates the three models of the Monte-Carlo exercise and an augmented version of sign restrictions, where the contribution of the monetary shock to real output in the long-run is zero. Amongst others, this approach dates back to Faust (1998), Sims (1998), and Christiano, Eichenbaum, and Evans (1999), who argued that for every reasonable identification, the monetary policy disturbance needs to explain a small share of the FEV of output in the long-run. This framework contains a zero restriction; in this case, convexity of the optimization problem requires more stringent conditions and a number of starting points is employed in the optimization algorithm, that always converges to the same infimum and supremum. The same applies to the model with constraints on the structural component of the monetary policy equation in Section 6.2.

The variables are the same as the Monte-Carlo simulation: real output, real consumption, real investment, real wages, hours worked, the inflation rate and interest rates. I have used the dataset constructed by Smets and Wouters (2007). This employs quarterly variables, and I have considered the first differences of logs, except for the federal funds rate. The model is therefore estimated using some variables differenced for stationarity; this implies that, for some covariates, the long-run effects of transitory shocks do not vanish. The reduced-form prior follows a flat Normal Inverse Wishart distribution and is common to any set of identifying restrictions; difference in estimation and inference therefore can not be attributed to the reduced-form, its prior, or sample bias. The cumulative impulse responses are shown for all the variables with the exception of the interest rate and inflation rate. The monetary shock is normalized to 15 basis points.

By using the distribution-free approach in Algorithm 3.2, Figure 3 characterizes the identified set of the impulse responses induced by dogmatic (panels a-g) and nondogmatic (panels a'-g') bounds on the FEVD. Specifically, it reports the posterior means of the set bounds (black solid lines), the Bayesian credibility region of the sets (black dashed lines), and the zero line (blue dashed lines). Figure 3 shows that a contractionary monetary shock induces a negative and significant response of the real variables, including output, in the short-run. At longer horizons, the effect of monetary disturbances tends to be no longer significant. The results are therefore consistent with the textbook theory according to which monetary shocks matter in the short-run, but are much less relevant at longer horizons. Remarkably, estimation and inference induced by nondogmatic approach is similar to that delivered by dogmatic bounds.<sup>18</sup>

---

<sup>18</sup>The main text reports the 68 per cent Bayesian credibility region; however, results are very robust to different credibility regions, e.g., with dogmatic and nondogmatic bounds on the FEVD, the output response in the short-run is still negative and statistically significant under the 95 per cent credibility region. Furthermore, to be thorough, for the case with uniform prior on the rotation matrix credibility regions up to 95 per cent are

Thus, identification does not strictly depend on specific values given to the bounds on the FEVD and the findings are extremely robust to reasonable doubts about the bounds. Figure 4 illustrates the impulse responses under a uniform distribution on the rotation matrix and fully confirms the previous results.

Next figures introduce the comparison between (dogmatic and nondogmatic) bounds on the FEVD and sign restrictions. In order to illustrate the difference in estimation and inference, note that the pictures need a different scale with respect to the previous ones. Panel (b) in Figure 5 and 6 displays the output response; with bounds on the FEVD, contractionary monetary shock induces a negative and significant response of the real output; on the other hand, sign restrictions with/without long-run constraint deliver a very large and disperse set, supporting the neutrality of monetary shocks in the short-run. The IRFs of the other variables confirm that the bounds on the FEV can shrink the set of structural parameters so that the economic implications dramatically differ. The sample uncertainty does not affect the results and bounds on the FEV yield very precise estimation, as opposed to sign restrictions. Figure 7 confirms that nondogmatic bounds on the FEVD greatly reduce the set of structural responses induced by sign restrictions.

Sign restrictions lead to extremely imprecise estimation, some hard-to-justify results and induce structural responses with different, and not rarely contradictory, economic implications; for example, a contractionary monetary shock of only 15 basis points induces an output variation between  $-1.80$  and  $+0.98$  per cent upon impact. Under sign restrictions, it is therefore challenging to obtain any meaningful, or informative, conclusion about both the magnitude and the sign of the effects of a monetary shock. On the other hand, dogmatic and nondogmatic bounds on the FEVD increase estimation precision, remove extreme or implausible results and allow to reach informative outcomes; for instance, upon impact output varies between  $-0.02$  and  $-0.77$  per cent.

Figure 8, 9, and 10 illustrate the impulse responses under a uniform distribution on the rotation matrix. For output (panel b), dogmatic and nondogmatic bounds on the FEVD drastically shrink the response set and lead to informative inference, whereas sign restrictions support the neutrality of monetary policy even in the short-run, and are generally uninformative. The same applies to the other variables.

---

reported.

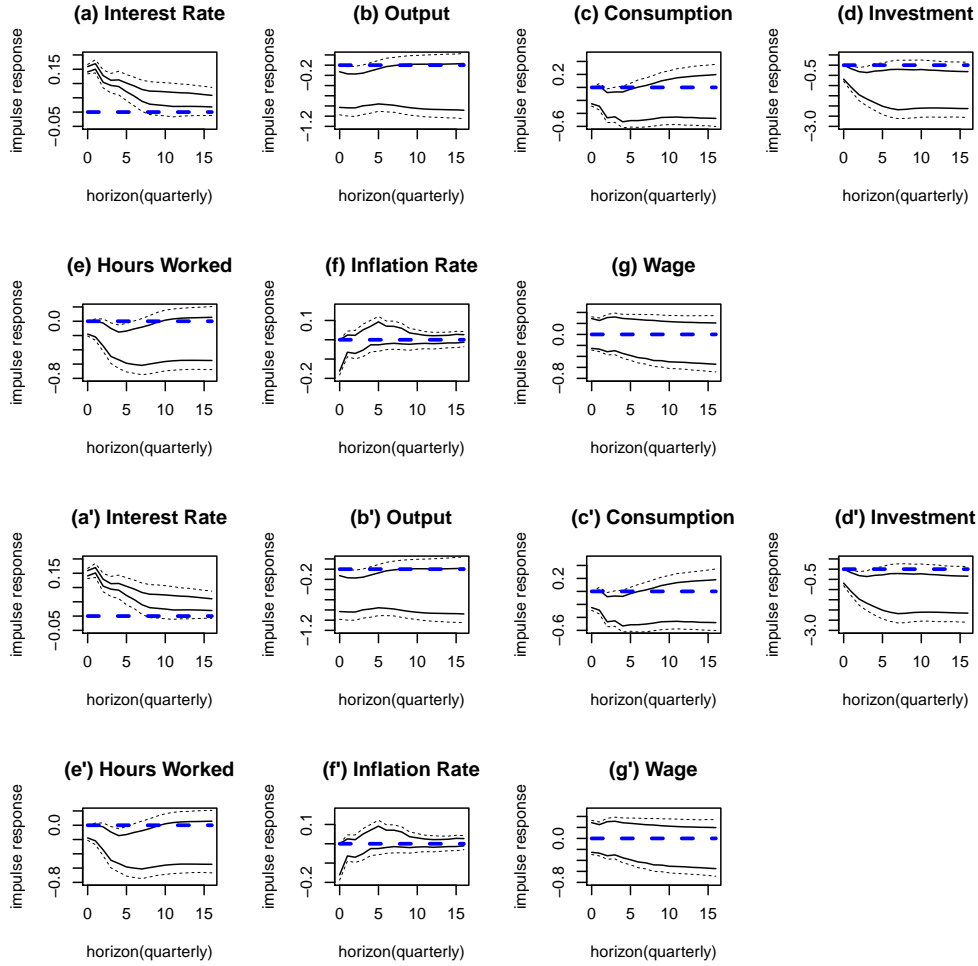


**Figure 3: Dogmatic and Nondogmatic Bounds on the FEVD: Impulse Responses Identified Set, Distribution-Free Approach**

For panels (a)-(g), the black solid lines plot the posterior means of the response set bounds for the model with dogmatic bounds on the FEVD; the black dashed lines plot the 68% Bayesian credibility region of the response set for the model with dogmatic bounds on the FEVD. For panels (a')-(g'), the black solid lines plot the posterior means of the response set bounds for the model with nondogmatic bounds on the FEVD; the black dashed lines plot the 68% Bayesian credibility region of the response set for the model with nondogmatic bounds on the FEVD. The blue dashed line is the zero line. Monetary policy shock size is set to 15 basis points; vertical axis is measured in percentage, with the exception of panel (a) and (a'), where 0.10 is equivalent to 10 basis points.

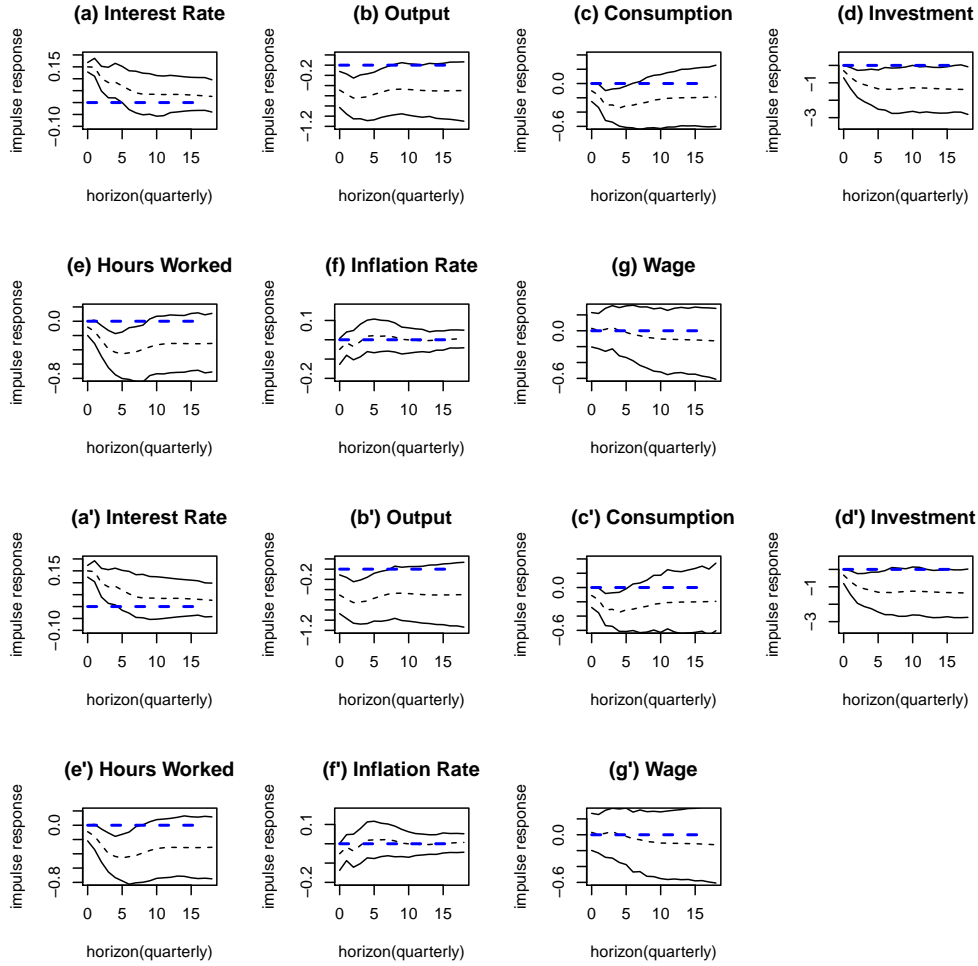


**Figure 4: Dogmatic and Nondogmatic Bounds on the FEVD: Impulse Responses, Uniform Prior Approach**

For panels (a)-(g), the black lines plot the 95% Bayesian credibility region (solid) and the posterior median (dashed) of the response under dogmatic bounds on the FEVD. For panels (a')-(g'), the black lines plot the 95% Bayesian credibility region (solid) and the posterior median (dashed) of the response under nondogmatic bounds on the FEVD. Monetary policy shock size is set to 15 basis points; vertical axis is measured in percentage, with the exception of panel (a) and (a'), where 0.10 is equivalent to 10 basis points.

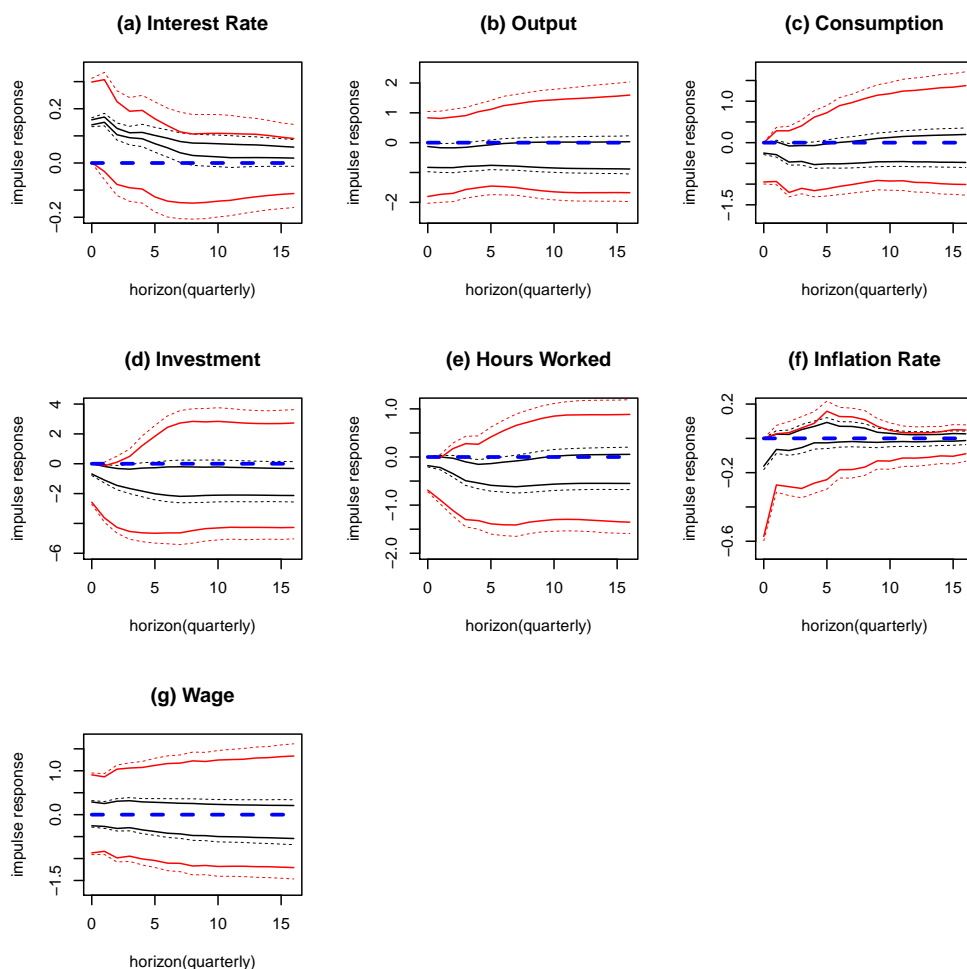


**Figure 5: Bounds on the FEVD vs Sign Restrictions: Impulse Responses Identified Set, Distribution-Free Approach**

In each panel, the black solid lines plot the posterior means of the response set bounds for the model with dogmatic bounds on the FEVD; the black dashed lines plot the 68% Bayesian credibility region of the response set for the model with dogmatic bounds on the FEVD; the red solid lines plot the posterior means of the response set bounds for the model with sign restrictions; the red dashed lines plot the 68% Bayesian credibility region of the response set for the model with sign restrictions. The blue dashed line is the zero line. Monetary policy shock size is set to 15 basis points; vertical axis is measured in percentage, with the exception of panel (a), where 0.10 is equivalent to 10 basis points.

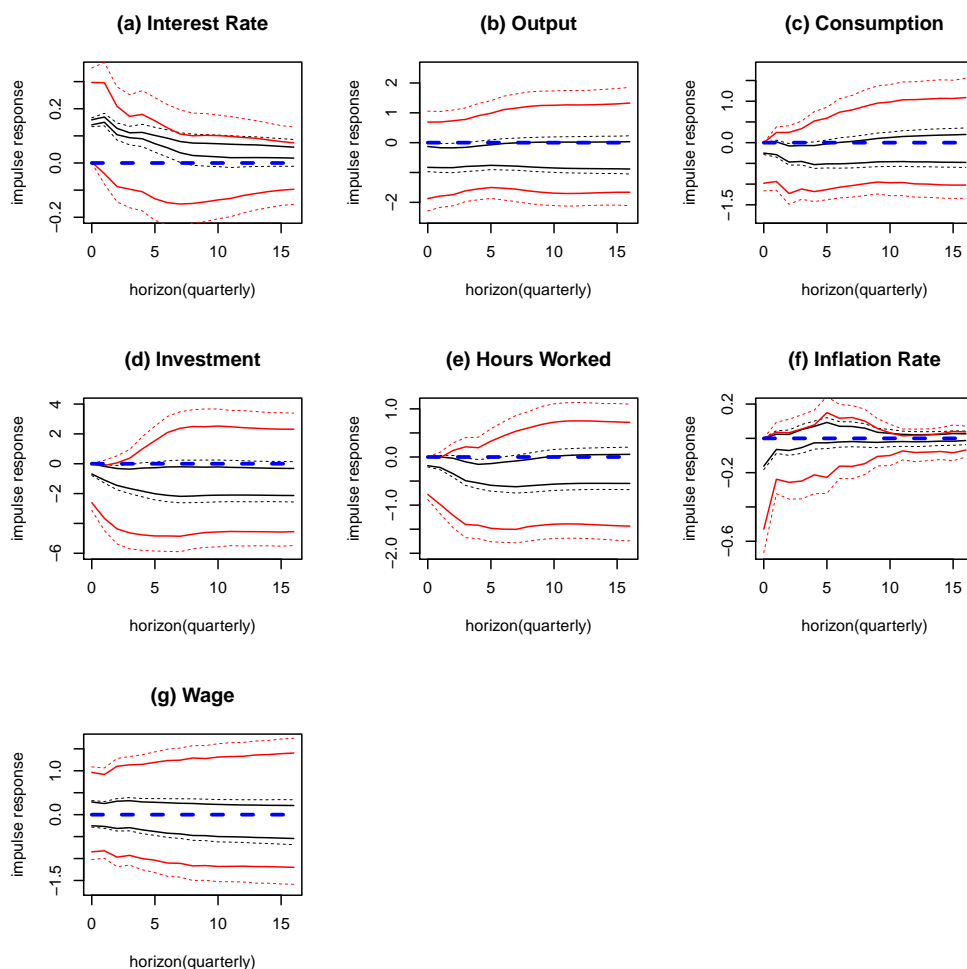


**Figure 6: Bounds on the FEVD vs Sign and Long-Run Restrictions: Impulse Responses Identified Set, Distribution-Free Approach**

In each panel, the black solid lines plot the posterior means of the response set bounds for the model with dogmatic bounds on the FEVD; the black dashed lines plot the 68% Bayesian credibility region of the response set for the model with dogmatic bounds on the FEVD; the red solid lines plot the posterior means of the response set bounds for the model with sign and long-run restrictions; the red dashed lines plot the 68% Bayesian credibility region of the response set for the model with sign and long-run restrictions. The blue dashed line is the zero line. Monetary policy shock size is set to 15 basis points; vertical axis is measured in percentage, with the exception of panel (a), where 0.10 is equivalent to 10 basis points.

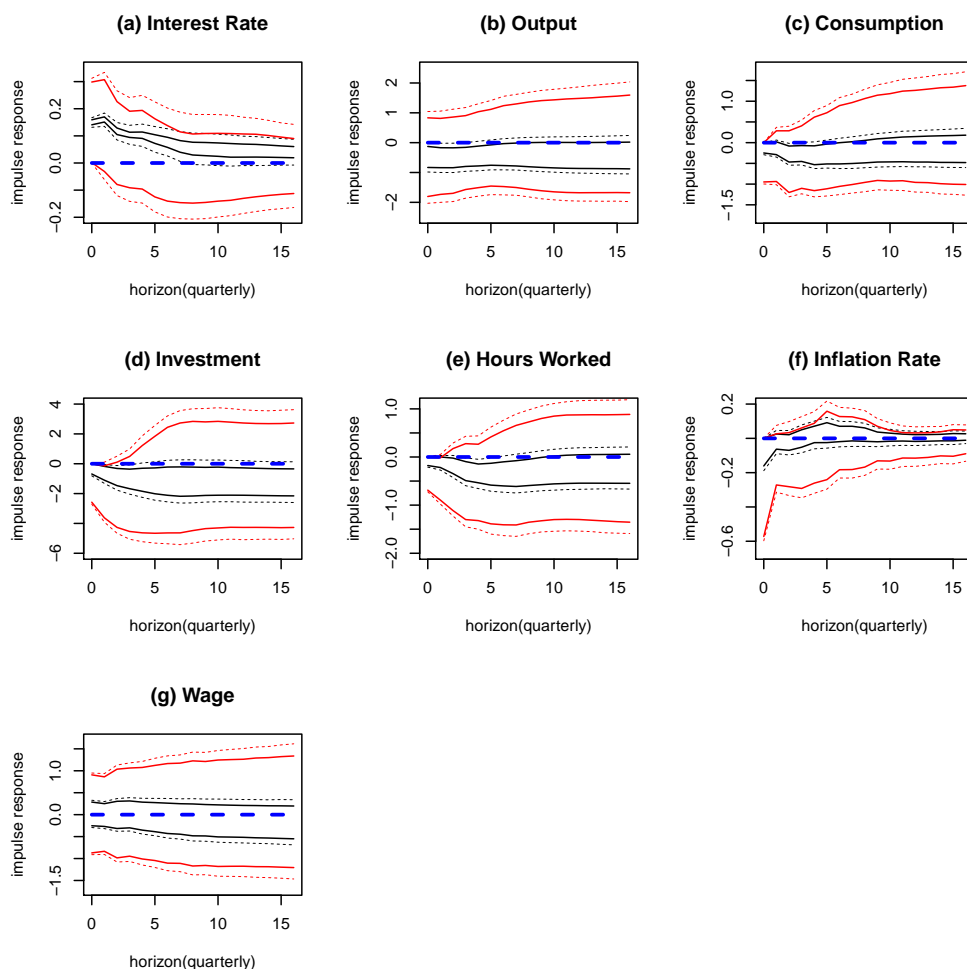


**Figure 7: NonDogmatic Bounds on the FEVD vs Sign Restrictions: Impulse Responses Identified Set, Distribution-Free Approach**

In each panel, the black solid lines plot the posterior means of the response set bounds for the model with nondogmatic bounds on the FEVD; the black dashed lines plot the 68% Bayesian credibility region of the response set for the model with nondogmatic bounds on the FEVD; the red solid lines plot the posterior means of the response set bounds for the model with sign restrictions; the red dashed lines plot the 68% Bayesian credibility region of the response set for the model with sign restrictions. The blue dashed line is the zero line. Monetary policy shock size is set to 15 basis points; vertical axis is measured in percentage, with the exception of panel (a), where 0.10 is equivalent to 10 basis points.

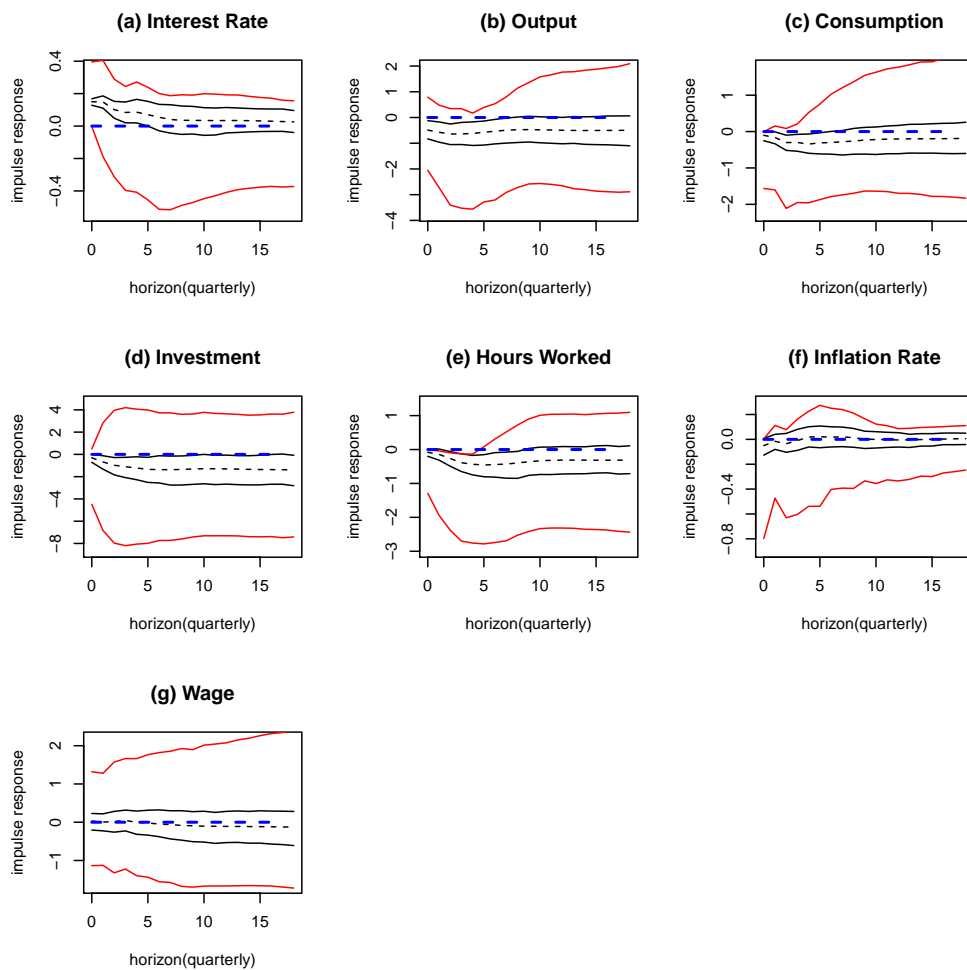


**Figure 8: Bounds on the FEVD vs Sign Restrictions: Impulse Responses, Uniform Prior Approach**

In each panel, the black lines plot the 95% Bayesian credibility region (solid) and the posterior median (dashed) of the response under dogmatic bounds on the FEVD; the red lines plot the 95% Bayesian credibility region of the response under sign restrictions. The blue dashed line is the zero line. Monetary policy shock size is set to 15 basis points; vertical axis is measured in percentage, with the exception of panel (a), where 0.10 is equivalent to 10 basis points.

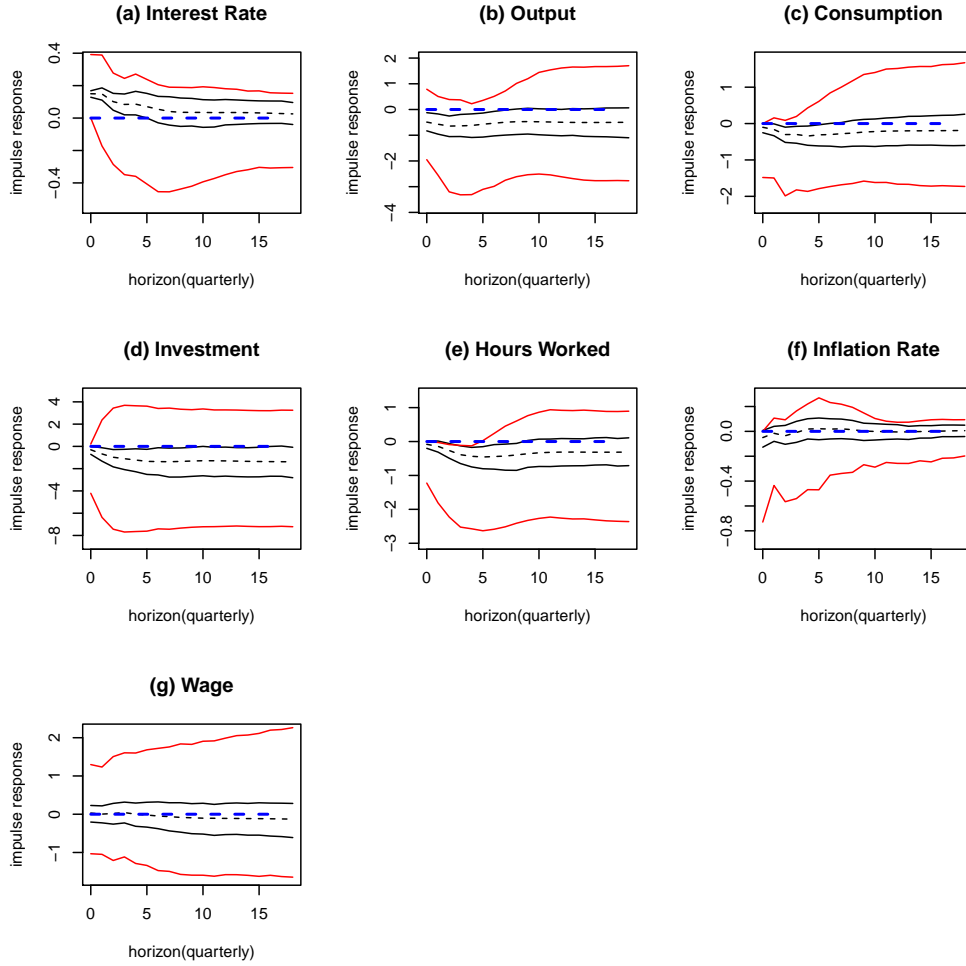


**Figure 9: Bounds on the FEVD vs Sign and Long-Run Restrictions: Impulse Responses, Uniform Prior Approach**

In each panel, the black lines plot the 95% Bayesian credibility region (solid) and the posterior median (dashed) of the response under dogmatic bounds on the FEVD; the red lines plot the 95% Bayesian credibility region of the response under sign and long-run restrictions. The blue dashed line is the zero line. Monetary policy shock size is set to 15 basis points; vertical axis is measured in percentage, with the exception of panel (a), where 0.10 is equivalent to 10 basis points.

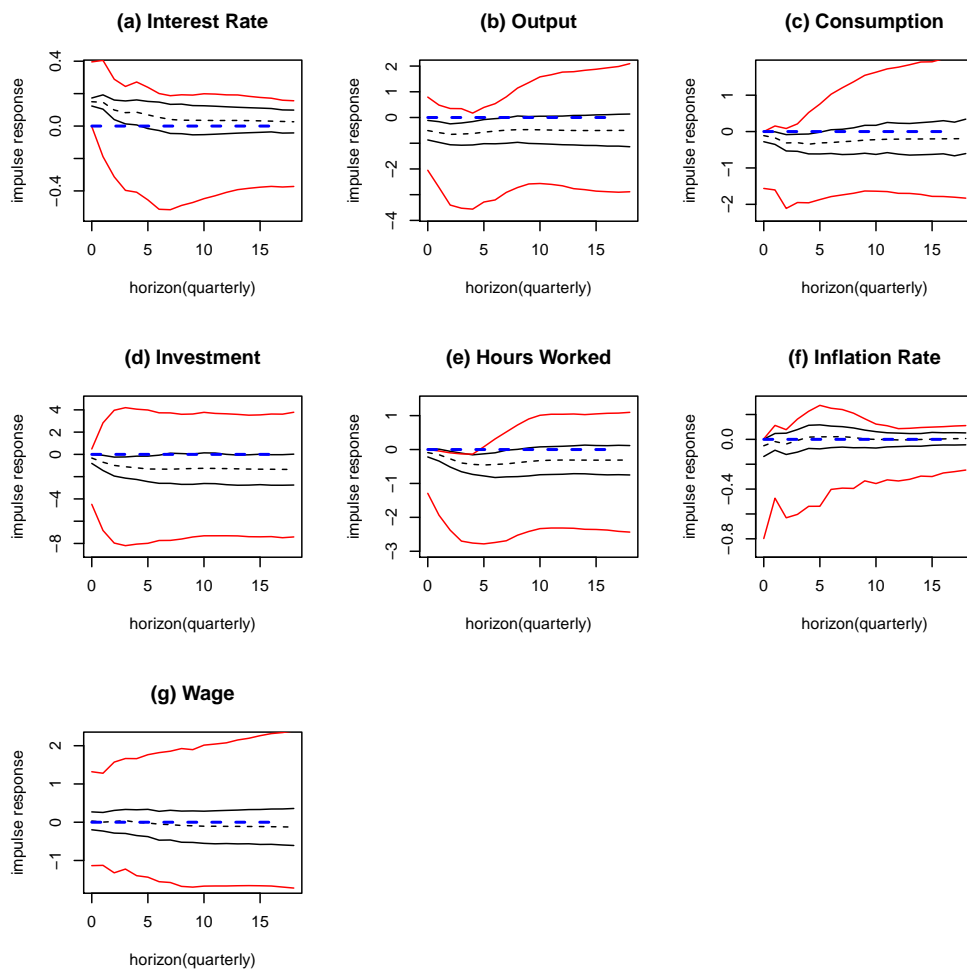


**Figure 10: NonDogmatic Bounds on the FEVD vs Sign Restrictions: Impulse Responses, Uniform Prior Approach**

In each panel, the black lines plot the 95% Bayesian credibility region (solid) and the posterior median (dashed) of the response under nondogmatic bounds on the FEVD; the red lines plot the 95% Bayesian credibility region of the response under sign restrictions. The blue dashed line is the zero line. Monetary policy shock size is set to 15 basis points; vertical axis is measured in percentage, with the exception of panel (a), where 0.10 is equivalent to 10 basis points.

## 6.2 Comparison with Alternative Methods

The previous results suggest that constraints on the FEVD lead to estimation and inference that are dramatically different from those with sign restrictions. This section makes a comparison with alternative schemes of shrinkage in set-identified frameworks. Specifically, the most recently used and increasingly common benchmarks in the field are restrictions on the structural components of monetary policy (Arias, Caldara, and Rubio-Ramirez, 2019), narrative inequality constraints (Antolín-Díaz and Rubio-Ramírez, 2018; Ludvigson, Ma, and Ng, 2018, 2019), and slope restrictions (Amir-Ahmadi and Drautzburg, 2018). On the other hand, in a small-scale SVAR, Baumeister and Hamilton (2018) incorporated information on both structural parameters and impact of shocks to exclude an expansionary effect of contractionary monetary shocks a-priori. Since dogmatic and nondogmatic bounds on the FEVD deliver very similar results, any comparison between the forementioned alternative methods of shrinkage and dogmatic bounds is common to nondogmatic bounds as well.

Amir-Ahmadi and Drautzburg (2018) ranked IRFs by magnitude. For the identification of monetary policy shocks, they enriched sign restrictions by assuming that nominal rates decline for two quarters after the initial shocks (slope restrictions). However, panel (b) in Figure 11 and 12 suggests that this strategy does not help much and does not sharpen the identification induced by sign restrictions.

Antolín-Díaz and Rubio-Ramírez (2018) used standard sign restrictions on IRFs and constraints on the HD and structural shocks around key historical events (narrative sign restrictions).<sup>19</sup> In addition to the sign restrictions, the model is restricted as follows: for the specific observation corresponding to the last quarter in 1979, the absolute value of the contribution of monetary policy shock to the federal funds rate is larger than the sum of the absolute value of the contributions of all other structural shocks; for the same period, the monetary policy shock must be of positive value. However, panel (b) in Figure 13, which uses a specific scale to exemplify the comparison, shows that there is still significant probability that the output can increase upon impact and in the short-run. On the other hand, bounds on the FEVD deliver different results and put evidence in favor of a significant and negative effect of contractionary monetary shocks on the real activity. The same applies to the comparison across the other variables.<sup>20</sup>

Finally, Arias, Caldara, and Rubio-Ramirez (2019) achieved set-identification of monetary policy shocks by restricting the systematic components of monetary policy, while impulse re-

---

<sup>19</sup>Ludvigson, Ma, and Ng (2018) and Ludvigson, Ma, and Ng (2019) used a similar approach to identify uncertainty and oil shocks.

<sup>20</sup>Estimation and inference procedure in Antolín-Díaz and Rubio-Ramírez (2018) is expressly constructed for imposing a uniform distribution on the rotation matrix, that is the case shown in Figure 13.

sponses were left unconstrained. The roots of this approach date back to Leeper, Sims, and Zha (1996), Leeper and Zha (2003), and Sims and Zha (2006), who argued that monetary policy choices do not evolve independently of economic conditions, and also Taylor (1993), who associated monetary policy changes with output and inflation. Let  $\gamma_y, \gamma_c, \gamma_I, \gamma_w, \gamma_l, \gamma_\pi$  denote the contemporaneous reaction of nominal rates to output, consumption, investment, real wages, hours worked and the inflation rate, respectively. Constraints on the seven-variable model are the following:  $\gamma_y > 0, \gamma_\pi > 0, \gamma_l > 0$  and  $\gamma_c = \gamma_I = \gamma_w = 0$ . This strategy provides mixed results; on the one hand, according to Figure 14 and 15, it supports the view that monetary shocks affect the real output in the short-run, but the estimation precision is lower than that induced by the bounds on the FEVD. On the other hand, as opposed to the bounds on the FEVD, the effect on interest rate, consumption, investment, and inflation rate is largely uninformative, regardless of the approach in relation to the rotation matrix. Note the different scale in Figure 14 and 15.

Overall, dogmatic and nondogmatic bounds on the FEVD reduce the identification uncertainty, increase the estimation precision and tend to remove unlikely implications of set-identification more than the current benchmarks in the literature.

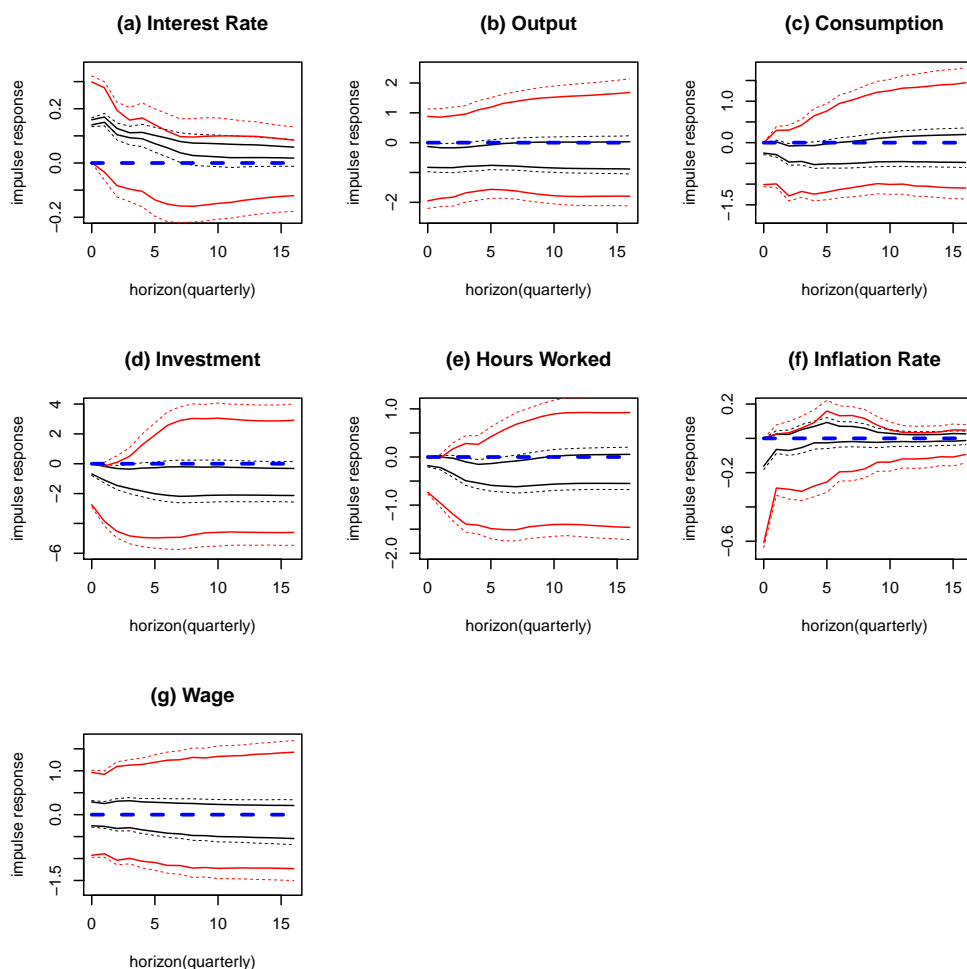


**Figure 11: Bounds on the FEVD vs Slope Restrictions: Impulse Responses Identified Set, Distribution-Free Approach**

In each panel, the black solid lines plot the posterior means of the response set bounds for the model with dogmatic bounds on the FEVD; the black dashed lines plot the 68% Bayesian credibility region of the response set for the model with dogmatic bounds on the FEVD; the red solid lines plot the posterior means of the response set bounds for the model with slope restrictions; the red dashed lines plot the 68% Bayesian credibility region of the response set for the model with slope restrictions. The blue dashed line is the zero line. Monetary policy shock size is set to 15 basis points; vertical axis is measured in percentage, with the exception of panel (a), where 0.10 is equivalent to 10 basis points.

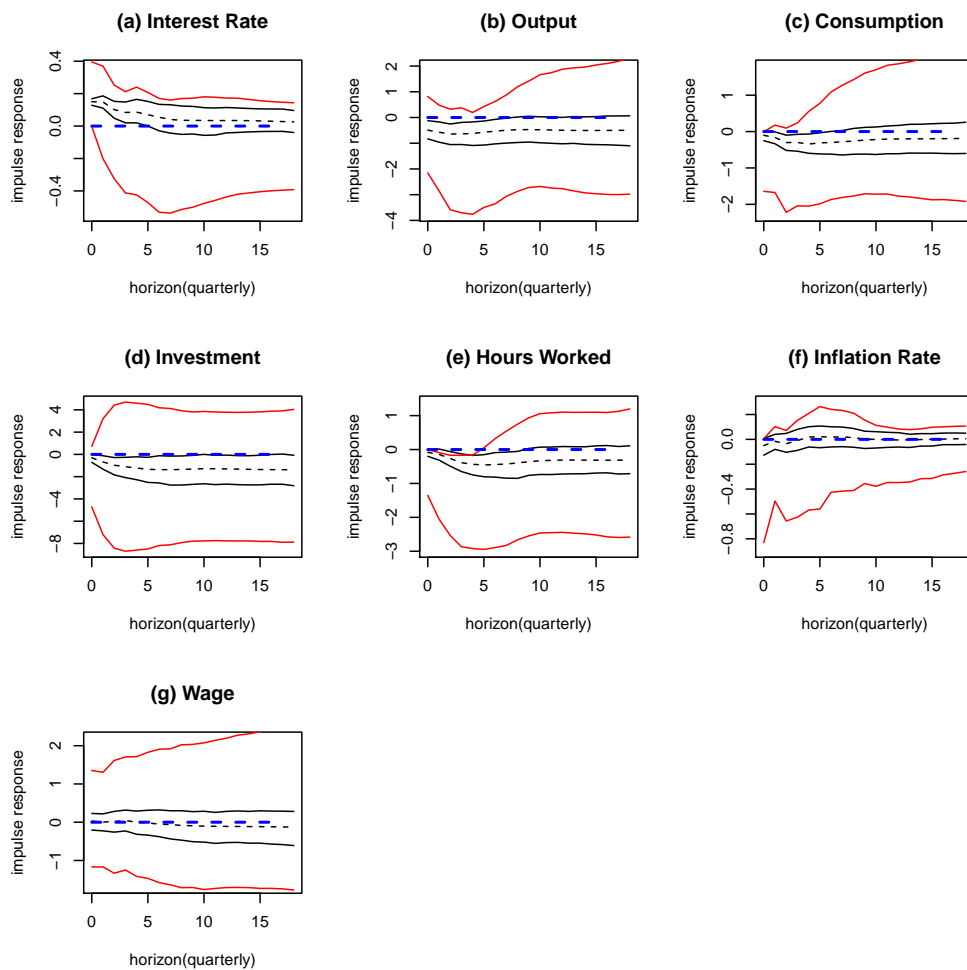


**Figure 12: Bounds on the FEVD vs Slope Restrictions: Impulse Responses, Uniform Prior Approach**

In each panel, the black lines plot the 95% Bayesian credibility region (solid) and the posterior median (dashed) of the response under dogmatic bounds on the FEVD; the red lines plot the 95% Bayesian credibility region of the response under slope restrictions. The blue dashed line is the zero line. Monetary policy shock size is set to 15 basis points; vertical axis is measured in percentage, with the exception of panel (a), where 0.10 is equivalent to 10 basis points.

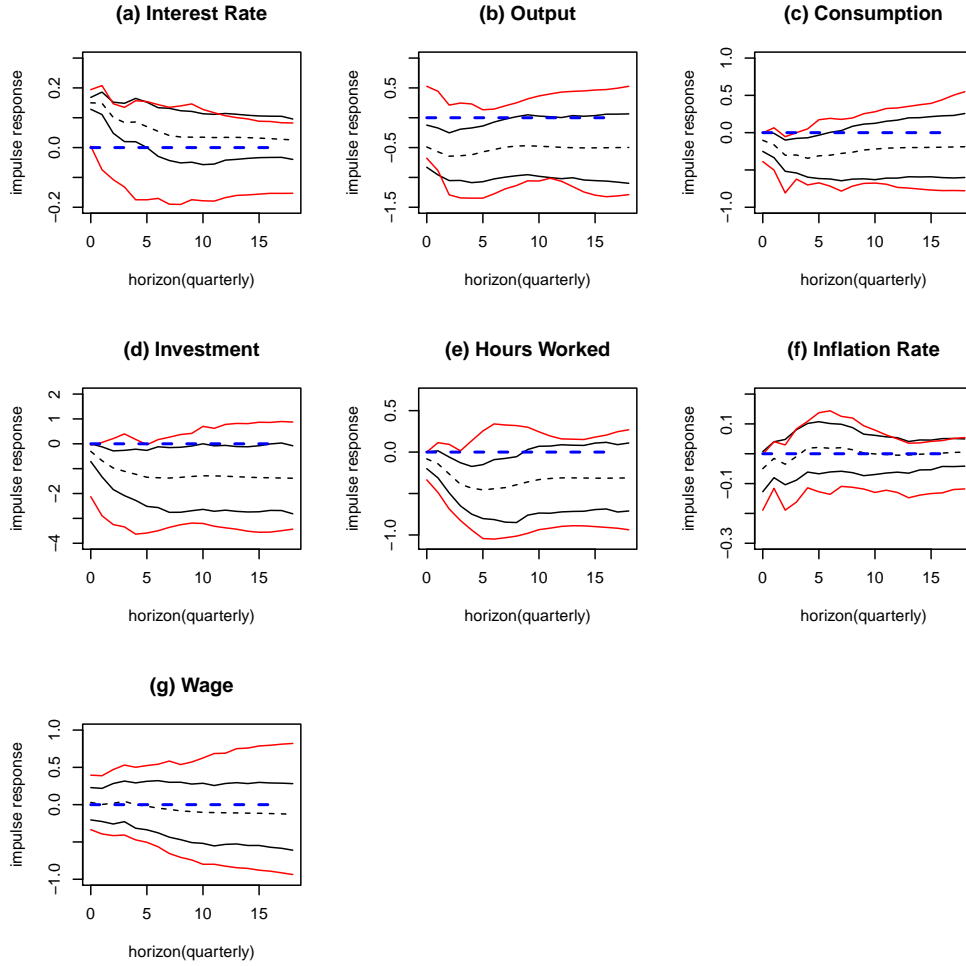


**Figure 13: Bounds on the FEVD vs Narrative Sign Restrictions: Impulse Responses, Uniform Prior Approach**

In each panel, the black lines plot the 95% Bayesian credibility region (solid) and the posterior median (dashed) of the response under dogmatic bounds on the FEVD; the red lines plot the 95% Bayesian credibility region of the response under narrative sign restrictions. The blue dashed line is the zero line. Monetary policy shock size is set to 15 basis points; vertical axis is measured in percentage, with the exception of panel (a), where 0.10 is equivalent to 10 basis points.

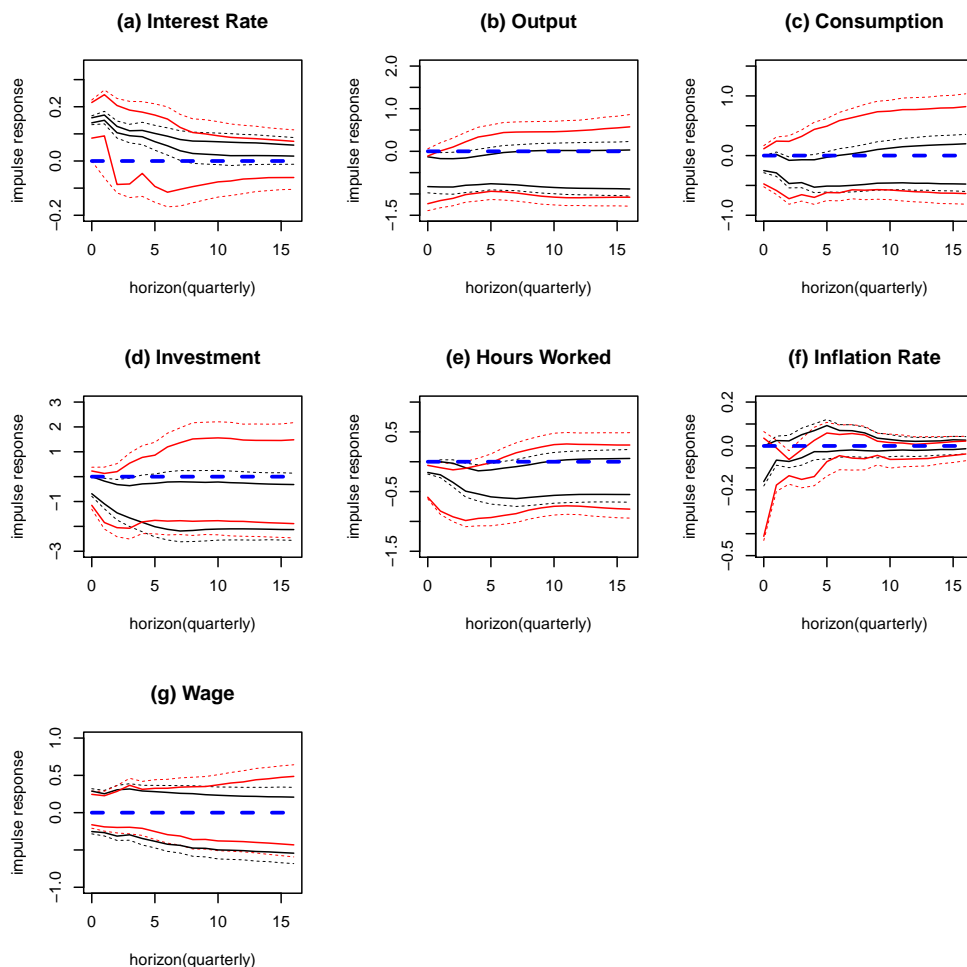


**Figure 14: Bounds on the FEVD vs Restrictions on the Monetary Policy Equation: Impulse Responses Identified Set, Distribution-Free Approach**

In each panel, the black solid lines plot the posterior means of the response set bounds for the model with dogmatic bounds on the FEVD; the black dashed lines plot the 68% Bayesian credibility region of the response set for the model with dogmatic bounds on the FEVD; the red solid lines plot the posterior means of the response set bounds for the model with restrictions on the monetary policy equation; the red dashed lines plot the 68% Bayesian credibility region of the response set for the model with restrictions on the monetary policy equation. The blue dashed line is the zero line. Monetary policy shock size is set to 15 basis points; vertical axis is measured in percentage, with the exception of panel (a), where 0.10 is equivalent to 10 basis points.

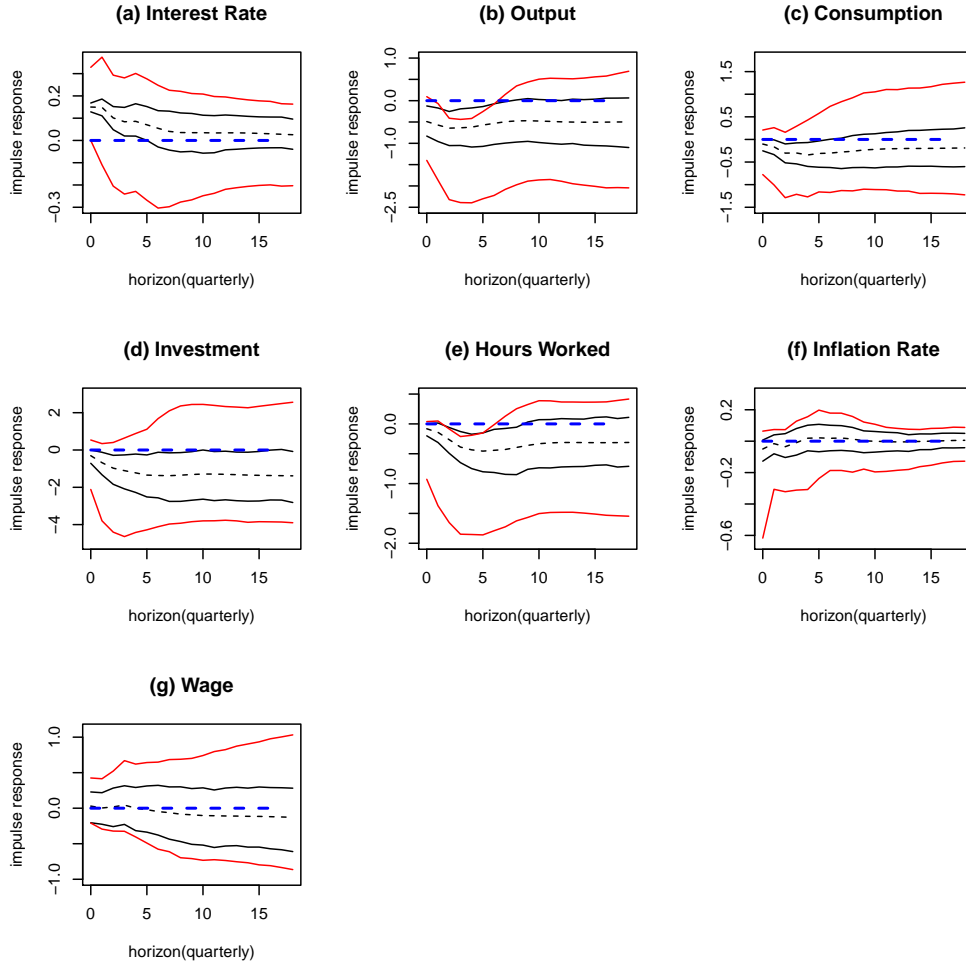


**Figure 15: Bounds on the FEVD vs Restrictions on the Monetary Policy Equation: Impulse Responses, Uniform Prior Approach**

In each panel, the black lines plot the 95% Bayesian credibility region (solid) and the posterior median (dashed) of the response under dogmatic bounds on the FEVD; the red lines plot the 95% Bayesian credibility region of the response under restrictions on the monetary policy equation. The blue dashed line is the zero line. Monetary policy shock size is set to 15 basis points; vertical axis is measured in percentage, with the exception of panel (a), where 0.10 is equivalent to 10 basis points.

### 6.3 Investigating the Mechanism

Section 6.1 and 6.2 show that few dogmatic or nondogmatic bounds on the FEVD dramatically affect estimation and inference without constraining key variables of interest. This section fully documents how, and to what extent, the mechanism works. In order to look into the machinery further, I have studied the unbounded FEVD of the sign-restricted SVAR in the data. Upon impact,  $0.00 \leq CFEV_i^i(0) \leq 0.75$ ,  $0.00 \leq CFEV_i^y(0) \leq 0.70$ ,  $0.00 \leq CFEV_i^c(0) \leq 0.67$ ,  $0.00 \leq CFEV_i^I(0) \leq 0.70$ ,  $0.00 \leq CFEV_i^l(0) \leq 0.72$ ,  $0.00 \leq CFEV_i^\pi(0) \leq 0.64$ , and  $0.00 \leq CFEV_i^w(0) \leq 0.62$  with a 99 per cent probability if only sign restrictions apply; the comparison with theory-driven bounds on the FEVD of  $i$  and  $\pi$  in Table 1 shows that the restrictions on the FEVD trim the structural parameters with a low contribution of the shock to the interest rate fluctuations and a high contribution to the variance of the inflation rate. Such a trimming alters the estimation and inference originally induced by sign restrictions.

The results above have highlighted that bounding the FEVD of nominal variables is highly informative. It seems reasonable to verify whether imposing bounds on the FEVD of additional variables affects the results reported above. This section therefore considers the following set of restrictions:

- *Augmented Bounds on the FEVD*

In addition to the sign restrictions, the FEVD is bounded as in Table 1:  $0.30 \leq CFEV_i^i(0) \leq 0.77$ ,  $0.00 \leq CFEV_i^c(0) \leq 0.20$ ,  $0.00 \leq CFEV_i^I(0) \leq 0.19$ ,  $0.00 \leq CFEV_i^l(0) \leq 0.12$ ,  $0.00 \leq CFEV_i^\pi(0) \leq 0.38$ , and  $0.00 \leq CFEV_i^w(0) \leq 0.10$ . The FEVD of real output is left unbounded.<sup>21</sup>

Figures 16 and 17 in Appendix show the results using augmented bounds on the FEVD are very similar to those employing only dogmatic or nondogmatic bounds on the FEVD of inflation and interest rate, despite with narrower sets because of added information. Furthermore, it is possible to obtain equally similar outcomes by just restricting the FEVD of consumption, investment, hours worked, and wages on their own.<sup>22</sup> Thus, restricting the bounds of the FEVD of  $i$  and  $\pi$  is sufficient to obtain the estimation and inference shown in Section 6.1 and 6.2, but it is not necessary. As a result, for the current application, the informativeness of bounds on the FEVD does not necessarily depend on constraining nominal variables because bounds on the FEVD of real variables are informative on their own.

Finally, the results are robust to the following checks: lag length three, four, six and seven; selecting the reduced-form prior tightness by maximising the marginal likelihood rather than

---

<sup>21</sup>The optimization problem in Algorithm 3.2 induced by this model is convex.

<sup>22</sup>In this scenario, condition (a) in Proposition 3.3 is satisfied and the optimization problem in Algorithm 3.2 is convex.

employing a flat specification; updating the dataset used by Smets and Wouters (2007); entering the endogenous variables in level; constructing non-cumulative impulse responses. Although some literature argued that set-identifying restrictions should be imposed in the short-run only (Canova and Paustian, 2011; Fry and Pagan, 2011),<sup>23</sup> as further check this paper also derives and imposes constraints up to 4 quarters after the shock. The results are very similar to what has been already shown.

## 6.4 Sensitivity Analysis

A sensitivity analysis in the form of perturbation about the dogmatic bounds on the FEVD is introduced with respect to the baseline scenario, where the error variance of inflation and interest rate is bounded as in Table 1; this exercise can be considered as a step in between dogmatic and nondogmatic bounds. In particular, the upper bound on the FEVD of the inflation rate to monetary shock is increased and set to 0.48; the lower bound on the FEVD of the interest rate is decreased to 0.20. As long as the monetary disturbance explains a non-negligible share of the interest rate unexpected fluctuations upon impact and its contribution to the error variance of inflation rate is somehow bounded from above, Figure 18 and 19 in Appendix show that perturbing the bounds does not affect the results. This confirms the main result provided by nondogmatic bounds, namely the findings do not strictly depend on specific values given to the restrictions; results are therefore very robust to reasonable changes to the bounds on the FEVD. The same applies if the bounds of the real variables in Section 6.3 are perturbed.

## 6.5 Misspecification

Step 1 and 2 in Section 4.1 derive dogmatic bounds on the FEVD robust to a variety of parametrizations; however, theory offers no uncontroversial guideline on the number and typology of variables to be included. Although this issue has been mitigated by Step 3, in which only bounds consistent with alternative models are used as identifying constraints, this section introduces misspecification between the estimated model and the framework where dogmatic theory-driven restrictions come from, i.e., the framework illustrated in Section 4.1.1. Specifically, I estimate the model without investment and real wages; in the sign-restricted model, a contractionary monetary policy shock reduces inflation, consumption, and hours worked, and increases interest rates. The framework with constraints on the FEVD restricts the nominal variables as in Table 1:  $0.30 \leq CFEV_i^i(0) \leq 0.77$  and  $CFEV_i^\pi(0) \leq 0.38$ . In other words,

---

<sup>23</sup>On the other hand, Inoue and Kilian (2013) have argued that medium-run sign restrictions can help identification. See Chapter 13 in Kilian and Lütkepohl (2017) for a survey.

restrictions are derived from a theoretical framework that is misspecified with respect to the estimated model. Figure 20 and 21 in Appendix display the results and confirm that sign restrictions are largely uninformative, as opposed to the bounds on the FEVD. Thus, the identification ability of the bounds seems to be robust to misspecification. Similar results are obtained by introducing monetary aggregates, such as borrowed and nonborrowed reserves in Uhlig (2005), and indices of financial conditions, such as the S&P index, in the estimated model.

## 7 Conclusion

Sign-restricted SVARs, which relax exclusion restrictions and rely on weaker assumptions on the sign of impulse responses, are becoming increasingly common. However this minimalist, or agnostic, approach comes at a cost. Sign restrictions usually deliver a set of structural parameters that have very different implications for IRFs, elasticities, HD and FEVD. On the one hand, obtaining precise estimation, informative inference and meaningful economic results is challenging, and on the other some of the admissible structural models may contain implausible implications.

This paper introduced dogmatic and nondogmatic bounds on the FEVD to sharpen identification, increase the estimation precision, reduce the set of admissible structural parameters and remove implausible implications of sign-restricted models. Firstly, in a bivariate and trivariate setting, I analytically proved that bounds on the FEVD deliver a strictly smaller set relative to sign restrictions. Interestingly, this also applies to variables that are not subject to restrictions. For higher dimensional SVARs, I established the necessary conditions in which the placing of bounds on the FEVD leads to a reduced identified set. Secondly, the paper also addressed the trade-off between sharp identification and computation, and established sufficient conditions to determine whether the identified set had a positive measure; an algorithm provided a computationally-fast practical check of the conditions. While recent studies (Giacomini and Kitagawa, 2018; Amir-Ahmadi and Drautzburg, 2018; Gafarov, Meier, and Olea, 2018) established the conditions for non-emptiness under zero and sign restrictions, this paper has advanced the relevant literature by investigating non-emptiness in the context of bounds on the FEVD.

In order to address the criticism by Baumeister and Hamilton (2015) over the role of prior for  $\mathbf{Q}$ , under a convexity criterion this paper presented a robust-prior procedure through a numerical optimizer, where the identified set, which was constrained by bounds on the FEVD, was distribution-free and did not depend on a specific prior over the rotation matrix. This is in line with the proposals made by Giacomini and Kitagawa (2018), Gafarov, Meier, and Olea

(2018), and Amir-Ahmadi and Drautzburg (2018) for sign and zero restrictions only.

I developed a procedure to derive dogmatic and nondogmatic bounds on the FEVD, which were consistent with the implications of a variety of popular DSGE models embodying different nominal, real, and financial frictions and competing parametrizations. While the dogmatic approach is the benchmark in the literature and treats the identifying restrictions as if known with certainty, the nondogmatic method introduced uncertainty about the bounds on the FEVD and made sure the identification did not strictly depend on a specific value given to the constraints on the FEVD. Results are therefore robust to doubts about the particular values given to the bounds.

A Monte-Carlo exercise documented the effectiveness of those dogmatic and nondogmatic bounds in recovering and identifying the data-generating process relative to sign restrictions.

While the latter typically suggest that contractionary monetary policy shocks have no effects on real variables and are even likely to increase real activity, an empirical application showed that a few dogmatic or nondogmatic bounds on the FEVD tend to be highly informative, increase the estimation precision, remove unreasonable effects of monetary shocks on real variables, and sharpen the inference of sign-restricted models. As shown by nondogmatic bounds and sensitivity analysis, estimation and inference are extremely robust to reasonable changes to the bounds on the FEVD. The approach in this paper was also more effective than alternative strategies of set-reduction, including long-run equality restrictions on the FEVD, constraints on the monetary policy equation (Arias, Caldara, and Rubio-Ramirez, 2019), narrative sign restrictions (Antolín-Díaz and Rubio-Ramírez, 2018), and the ranking of IRFs (Amir-Ahmadi and Drautzburg, 2018). The results are very robust to misspecification.

## References

- AMIR-AHMADI, P., AND T. DRAUTZBURG (2018): “Identification through Heterogeneity,” *FEB of Philadelphia Working Paper*.
- ANTOLÍN-DÍAZ, J., AND J. F. RUBIO-RAMÍREZ (2018): “Narrative Sign Restrictions for SVARs,” *American Economic Review*, 108(10), 2802–2829.
- ARIAS, J. E., D. CALDARA, AND J. F. RUBIO-RAMÍREZ (2019): “The Systematic Component of Monetary Policy in SVARs: An Agnostic Identification Procedure,” *Journal of Monetary Economics*, 101, 1–13.
- ARIAS, J. E., J. F. RUBIO-RAMÍREZ, AND D. WAGGONER (2018): “Inference Based on SVARs Identified with Sign and Zero Restrictions: Theory and Applications,” *Econometrica*, 86(2), 685–720.
- BAUMEISTER, C., AND J. D. HAMILTON (2015): “Sign Restrictions, Structural Vector Autoregressions, and Useful Prior Information,” *Econometrica*, 83(5), 1963–1999.
- (2018): “Inference in Structural Vector Autoregressions when the Identifying Assumptions Are Not Fully Believed: Re-evaluating the Role of Monetary Policy in Economic Fluctuations,” *Journal of Monetary Economics*, 100, 48–65.
- (2019): “Structural Interpretation of Vector Autoregressions with Incomplete Identification: Revisiting the Role of Oil Supply and Demand Shocks,” *American Economic Review*, 109(5), 1873–1910.
- BERNANKE, B. S., AND I. MIHOV (1998): “Measuring Monetary Policy,” *The Quarterly Journal of Economics*, 113(3), 869–902.
- BLANCHARD, O. J., AND D. QUAH (1989): “The Dynamic Effects of Aggregate Demand and Supply Disturbances,” *American Economic Review*, 79(4), 655–673.
- CANOVA, F., AND G. D. NICOLO (2002): “Monetary Disturbances Matter for Business Fluctuations in the G-7,” *Journal of Monetary Economics*, 49(6), 1121–1159.
- CANOVA, F., AND M. PAUSTIAN (2011): “Business Cycle Measurement with Some Theory,” *Journal of Monetary Economics*, 58(4), 345–361.
- CARRIERO, A., T. E. CLARK, AND M. MARCELLINO (2018): “Endogenous Uncertainty,” *Federal Reserve Bank of Cleveland Working Paper*.

- CHRISTIANO, L. J., M. EICHENBAUM, AND C. L. EVANS (1999): “Monetary Policy Shock: What Have We Learned and to What End?,” in *Handbook of Macroeconomics*, ed. by J. B. Taylor, and M. Woodford. Elsevier.
- CHRISTIANO, L. J., R. MOTTO, AND M. ROSTAGNO (2014): “Risk Shocks,” *American Economic Review*, 104(1), 27–65.
- CURDIA, V., AND M. WOODFORD (2010): “Credit Spreads and Monetary Policy,” *Journal of Money, Credit and Banking*, 42, 3–35.
- DEDOLA, L., AND S. NERI (2007): “What Does a Technology Shock Do? A VAR Analysis with Model-Based Sign Restrictions,” *Journal of Monetary Economics*, 54(2), 512–549.
- DEDOLA, L., G. RIVOLTA, AND L. STRACCA (2017): “If the Fed Sneezes, Who Catches a Cold?,” *Journal of International Economics*, 108(Supplement 1), S23–S41.
- DEL NEGRO, M., AND F. SCHORFHEIDE (2004): “Priors from General Equilibrium Models for VARs,” *International Economic Review*, 45(2), 643–673.
- DI TRAGLIA, F., AND C. GARCÍA-JIMENO (2016): “A Framework for Eliciting, Incorporating, and Disciplining Identification Beliefs in Linear Models,” *NBER Working Paper*.
- FAUST, J. (1998): “The Robustness of Identified VAR Conclusions about Money,” *Carnegie-Rochester Conference Series on Public Policy*, 48, 207–244.
- FRY, R., AND A. PAGAN (2011): “Sign Restrictions in Structural Vector Autoregressions: A Critical Review,” *Journal of Economic Literature*, 49(4), 938–960.
- FUJITA, S. (2011): “Dynamics of Worker Flows and Vacancies: Evidence from the Sign Restriction Approach,” *Journal of Applied Econometrics*, 26(1), 89–121.
- GAFAROV, B., M. MEIER, AND J. L. M. OLEA (2018): “Delta-Method Inference for a Class of Set-Identified SVARs,” *Journal of Econometrics*, 203(2), 316–327.
- GERTLER, M., AND P. KARADI (2011): “A Model of Unconventional Monetary Policy,” *Journal of Monetary Economics*, 58(1), 17–34.
- GIACOMINI, R., AND T. KITAGAWA (2018): “Robust Inference about Partially-Identified SVARs,” *Cemmap Working Paper*.
- GIACOMINI, R., T. KITAGAWA, AND A. VOLPICELLA (2017): “Uncertain Identification,” *Cemmap Working Paper*.

- INOUE, A., AND L. KILIAN (2013): “Inference on Impulse Response Functions in Structural VAR Models,” *Journal of Econometrics*, 177(1), 1–13.
- JURADO, K., S. C. LUDVIGSON, AND S. NG (2015): “Measuring Uncertainty,” *American Economic Review*, 105(3), 1177–1216.
- JUSTINIANO, A., G. E. PRIMICERI, AND A. TAMBALOTTI (2011): “Investment Shocks and the Relative Price of Investment,” *Review of Economic Dynamics*, 14(1), 102–121.
- KILIAN, L., AND H. LÜTKEPOHL (2017): *Structural Vector Autoregressive Analysis*. Cambridge University Press.
- KILIAN, L., AND D. MURPHY (2012): “Why Agnostic Sign Restrictions Are Not Enough: Understanding the Dynamics of Oil Market VAR Models,” *Journal of the European Economic Association*, 10(5), 1166–1188.
- LEEPER, E., C. SIMS, AND T. ZHA (1996): “What Does Monetary Policy Do?,” *Brookings Papers on Economic Activity*, 2, 1–78.
- LEEPER, E. M., AND T. ZHA (2003): “Modest Policy Interventions,” *Journal of Monetary Economics*, 50(8), 1673–1700.
- LIPPI, F., AND A. NOBILI (2012): “Oil and the Macroeconomy: A Quantitative Structural Analysis,” *Journal of the European Economic Association*, 10(5), 1059–1083.
- LOVCHA, Y., AND À. PÉREZ LABORDA (2016): “The Variance-Frequency Decomposition as an Instrument for VAR Identification: An Application to Technology Shocks,” *CREIP Working Paper*.
- LUDVIGSON, S. C., S. MA, AND S. NG (2018): “Shock Restricted Structural Vector-Autoregressions,” *NBER Working Paper*.
- (2019): “Uncertainty and Business Cycles: Exogenous Impulse or Endogenous Response?,” *NBER Working Paper*.
- MOUNTFORD, A. (2005): “Leaning Into the Wind: A Structural VAR Investigation of UK Monetary Policy,” *Oxford Bulletin of Economics and Statistics*, 67(5), 597–621.
- PAPPA, E. (2009): “The Effects of Fiscal Shocks on Employment and the Real Wage,” *International Economic Review*, 50(1), 217–244.

- PAUSTIAN, M. (2007): “Assessing Sign Restrictions,” *The BE Journal of Macroeconomics*, 7(1), Article 23.
- PEERSMAN, G., AND R. STRAUB (2009): “Technology Shocks and Robust Sign Restrictions in a Euro Area SVAR,” *International Economic Review*, 50(3), 727–750.
- RAFIQ, S., AND S. MALLICK (2008): “The Effect of Monetary Policy on Output in EMU3: A Sign Restriction Approach,” *Journal of Macroeconomics*, 30(4), 1756–1791.
- ROTHENBERG, T. J. (1971): “Identification in parametric models,” *Econometrica*, 39(3), 577–591.
- RUBIO-RAMIREZ, J., D. WAGGONER, AND T. ZHA (2010): “Structural Vector Autoregressions: Theory of Identification and Algorithm for Inference,” *The Review of Economic Studies*, 77(2), 665–696.
- SCHOLL, A., AND H. UHLIG (2008): “New Evidence on the Puzzles: Results from Agnostic Identification on Monetary Policy and Exchange Rates,” *Journal of International Economics*, 76(1), 1–13.
- SCHORFHEIDE, F. (2017): “Macroeconometrics - A Discussion,” in *Advances in Economics and Econometrics*, ed. by M. B. Honore, A. Pakes, and L. Samuelson, vol. 2, pp. 128–142. Cambridge University Press.
- SIMS, C. (1980): “Macroeconomics and Reality,” *Econometrica*, 48(1), 1–48.
- SIMS, C., AND T. ZHA (2006): “Does Monetary Policy Generate Recessions?,” *Macroeconomic Dynamics*, 10, 231–272.
- SIMS, C. A. (1998): “Comment on Glenn Rudebusch’s” Do Measures of Monetary Policy in a VAR Make Sense?,” *International Economic Review*, 39(4), 933–941.
- SMETS, F., AND R. WOUTERS (2005): “Comparing Shocks and Frictions in US and Euro Area Business cycles: A Bayesian DSGE Approach,” *Journal of Applied Econometrics*, 20(2), 161–183.
- SMETS, F., AND R. WOUTERS (2007): “Shocks and Frictions in US Business Cycles: A Bayesian DSGE Approach,” *American Economic Review*, 97(3), 586–606.
- SUTHERLAND, W. A. (2009): *Introduction to Metric and Topological Spaces*. Oxford University Press, second edn.

- TAYLOR, J. B. (1993): “Discretion versus Policy Rules in Practice,” in *Carnegie-Rochester Conference Series on Public Policy*, vol. 39, pp. 195–214. Elsevier.
- UHLIG, H. (2004a): “Do Technology Shocks Lead to a Fall in Total Hours Worked?,” *Journal of the European Economic Association*, 2(2-3), 361–371.
- (2004b): “What Moves GNP?,” in *Econometric Society 2004 North American Winter Meetings*, no. 636. Econometric Society.
- UHLIG, H. (2005): “What are the Effects of Monetary Policy on Output? Results from an Agnostic Identification Procedure,” *Journal of Monetary Economics*, 52(2), 381–419.
- UHLIG, H. (2017): “Shocks, Sign Restrictions, and Identification,” in *Advances in Economics and Econometrics*, ed. by M. B. Honore, A. Pakes, and L. Samuelson, vol. 2, pp. 95–127. Cambridge University Press.
- VARGAS-SILVA, C. (2008): “Monetary Policy and the US Housing Market: a VAR Analysis Imposing Sign Restrictions,” *Journal of Macroeconomics*, 30(3), 977–990.

# Appendices

## A Appendix

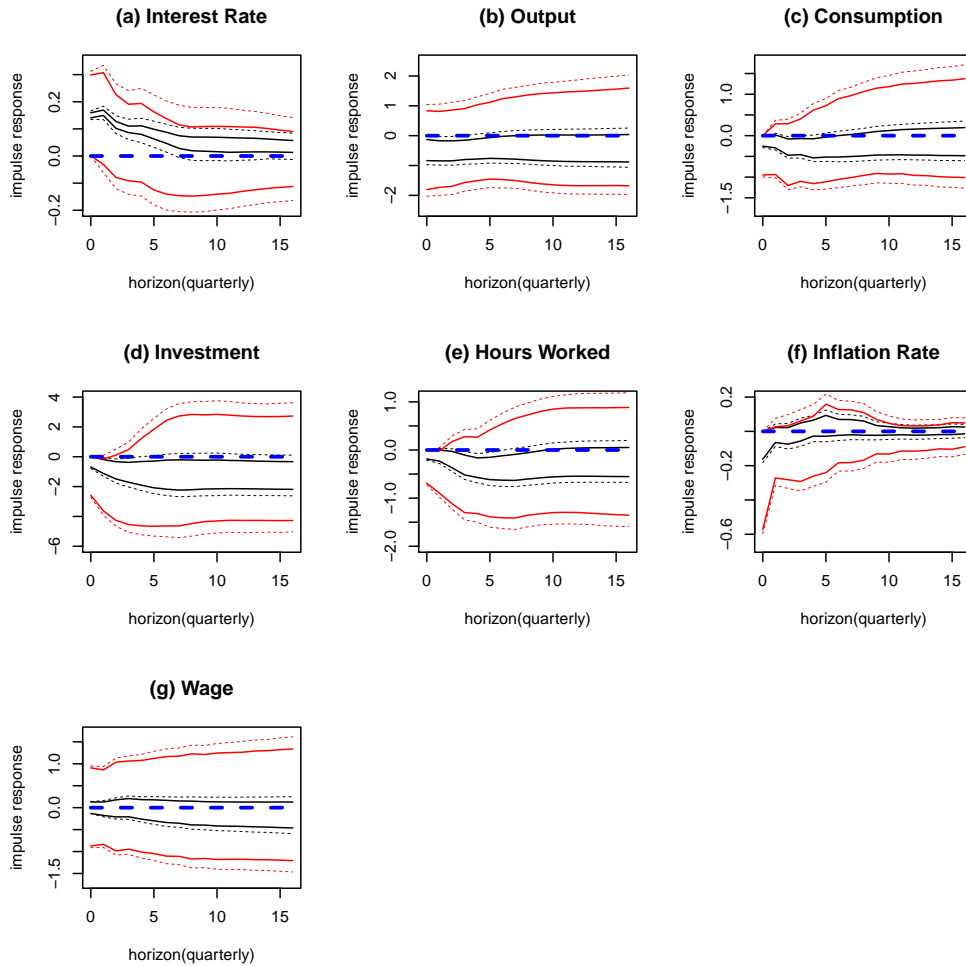


**Figure 16: Augmented Bounds on the FEVD vs Sign Restrictions: Impulse Responses Identified Set, Distribution-Free Approach**

In each panel, the black solid lines plot the posterior means of the response set bounds for the model with augmented bounds on the FEVD; the black dashed lines plot the 68% Bayesian credibility region of the response set for the model with augmented bounds on the FEVD; the red solid lines plot the posterior means of the response set bounds for the model with sign restrictions; the red dashed lines plot the 68% Bayesian credibility region of the response set for the model

with sign restrictions. The blue dashed line is the zero line. Monetary policy shock size is set to 15 basis points; vertical axis is measured in percentage, with the exception of panel (a), where 0.10 is equivalent to 10 basis points.

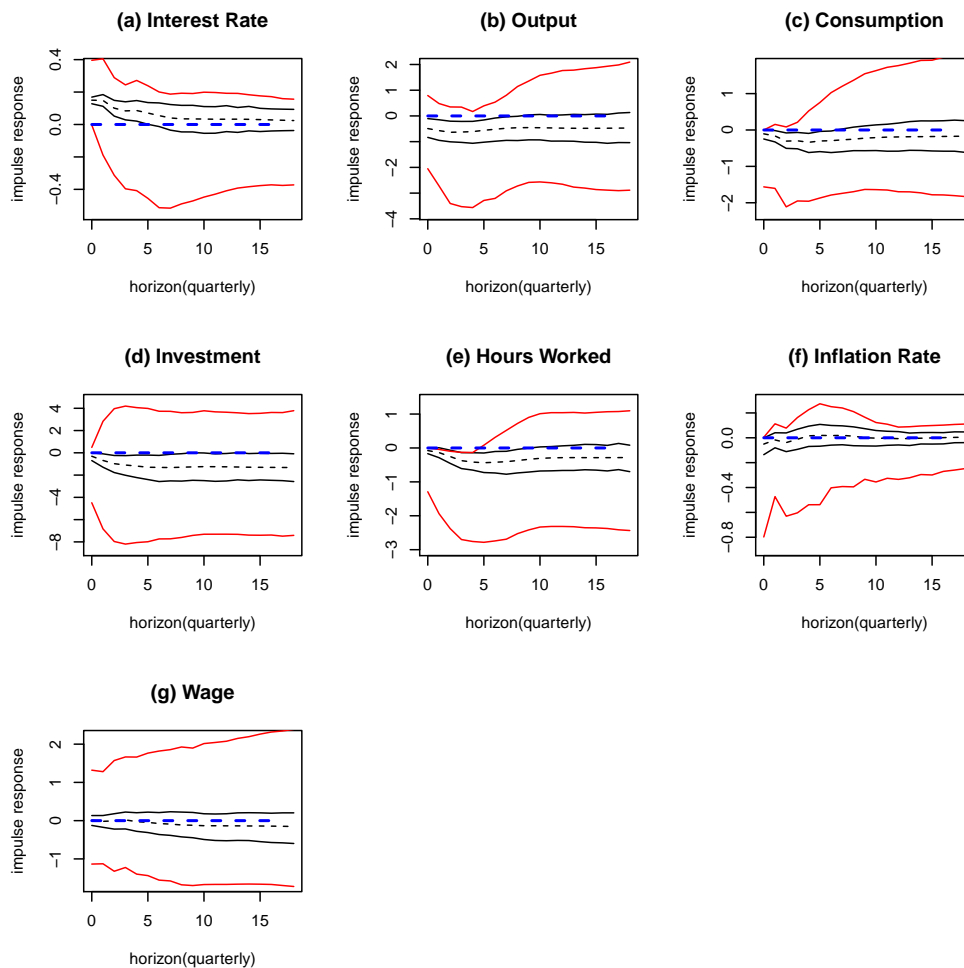


**Figure 17: Augmented Bounds on the FEVD vs Sign Restrictions: Impulse Responses, Uniform Prior Approach**

In each panel, the black lines plot the 95% Bayesian credibility region (solid) and the posterior median (dashed) of the response under augmented bounds on the FEVD; the red lines plot the 95% Bayesian credibility region of the response under sign restrictions. The blue dashed line is the zero line. Monetary policy shock size is set to 15 basis points; vertical axis is measured in percentage, with the exception of panel (a), where 0.10 is equivalent to 10 basis points.

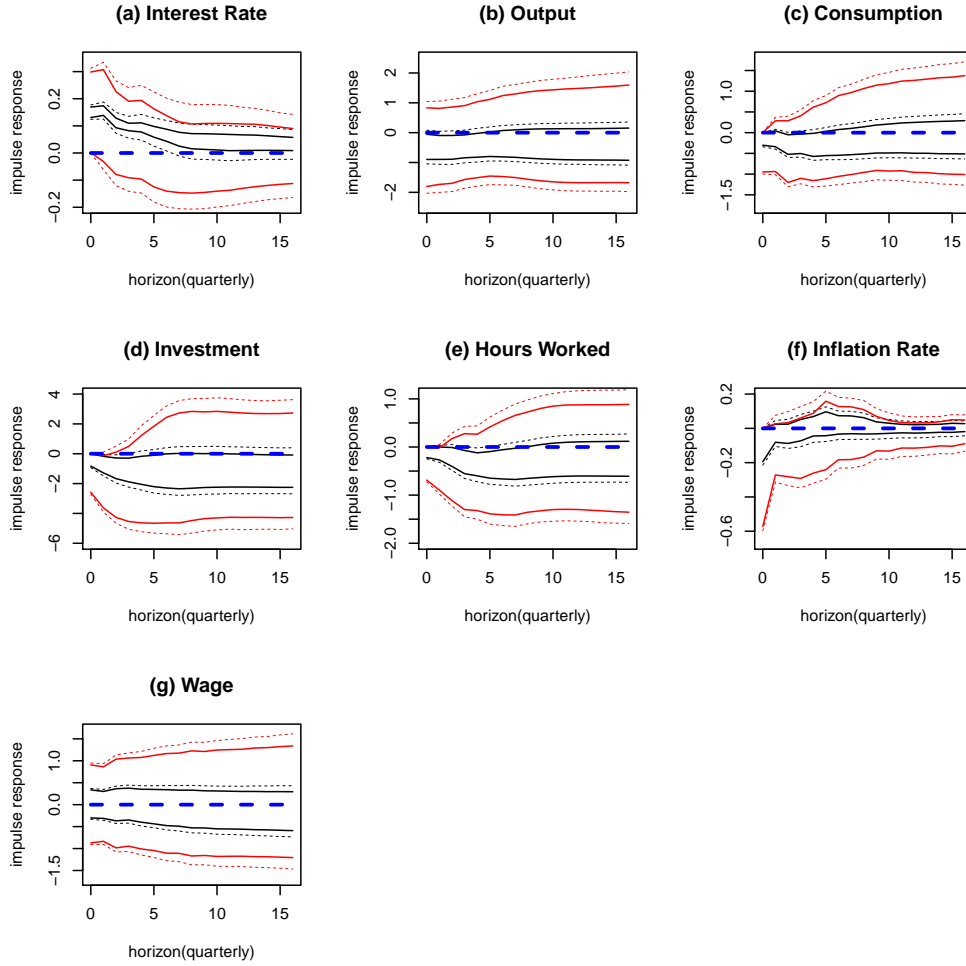


**Figure 18: Perturbed Bounds on the FEVD vs Sign Restrictions: Impulse Responses Identified Set, Distribution-Free Approach**

In each panel, the black solid lines plot the posterior means of the response set bounds for the model with perturbed bounds on the FEVD; the black dashed lines plot the 68% Bayesian credibility region of the response set for the model with perturbed bounds on the FEVD; the red solid lines plot the posterior means of the response set bounds for the model with sign restrictions; the red dashed lines plot the 68% Bayesian credibility region of the response set for the model with sign restrictions. The blue dashed line is the zero line. Monetary policy shock size is set to 15 basis points; vertical axis is measured in percentage, with the exception of panel (a), where 0.10 is equivalent to 10 basis points.

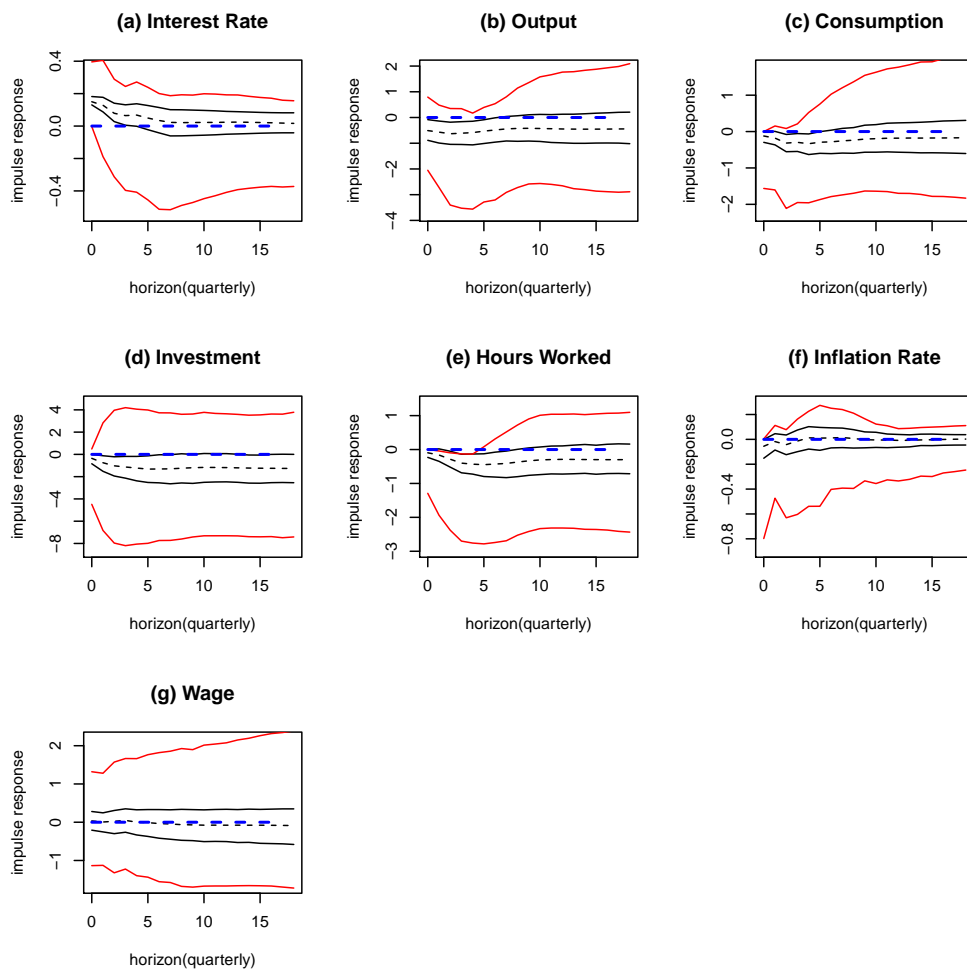


**Figure 19: Perturbed Bounds on the FEVD vs Sign Restrictions: Impulse Responses, Uniform Prior Approach**

In each panel, the black lines plot the 95% Bayesian credibility region (solid) and the posterior median (dashed) of the response under perturbed bounds on the FEVD; the red lines plot the 95% Bayesian credibility region of the response under sign restrictions. The blue dashed line is the zero line. Monetary policy shock size is set to 15 basis points; vertical axis is measured in percentage, with the exception of panel (a), where 0.10 is equivalent to 10 basis points.

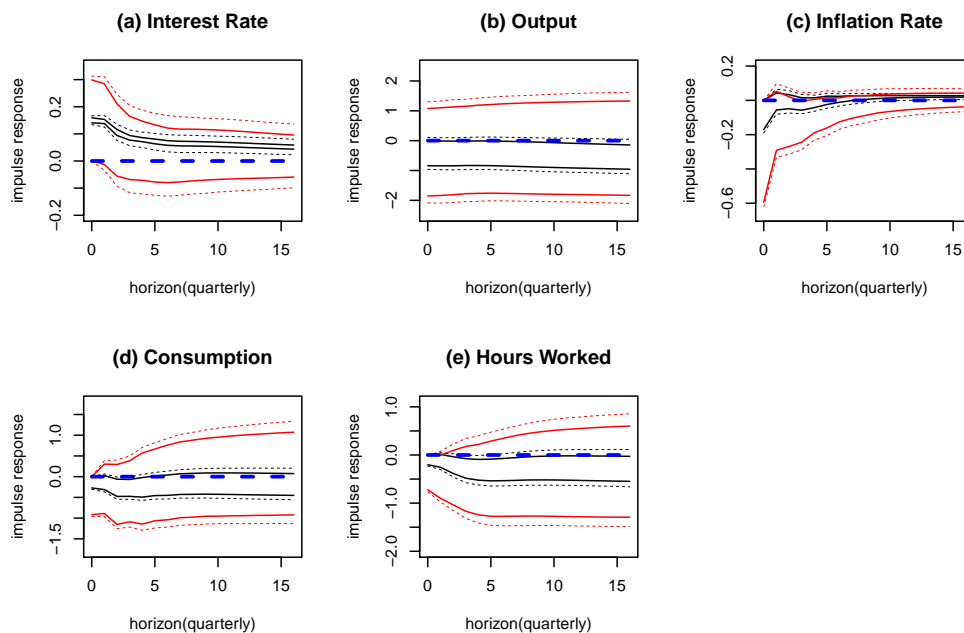


**Figure 20: Bounds on the FEVD vs Sign Restrictions, Misspecified Model: Impulse Responses Identified Set, Distribution-Free Approach**

For the misspecification in Section 6.5, in each panel the black solid lines plot the posterior means of the response set bounds for the model with dogmatic bounds on the FEVD; the black dashed lines plot the 68% Bayesian credibility region of the response set for the model with dogmatic bounds on the FEVD; the red solid lines plot the posterior means of the response set bounds for the model with sign restrictions; the red dashed lines plot the 68% Bayesian credibility region of the response set for the model with sign restrictions. The blue dashed line is the zero line. Monetary policy shock size is set to 15 basis points; vertical axis is measured in percentage, with the exception of panel (a), where 0.10 is equivalent to 10 basis points.

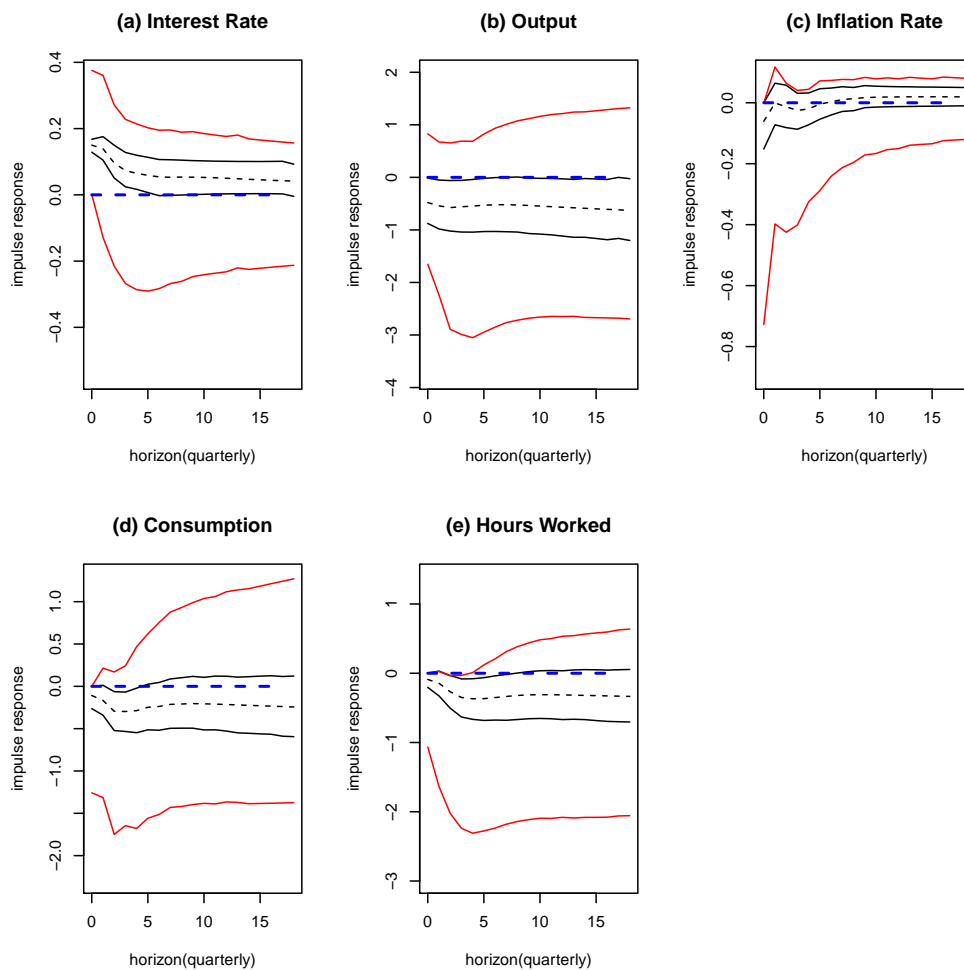


**Figure 21: Bounds on the FEVD vs Sign Restrictions, Misspecified Model: Impulse Responses, Uniform Prior Approach**

For the misspecification in Section 6.5, in each panel the black lines plot the 95% Bayesian credibility region (solid) and the posterior median (dashed) of the response under dogmatic bounds on the FEVD; the red lines plot the 95% Bayesian credibility region of the response under sign restrictions. The blue dashed line is the zero line. Monetary policy shock size is set to 15 basis points; vertical axis is measured in percentage, with the exception of panel (a), where 0.10 is equivalent to 10 basis points.

## B Technical Appendix

### B.1 Bivariate Setting

#### Proposition 3.1.

This proof proceeds as follows: firstly, it derives the identified sets in (3.7) and (3.8); it then compares the two sets.

Following Uhlig (2005),  $\mathbf{A}_0$  can be parametrized via the Cholesky matrix  $\mathbf{\Sigma}_{tr}$  and a rotation matrix  $\mathbf{Q} = \begin{pmatrix} \cos \rho & -\sin \rho \\ \sin \rho & \cos \rho \end{pmatrix}$  with spherical coordinate  $\rho \in [0, 2\pi]$ . The structural matrix of impact responses can be written as

$$\mathbf{IR}^0 = \mathbf{A}_0^{-1} = \mathbf{\Sigma}_{tr}\mathbf{Q} = \begin{pmatrix} \sigma_{11} \cos \rho & -\sigma_{11} \sin \rho \\ \sigma_{21} \cos \rho + \sigma_{22} \sin \rho & -\sigma_{21} \sin \rho + \sigma_{22} \cos \rho \end{pmatrix}$$

and the parameter of interest is  $\alpha \equiv \sigma_{11} \cos \rho$ , where  $\boldsymbol{\phi} = (\sigma_{11}, \sigma_{21}, \sigma_{22}) \in \boldsymbol{\Phi} = \mathbb{R}_+ \times \mathbb{R} \times \mathbb{R}_+$ . Following Christiano, Eichenbaum, and Evans (1999), I impose the sign normalization restrictions by constraining the diagonal elements of  $\mathbf{A}_0$  to being nonnegative,

$$\sigma_{22} \cos \rho - \sigma_{21} \sin \rho \geq 0 \tag{B.1}$$

and

$$\sigma_{11} \cos \rho \geq 0. \tag{B.2}$$

The identifying sign restrictions *SR1* and *SR2* in Section 3.2.1 are expressed as

$$\sigma_{11} \sin \rho \geq 0, \tag{B.3}$$

$$-\sigma_{22} \sin \rho - \sigma_{21} \cos \rho \leq 0. \tag{B.4}$$

Given  $\boldsymbol{\phi}$ , the identified set for  $\alpha = \sigma_{11} \cos \rho$  is given by its range as  $\rho$  varies over the range characterized by the restrictions (B.1) - (B.4).

Assume  $\sigma_{21} > 0$ . Constraints (B.2) and (B.3) induce  $\rho \in [0, \frac{\pi}{2}]$ ; constraints (B.1) and (B.4) imply  $\rho \in [\arctan(-\sigma_{21}/\sigma_{22}), \arctan(\sigma_{22}/\sigma_{21})]$ . Intersecting the two intervals leads to  $[0, \arctan(\sigma_{22}/\sigma_{21})]$  as the identified set for  $\rho$ . Thus, for  $\sigma_{21} > 0$  the identified set for  $\alpha$  in (3.7) follows. A similar argument applies for  $\sigma_{21} \leq 0$ :

$$IS_\alpha(\boldsymbol{\phi}) \equiv \begin{cases} \left[ \sigma_{11} \cos \left( \arctan \left( \frac{\sigma_{22}}{\sigma_{21}} \right) \right), \sigma_{11} \right], & \text{for } \sigma_{21} > 0, \\ \left[ 0, \sigma_{11} \cos \left( \arctan \left( -\frac{\sigma_{21}}{\sigma_{22}} \right) \right) \right], & \text{for } \sigma_{21} \leq 0. \end{cases} \tag{B.5}$$

*FEVR* assumes that the contribution of shock  $\epsilon_2$  to the total error variance of  $y_1$  is bounded between  $\underline{k}$  and  $\bar{k}$ . Following the notation introduced in Section 3, this restriction can be written as

$$\underline{k} \leq CFEV_{\epsilon_2}^{y_1}(0) = \frac{FEV_{\epsilon_2}^{y_1}(0)}{FEV^{y_1}(0)} \leq \bar{k}, \quad (\text{B.6})$$

where  $0 \leq \underline{k} < \bar{k} \leq 1$ . Given specification of  $\mathbf{IR}^0$ , note that

$$\begin{aligned} FEV_{\epsilon_2}^{y_1}(0) &= \sigma_{11} \sin^2 \rho, \\ FEV^{y_1}(0) &= \sigma_{11}^2 \sin^2 \rho + \sigma_{11}^2 \cos^2 \rho = \sigma_{11}^2. \end{aligned}$$

Thus, restriction (B.6) can be written as

$$\underline{k} \leq \sin^2 \rho \leq \bar{k} \quad (\text{B.7})$$

and imposes quadratic constraints on  $\mathbf{Q}$ . Under constraints (B.1) - (B.4) and (B.7), the argument used above leads to the identified set for  $\alpha$  in (3.8):

$$IS_\alpha(\phi) \equiv \begin{cases} \left[ \sigma_{11} \cos(\arcsin \sqrt{\bar{k}}), \sigma_{11} \cos(\arcsin \sqrt{\underline{k}}) \right] \\ \text{for } \{\sigma_{21} > 0, \bar{k} < \bar{k}^*(\phi)\} \cup \{\sigma_{21} \leq 0, \underline{k} > \underline{k}^*(\phi)\}, \\ \left[ \sigma_{11} \cos\left(\arctan\left(\frac{\sigma_{22}}{\sigma_{21}}\right)\right), \sigma_{11} \cos(\arcsin \sqrt{\bar{k}}) \right] \\ \text{for } \sigma_{21} > 0, \bar{k} \geq \bar{k}^*(\phi), \\ \left[ \sigma_{11} \cos(\arcsin \sqrt{\bar{k}}), \sigma_{11} \cos\left(\arctan\left(-\frac{\sigma_{21}}{\sigma_{22}}\right)\right) \right] \\ \text{for } \sigma_{21} \leq 0, \underline{k} \leq \underline{k}^*(\phi), \end{cases} \quad (\text{B.8})$$

where  $\bar{k}^*(\phi) = \sin^2(\arctan(\frac{\sigma_{22}}{\sigma_{21}}))$  and  $\underline{k}^*(\phi) = \sin^2(\arctan(-\frac{\sigma_{21}}{\sigma_{22}}))$ .

Firstly, assume that  $\underline{k} \neq 0$  and  $\bar{k} \neq 1$ . For  $\sigma_{21} > 0$ ,  $\bar{k} < \bar{k}^*(\phi)$ ,  $IS_\alpha(\phi)$  in (B.8) is strictly smaller than  $IS_\alpha(\phi)$  in (B.5) because  $\sigma_{11} \cos(\arcsin \sqrt{\bar{k}}) < \sigma_{11}$  and  $\sigma_{11} \cos(\arcsin \sqrt{\bar{k}}) > \sigma_{11} \cos\left(\arctan\left(\frac{\sigma_{22}}{\sigma_{21}}\right)\right)$ . For  $\sigma_{21} \leq 0$ ,  $\underline{k} > \underline{k}^*(\phi)$ , the reduction in the identified set follows from the fact that  $\sigma_{11} \cos(\arcsin \sqrt{\bar{k}}) > 0$  and  $\sigma_{11} \cos(\arcsin \sqrt{\bar{k}}) < \sigma_{11} \cos\left(\arctan\left(-\frac{\sigma_{21}}{\sigma_{22}}\right)\right)$ . The same argument applies under  $\sigma_{21} > 0$ ,  $\bar{k} \geq \bar{k}^*(\phi)$  and  $\sigma_{21} \leq 0$ ,  $\underline{k} \leq \underline{k}^*(\phi)$ .

Secondly, suppose that  $\underline{k} = 0$  and  $\bar{k} \neq 1$ . The identified set in (B.8) then becomes

$$IS_\alpha(\phi) \equiv \begin{cases} \left[ \sigma_{11} \cos(\arcsin \sqrt{\bar{k}}), \sigma_{11} \right] \\ \text{for } \sigma_{21} > 0, \bar{k} < \bar{k}^*(\phi), \\ \left[ \sigma_{11} \cos\left(\arctan\left(\frac{\sigma_{22}}{\sigma_{21}}\right)\right), \sigma_{11} \right] \\ \text{for } \sigma_{21} > 0, \bar{k} \geq \bar{k}^*(\phi), \\ \left[ \sigma_{11} \cos(\arcsin \sqrt{\bar{k}}), \sigma_{11} \cos\left(\arctan\left(-\frac{\sigma_{21}}{\sigma_{22}}\right)\right) \right] \\ \text{for } \sigma_{21} \leq 0. \end{cases} \quad (\text{B.9})$$

For  $\sigma_{21} > 0$ ,  $\bar{k} \geq \bar{k}^*(\phi)$ ,  $IS_\alpha(\phi)$  in (B.9) is equivalent to  $IS_\alpha(\phi)$  in (B.5); otherwise, the identified set in (B.9) is strictly smaller.

Finally, assume that  $\underline{k} \neq 0$  and  $\bar{k} = 1$ . The identified set in (B.8) is now

$$IS_\alpha(\phi) \equiv \begin{cases} \left[ \sigma_{11} \cos \left( \arctan \left( \frac{\sigma_{22}}{\sigma_{21}} \right) \right), \sigma_{11} \cos(\arcsin \sqrt{\underline{k}}) \right] \\ \text{for } \sigma_{21} > 0, \\ \left[ 0, \sigma_{11} \cos(\arcsin \sqrt{\underline{k}}) \right] \\ \text{for } \sigma_{21} \leq 0, \underline{k} > \underline{k}^*(\phi), \\ \left[ 0, \sigma_{11} \cos \left( \arctan \left( -\frac{\sigma_{21}}{\sigma_{22}} \right) \right) \right] \\ \text{for } \sigma_{21} \leq 0, \underline{k} \leq \underline{k}^*(\phi). \end{cases} \quad (\text{B.10})$$

For  $\sigma_{21} \leq 0$ ,  $\underline{k} \leq \underline{k}^*(\phi)$ ,  $IS_\alpha(\phi)$  in (B.10) is equivalent to  $IS_\alpha(\phi)$  in (B.5); otherwise, the identified set in (B.10) is strictly smaller.

■

### Proposition 3.2.

*FEVR2* assumes that the contribution of shock  $\epsilon_1$  to the total error variance of  $y_2$  is bounded between  $\underline{k}$  and  $\bar{k}$ . Following the notation introduced in Section 3, this restriction can be written as

$$\underline{k} \leq CFEV_{\epsilon_1}^{y_2}(0) = \frac{FEV_{\epsilon_1}^{y_2}(0)}{FEV^{y_2}(0)} \leq \bar{k}, \quad (\text{B.11})$$

where  $0 \leq \underline{k} < \bar{k} \leq 1$ . Given specification of  $\mathbf{IR}^0$ , note that

$$\begin{aligned} FEV_{\epsilon_1}^{y_2}(0) &= (\sigma_{21} \cos \rho + \sigma_{22} \sin \rho)^2, \\ FEV^{y_2}(0) &= \sigma_{21}^2 + \sigma_{22}^2. \end{aligned}$$

Thus, restriction (B.11) can be written as

$$\underline{k} \leq \frac{(\sigma_{21} \cos \rho + \sigma_{22} \sin \rho)^2}{\sigma_{21}^2 + \sigma_{22}^2} \leq \bar{k}. \quad (\text{B.12})$$

The argument in the previous proof delivers Proposition 3.2. ■

## B.2 Trivariate Setting

### Proposition 3.3.

This proof firstly derives the identified sets in (3.10) and (3.11) and then makes the comparison.

In the trivariate setting,  $\mathbf{Q}$  can be written as the product of three Givens matrices  $\mathbf{Q}_{12}$ ,  $\mathbf{Q}_{13}$  and  $\mathbf{Q}_{23}$ , each rotating a different pair of columns of the matrix to be transformed:

$$\mathbf{Q} = \begin{pmatrix} \cos \rho_{12} & -\sin \rho_{12} & 0 \\ \sin \rho_{12} & \cos \rho_{12} & 0 \\ 0 & 0 & 1 \end{pmatrix} \begin{pmatrix} \cos \rho_{13} & 0 & -\sin \rho_{13} \\ 0 & 1 & 0 \\ \sin \rho_{13} & 0 & \cos \rho_{13} \end{pmatrix} \begin{pmatrix} 1 & 0 & 0 \\ 0 & \cos \rho_{23} & -\sin \rho_{23} \\ 0 & \sin \rho_{23} & \cos \rho_{23} \end{pmatrix}.$$

For simplicity, the main text limits the analysis to the case where  $\rho_{12} = \rho_{23} = 0$ , namely  $\mathbf{Q}_{12} = \mathbf{Q}_{23} = \mathbf{I}_3$ ,  $\mathbf{Q} = \mathbf{Q}_{13}$  and  $\rho = \rho_{13}$ . Thus, there are the following sign normalizations:

$$\sigma_{11} \cos \rho \geq 0, \tag{B.13}$$

$$\sigma_{22} \geq 0, \tag{B.14}$$

which is always satisfied, and

$$-\sigma_{31} \sin \rho + \sigma_{33} \cos \rho \geq 0. \tag{B.15}$$

The identifying sign restrictions *SR1*, *SR2* and *SR3* in Section 3.2.2 are

$$\sigma_{11} \sin \rho \geq 0, \tag{B.16}$$

$$\sigma_{21} \cos \rho \geq 0, \tag{B.17}$$

$$\sigma_{31} \cos \rho + \sigma_{33} \sin \rho \geq 0. \tag{B.18}$$

Under constraints (B.13) - (B.18), the argument used for Proposition 3.1 leads to the identified set for  $\alpha \equiv \sigma_{11} \cos \rho$  in (3.10):

$$IS_\alpha(\phi) \equiv \begin{cases} \left[ \sigma_{11} \cos \left( \arctan \left( \frac{\sigma_{33}}{\sigma_{31}} \right) \right), \sigma_{11} \right], & \text{for } \sigma_{31} > 0, \\ \left[ 0, \sigma_{11} \cos \left( \arctan \left( -\frac{\sigma_{31}}{\sigma_{33}} \right) \right) \right], & \text{for } \sigma_{31} \leq 0, \end{cases} \tag{B.19}$$

where sign restrictions are defined if and only if  $\sigma_{21} \geq 0$ .

*FEVR3* assumes that the contribution of shock  $\epsilon_3$  to the total error variance of  $y_2$  is bounded between  $\underline{k}$  and  $\bar{k}$ . This restriction can be written as

$$\underline{k} \leq CFEV_{\epsilon_3}^{y_2}(0) = \frac{FEV_{\epsilon_3}^{y_2}(0)}{FEV^{y_2}(0)} \leq \bar{k}, \tag{B.20}$$

where  $0 \leq \underline{k} < \bar{k} \leq 1$ . Given specification of  $\mathbf{IR}^0$ , note that

$$\begin{aligned} FEV_{\epsilon_3}^{y_2}(0) &= \sigma_{21}^2 \sin^2 \rho, \\ FEV^{y_2}(0) &= \sigma_{21}^2 + \sigma_{22}^2. \end{aligned}$$

Thus, restriction (B.20) can be written as

$$\underline{k} \leq \frac{\sigma_{21}^2 \sin^2 \rho}{\sigma_{21}^2 + \sigma_{22}^2} \leq \bar{k}. \quad (\text{B.21})$$

Constraints (B.13) - (B.18) and (B.21) yields the identified set in (3.11):

$$IS_\alpha(\phi) \equiv \begin{cases} \left[ \left[ \sigma_{11} \cos \left( \arcsin \left( \frac{\sqrt{k(\sigma_{21}^2 + \sigma_{22}^2)}}{\sigma_{21}} \right) \right), \sigma_{11} \cos \left( \arcsin \left( \frac{\sqrt{k(\sigma_{21}^2 + \sigma_{22}^2)}}{\sigma_{21}} \right) \right) \right], \right. \\ \text{for } \{\sigma_{31} > 0, \bar{k} < \bar{k}^*(\phi)\} \cup \{\sigma_{31} \leq 0, \underline{k} > \underline{k}^*(\phi)\}, \\ \left[ \sigma_{11} \cos \left( \arctan \left( \frac{\sigma_{33}}{\sigma_{31}} \right) \right), \sigma_{11} \cos \left( \arcsin \left( \frac{\sqrt{k(\sigma_{21}^2 + \sigma_{22}^2)}}{\sigma_{21}} \right) \right) \right], \\ \text{for } \sigma_{31} > 0, \bar{k} \geq \bar{k}^*(\phi), \\ \left[ \sigma_{11} \cos \left( \arcsin \left( \frac{\sqrt{k(\sigma_{21}^2 + \sigma_{22}^2)}}{\sigma_{21}} \right) \right), \sigma_{11} \cos \left( \arctan \left( -\frac{\sigma_{31}}{\sigma_{33}} \right) \right) \right], \\ \text{for } \sigma_{31} \leq 0, \underline{k} \leq \underline{k}^*(\phi), \end{cases} \quad (\text{B.22})$$

where  $\underline{k}^*(\phi) = \frac{\sigma_{21}^2}{\sigma_{21}^2 + \sigma_{22}^2} \sin^2 \left( \arctan \left( -\frac{\sigma_{31}}{\sigma_{33}} \right) \right)$ ,  $\bar{k}^*(\phi) = \frac{\sigma_{21}^2}{\sigma_{21}^2 + \sigma_{22}^2} \sin^2 \left( \arctan \left( \frac{\sigma_{33}}{\sigma_{31}} \right) \right)$ , and  $\sigma_{21} \geq 0$ .

Assume that  $\underline{k} \neq 0$  and  $\bar{k} \neq 1$ . For  $\sigma_{31} > 0$ ,  $\bar{k} < \bar{k}^*(\phi)$ ,  $IS_\alpha(\phi)$  in (B.22) is strictly smaller than  $IS_\alpha(\phi)$  in (B.19) because  $\sigma_{11} \cos \left( \arcsin \left( \frac{\sqrt{k(\sigma_{21}^2 + \sigma_{22}^2)}}{\sigma_{21}} \right) \right) < \sigma_{11}$  and  $\sigma_{11} \cos \left( \arcsin \left( \frac{\sqrt{k(\sigma_{21}^2 + \sigma_{22}^2)}}{\sigma_{21}} \right) \right) > \sigma_{11} \cos \left( \arctan \left( \frac{\sigma_{33}}{\sigma_{31}} \right) \right)$ . For  $\sigma_{31} \leq 0$ ,  $\underline{k} > \underline{k}^*(\phi)$ , the reduction in the identified set follows from the fact that  $\sigma_{11} \cos \left( \arcsin \left( \frac{\sqrt{k(\sigma_{21}^2 + \sigma_{22}^2)}}{\sigma_{21}} \right) \right) > 0$  and  $\sigma_{11} \cos \left( \arcsin \left( \frac{\sqrt{k(\sigma_{21}^2 + \sigma_{22}^2)}}{\sigma_{21}} \right) \right) < \sigma_{11} \cos \left( \arctan \left( -\frac{\sigma_{31}}{\sigma_{33}} \right) \right)$ . The same argument applies under  $\sigma_{31} > 0$ ,  $\bar{k} \geq \bar{k}^*(\phi)$  and  $\sigma_{31} \leq 0$ ,  $\underline{k} \leq \underline{k}^*(\phi)$ .

Suppose that  $\underline{k} = 0$  and  $\bar{k} \neq 1$ . The identified set in (B.22) then becomes

$$IS_\alpha(\phi) \equiv \begin{cases} \left[ \sigma_{11} \cos \left( \arcsin \left( \frac{\sqrt{\underline{k}(\sigma_{21}^2 + \sigma_{22}^2)}}{\sigma_{21}} \right) \right), \sigma_{11} \right], \\ \text{for } \{\sigma_{31} > 0, \bar{k} < \bar{k}^*(\phi)\}, \\ \left[ \sigma_{11} \cos \left( \arctan \left( \frac{\sigma_{33}}{\sigma_{31}} \right) \right), \sigma_{11} \right], \\ \text{for } \sigma_{31} > 0, \bar{k} \geq \bar{k}^*(\phi), \\ \left[ \sigma_{11} \cos \left( \arcsin \left( \frac{\sqrt{\underline{k}(\sigma_{21}^2 + \sigma_{22}^2)}}{\sigma_{21}} \right) \right), \sigma_{11} \cos \left( \arctan \left( -\frac{\sigma_{31}}{\sigma_{33}} \right) \right) \right], \\ \text{for } \sigma_{31} \leq 0, \end{cases} \quad (\text{B.23})$$

where  $\sigma_{21} \geq 0$ . For  $\sigma_{31} > 0$ ,  $\bar{k} \geq \bar{k}^*(\phi)$ ,  $IS_\alpha(\phi)$  in (B.23) is equivalent to  $IS_\alpha(\phi)$  in (B.19); otherwise, the identified set in (B.23) is strictly smaller.

Finally, assume that  $\underline{k} \neq 0$  and  $\bar{k} = 1$ . The identified set in (B.22) is

$$IS_\alpha(\phi) \equiv \begin{cases} \left[ \sigma_{11} \cos \left( \arctan \left( \frac{\sigma_{33}}{\sigma_{31}} \right) \right), \sigma_{11} \cos \left( \arcsin \left( \frac{\sqrt{\underline{k}(\sigma_{21}^2 + \sigma_{22}^2)}}{\sigma_{21}} \right) \right) \right], \\ \text{for } \sigma_{31} > 0, \\ \left[ 0, \sigma_{11} \cos \left( \arcsin \left( \frac{\sqrt{\underline{k}(\sigma_{21}^2 + \sigma_{22}^2)}}{\sigma_{21}} \right) \right) \right], \\ \text{for } \sigma_{31} \leq 0, \underline{k} > \underline{k}^*(\phi), \\ \left[ 0, \sigma_{11} \cos \left( \arctan \left( -\frac{\sigma_{31}}{\sigma_{33}} \right) \right) \right], \\ \text{for } \sigma_{31} \leq 0, \underline{k} \leq \underline{k}^*(\phi), \end{cases} \quad (\text{B.24})$$

where  $\sigma_{21} \geq 0$ . For  $\sigma_{31} \leq 0$ ,  $\underline{k} \leq \underline{k}^*(\phi)$ ,  $IS_\alpha(\phi)$  in (B.24) is equivalent to  $IS_\alpha(\phi)$  in (B.19); otherwise, the identified set in (B.24) is strictly smaller.

■

### B.3 Non-Emptiness and Shrinkage

The proofs given below use the following notation and concepts.  $\mathbf{Q} = [\mathbf{q}_1, \dots, \mathbf{q}_n] \in \Theta(n)$  is a  $n \times n$  orthonormal matrix belonging to the space of  $n \times n$  orthonormal matrices  $\Theta(n)$ , where  $n$  is the number of endogenous variables in a VAR(p) model. It follows that  $\mathbf{Q}' = \mathbf{Q}^{-1}$  and  $\mathbf{q}_j \in \mathcal{R}^n$ ,  $\mathbf{q}'_j \mathbf{q}_i = 0$  for  $j \neq i$ ,  $\sum_{j=1}^n \mathbf{q}_j \mathbf{q}'_j = \mathbf{I}_n$ , and  $\|\mathbf{q}_j\| = 1$  for every  $j \in \{1, \dots, n\}$ .  $\phi = (\mathbf{B}, \Sigma) \in \Phi$  collects the reduced-form parameters and  $\Phi \subset \mathcal{R}^{n+n^2p} \times \Xi$ , where  $\Xi$  is the space of  $n \times n$  symmetric positive semidefinite matrices; see Section 2.1 in the main text for definition of  $\mathbf{B}$  and  $\Sigma$ . The domain of  $\Phi$  is restricted such that the VAR(p) is invertible into a VMA( $\infty$ ).  $g_{ij}^h(\phi, \mathbf{Q}) \equiv \mathbf{e}'_i \mathbf{C}_h(\mathbf{B}) \Sigma_{tr} \mathbf{Q} \mathbf{e}_j \equiv \mathbf{c}'_{ih}(\phi) \mathbf{q}_j \in \mathcal{R}$  is the  $(i, j)$ -th element of  $\mathbf{I}\mathbf{R}^h$  for  $i, j \in \{1, \dots, n\}$  and  $h = 0, 1, \dots$ .

Let  $\mathcal{Q}(\phi|\mathbf{F}, \mathbf{S}, \mathbf{\Gamma})$  denote the set of  $\mathbf{Q}$ 's that satisfy sign normalizations, zero restrictions (2.5), sign restrictions (2.7), and restrictions on the FEVD (3.4); let  $\mathbf{F}, \mathbf{S}, \mathbf{\Gamma}$  denote a shorthand notation for zero restrictions, sign restrictions, constraints on the FEVD, respectively.  $IS_g(\phi|\mathbf{F}, \mathbf{S}, \mathbf{\Gamma}) = \{g_{ij}^h(\phi, \mathbf{Q}) : \mathbf{Q} \in \mathcal{Q}(\phi|\mathbf{F}, \mathbf{S}, \mathbf{\Gamma})\}$  is the identified set for the object of interest, defined as a set-valued map from  $\phi$  to a subset in  $\mathcal{R}$  that delivers the range of  $g_{ij}^h(\phi, \mathbf{Q})$  when  $\mathbf{Q}$  varies over  $\mathcal{Q}(\mathbf{Q}|\mathbf{F}, \mathbf{S}, \mathbf{\Gamma})$ . Let  $f_j$  represent the number of zero restrictions constraining  $\mathbf{q}_j$ ;  $\mathcal{I}_S \subset \{1, 2, \dots, n\}$  is the set of indices such that  $j \in \mathcal{I}_S$  if some of the impulse responses to the  $j$ -th structural shock are sign-constrained; let  $\mathcal{I}_{FEV}$  be a set of indices such that  $j \in \mathcal{I}_{FEV}$  if shock  $j$  is restricted as in (3.3);  $\Lambda_j$  is a set of indices such that  $z \in \Lambda_j$ , where  $j \in \mathcal{I}_{FEV}$ , if the FEV of variable  $z \in \{1, \dots, n\}$  to shock  $j$  is bounded as in (3.3).

Let  $\mathbf{\Upsilon}_S^z(\phi) = \frac{\mathbf{\Upsilon}^z(\phi) + (\mathbf{\Upsilon}^z(\phi))'}{2}$  denote the symmetric part of  $\mathbf{\Upsilon}^z(\phi)$ , where  $z \in \Lambda_j$ ;  $\lambda_{l,j}^z$  for  $l = \{1, \dots, n\}$  are the  $n$  real eigenvalues of  $\mathbf{\Upsilon}_S^z(\phi)$ . Note that  $\lambda_{max,j}^z = \max\{\lambda_{1,j}^z, \dots, \lambda_{n,j}^z\}$  and  $\lambda_{min,j}^z = \min\{\lambda_{1,j}^z, \dots, \lambda_{n,j}^z\}$ . Finally, let  $\tilde{\mathbf{q}}$  be the eigenvector associated to  $\lambda_{l,j}^z$ , namely  $\mathbf{\Upsilon}_S^z(\phi)\tilde{\mathbf{q}} = \lambda_{l,j}^z\tilde{\mathbf{q}}$ .

**Proof of Proposition 3.4.**

Under  $\mathcal{I}_{FEV} = \{j^*\}$ , the whole set of restrictions on the FEVD is reduced to

$$\underline{k}_{j^*}^z \leq \mathbf{q}'_{j^*} \mathbf{\Upsilon}^z(\phi) \mathbf{q}_{j^*} \leq \bar{k}_{j^*}^z \text{ for } z \in \Lambda_{j^*}. \quad (\text{B.25})$$

$\mathbf{\Upsilon}^z(\phi)$  is a positive semidefinite  $n \times n$  real matrix and can be as such decomposed into its symmetric and antisymmetric part:

$$\mathbf{\Upsilon}^z(\phi) \equiv \mathbf{\Upsilon}_S^z(\phi) + \mathbf{\Upsilon}_{AS}^z(\phi),$$

where  $\mathbf{\Upsilon}_S^z(\phi) = \frac{\mathbf{\Upsilon}^z(\phi) + (\mathbf{\Upsilon}^z(\phi))'}{2}$  and  $\mathbf{\Upsilon}_{AS}^z(\phi) = \frac{\mathbf{\Upsilon}^z(\phi) - (\mathbf{\Upsilon}^z(\phi))'}{2}$ . This implies the following:

$$\begin{aligned} & \mathbf{q}'_{j^*} \mathbf{\Upsilon}^z(\phi) \mathbf{q}_{j^*} = \\ & \mathbf{q}'_{j^*} (\mathbf{\Upsilon}_S^z(\phi) + \mathbf{\Upsilon}_{AS}^z(\phi)) \mathbf{q}_{j^*} = \\ & \mathbf{q}'_{j^*} \left( \frac{\mathbf{\Upsilon}^z(\phi) + (\mathbf{\Upsilon}^z(\phi))'}{2} + \frac{\mathbf{\Upsilon}^z(\phi) - (\mathbf{\Upsilon}^z(\phi))'}{2} \right) \mathbf{q}_{j^*} = \\ & \mathbf{q}'_{j^*} \left( \frac{\mathbf{\Upsilon}^z(\phi) + (\mathbf{\Upsilon}^z(\phi))'}{2} \right) \mathbf{q}_{j^*} + \mathbf{q}'_{j^*} \left( \frac{\mathbf{\Upsilon}^z(\phi) - (\mathbf{\Upsilon}^z(\phi))'}{2} \right) \mathbf{q}_{j^*} = \\ & \mathbf{q}'_{j^*} \left( \frac{\mathbf{\Upsilon}^z(\phi) + (\mathbf{\Upsilon}^z(\phi))'}{2} \right) \mathbf{q}_{j^*} = \\ & \mathbf{q}'_{j^*} \mathbf{\Upsilon}_S^z(\phi) \mathbf{q}_{j^*} \\ & \text{for } z \in \Lambda_{j^*}, \end{aligned} \quad (\text{B.26})$$

where the second last equality comes from the fact that  $\mathbf{q}'_{j^*} \left( \frac{\mathbf{\Upsilon}^z(\phi) - (\mathbf{\Upsilon}^z(\phi))'}{2} \right) \mathbf{q}_{j^*} = 0$ . Thus, restrictions (B.25) can be written as

$$\underline{k}_{j^*}^z \leq \mathbf{q}'_{j^*} \mathbf{\Upsilon}_S^z(\phi) \mathbf{q}_{j^*} \leq \bar{k}_{j^*}^z \text{ for } z \in \Lambda_{j^*}, \quad (\text{B.27})$$

where  $\mathbf{\Upsilon}_S^z(\phi) = \frac{\mathbf{\Upsilon}^z(\phi) + (\mathbf{\Upsilon}^z(\phi))'}{2}$ .

$\mathbf{\Upsilon}_S^z(\phi)$  is symmetric and can be as such diagonalized; thus, there must exist an orthogonal matrix  $\mathbf{P}$  such that

$$\mathbf{P}' \mathbf{\Upsilon}_S^z(\phi) \mathbf{P} = \mathbf{D}^z,$$

where  $\mathbf{D}^z$  is a diagonal matrix

$$\mathbf{D}^z = \begin{bmatrix} \lambda_{1,j^*}^z & 0 & \dots & 0 \\ 0 & \lambda_{2,j^*}^z & \dots & 0 \\ \vdots & \dots & \ddots & \vdots \\ 0 & 0 & \dots & \lambda_{n,j^*}^z \end{bmatrix}$$

and diagonal entries  $\lambda_{1,j^*}^z, \dots, \lambda_{n,j^*}^z$  are real eigenvalues of  $\mathbf{\Upsilon}_S^z(\phi)$ .

Suppose that the  $n \times 1$  orthogonal eigenvector associated to a specific  $\lambda_{l,j^*}^z \in \{\lambda_{1,j^*}^z, \dots, \lambda_{n,j^*}^z\}$  is  $\tilde{\mathbf{q}}$ :

$$\mathbf{\Upsilon}_S^z(\phi) \tilde{\mathbf{q}} = \lambda_{l,j^*}^z \tilde{\mathbf{q}} \quad (\text{B.28})$$

It follows that

$$\tilde{\mathbf{q}}' \mathbf{\Upsilon}_S^z(\phi) \tilde{\mathbf{q}} = \lambda_{l,j^*}^z \tilde{\mathbf{q}}' \tilde{\mathbf{q}} = \lambda_{l,j^*}^z, \quad (\text{B.29})$$

where the last equality comes from the fact that  $\tilde{\mathbf{q}}' \tilde{\mathbf{q}} = 1$  by construction. Combining (B.26) and (B.29) yields

$$\tilde{\mathbf{q}}' \mathbf{\Upsilon}^z(\phi) \tilde{\mathbf{q}} = \lambda_{l,j^*}^z. \quad (\text{B.30})$$

If  $\underline{k}_{j^*}^z \leq \lambda_{l,j^*}^z \leq \bar{k}_{j^*}^z$  (condition (a)), constraint  $\underline{k}_{j^*}^z \leq \mathbf{q}'_{j^*} \mathbf{\Upsilon}^z(\phi) \mathbf{q}_{j^*} \leq \bar{k}_{j^*}^z$  is then satisfied for  $\mathbf{q}_{j^*} = \tilde{\mathbf{q}}$ . Under condition (b),  $\tilde{\mathbf{q}}$  satisfies remaining bounds on the FEVD, zero restrictions, and sign restrictions. This implies that there must exist a matrix  $\tilde{\mathbf{Q}} = [\mathbf{q}_1, \dots, \tilde{\mathbf{q}}, \dots, \mathbf{q}_n] \in \mathcal{Q}(\phi|\mathbf{F}, \mathbf{S}, \mathbf{\Gamma})$ . In turn, this leads to  $\mathcal{Q}(\phi|\mathbf{F}, \mathbf{S}, \mathbf{\Gamma}) \neq \emptyset$ . Given the map between the impulse response identified set  $IS_g(\phi|\mathbf{F}, \mathbf{S}, \mathbf{\Gamma})$  and  $\mathcal{Q}(\phi|\mathbf{F}, \mathbf{S}, \mathbf{\Gamma})$ ,  $IS_g(\phi|\mathbf{F}, \mathbf{S}, \mathbf{\Gamma}) \neq \emptyset$  for every  $i, j^* \in \{1, \dots, n\}$ ,  $z, z^* \in \Lambda_{j^*}$ , and  $h = 0, 1, \dots$ . Since  $|g_{ij^*}^h| \leq \|\mathbf{c}_{ih}(\phi)\| < \infty$  for any

$i \in \{1, \dots, n\}$ ,  $j^* \in \{1, \dots, n\}$ , and  $h = 0, 1, \dots$ , where  $\|\mathbf{c}_{ih}(\boldsymbol{\phi})\|$  is bounded due to the restriction on  $\boldsymbol{\phi}$  such that reduced-form VAR is invertible to VMA( $\infty$ ), the boundedness of the identified set follows.

■

### Proof of Proposition 3.5.

This proof extensively builds on the arguments used above.

If  $IS_g(\boldsymbol{\phi}|\mathbf{F}, \mathbf{S}, \boldsymbol{\Gamma}) \subset IS_g(\boldsymbol{\phi}|\mathbf{F}, \mathbf{S})$ , then  $\mathcal{Q}(\boldsymbol{\phi}|\mathbf{F}, \mathbf{S}, \boldsymbol{\Gamma}) \subset \mathcal{Q}(\boldsymbol{\phi}|\mathbf{F}, \mathbf{S})$  must hold. This implies that there must exist  $\tilde{\mathbf{Q}} = [\mathbf{q}_1, \dots, \tilde{\mathbf{q}}, \dots, \mathbf{q}_n]$  such that  $\tilde{\mathbf{Q}} \notin \mathcal{Q}(\boldsymbol{\phi}|\mathbf{F}, \mathbf{S}, \boldsymbol{\Gamma})$  and  $\tilde{\mathbf{Q}} \in \mathcal{Q}(\boldsymbol{\phi}|\mathbf{F}, \mathbf{S})$ .

This leads to

$$\exists z \in \Lambda_{j^*} \mid \tilde{\mathbf{q}}' \boldsymbol{\Upsilon}^z(\boldsymbol{\phi}) \tilde{\mathbf{q}} > \bar{k}_{j^*}^z \cup \tilde{\mathbf{q}}' \boldsymbol{\Upsilon}^z(\boldsymbol{\phi}) \tilde{\mathbf{q}} < \underline{k}_{j^*}^z \quad (\text{B.31})$$

and

$$\mathbf{S}_{j^*}(\boldsymbol{\phi}) \tilde{\mathbf{q}} \geq \mathbf{0}, \quad \mathbf{F}_{j^*}(\boldsymbol{\phi}) \tilde{\mathbf{q}} = \mathbf{0}. \quad (\text{B.32})$$

From the previous proof, it is easy to see that

$$\lambda_{min, j^*}^z = \min_{\mathbf{q}_{j^*}} \mathbf{q}'_{j^*} \boldsymbol{\Upsilon}^z(\boldsymbol{\phi}) \mathbf{q}_{j^*} \quad (\text{B.33})$$

and

$$\lambda_{max, j^*}^z = \max_{\mathbf{q}_{j^*}} \mathbf{q}'_{j^*} \boldsymbol{\Upsilon}^z(\boldsymbol{\phi}) \mathbf{q}_{j^*}. \quad (\text{B.34})$$

Combining (A.31), (A.32), (A.33), and (A.34) delivers  $\exists z \in \Lambda_{j^*} \mid \lambda_{min, j^*}^z < \underline{k}_{j^*}^z$  or  $\lambda_{max, j^*}^z > \bar{k}_{j^*}^z$ .

■

## B.4 Convexity

### Proof of Proposition 3.6.

Let  $\Lambda_{j^*} = \Lambda_{j^*}^{(a)} \cup \Lambda_{j^*}^{(b)} \cup \Lambda_{j^*}^{(ab)}$ , where  $z \in \Lambda_{j^*}^{(a)}$  if  $z$  satisfies condition (a) only,  $z \in \Lambda_{j^*}^{(b)}$  if  $z$  satisfies condition (b) only, and  $z \in \Lambda_{j^*}^{(ab)}$  if  $z$  satisfies condition (a) and (b). For simplicity and without loss of generality, suppose that  $\Lambda_{j^*}^{(ab)} = \emptyset$ .

For  $z \in \Lambda_{j^*}^{(a)}$ , the set of identifying assumptions on the FEVD is

$$\mathbf{q}'_{j^*} \boldsymbol{\Upsilon}^z(\boldsymbol{\phi}) \mathbf{q}_{j^*} \leq \bar{k}_{j^*}^z \text{ for any } z \in \Lambda_{j^*}^{(a)}, \quad (\text{B.35})$$

because  $\underline{k}_{j^*}^z = 0$  under condition (a).

Focus on condition (b). Let  $z \in \Lambda_{j^*}^{(b)}$  and suppose that  $\tilde{h} = 0$ . Firstly, let us derive how bounds on the FEVD can be written. From Section 3, for any  $z \in \Lambda_{j^*}^{(b)}$

$$\Upsilon^z(\phi) = \frac{\sum_{h=0}^{\tilde{h}} \mathbf{c}_{zh}(\phi) \mathbf{c}'_{zh}(\phi)}{\sum_{h=0}^{\tilde{h}} \mathbf{c}'_{zh}(\phi) \mathbf{c}_{zh}(\phi)}. \quad (\text{B.36})$$

Since  $\tilde{h} = 0$ ,

$$\Upsilon^z(\phi) = \frac{\mathbf{c}_{z0}(\phi) \mathbf{c}'_{z0}(\phi)}{\mathbf{c}'_{z0}(\phi) \mathbf{c}_{z0}(\phi)}. \quad (\text{B.37})$$

This implies that

$$\begin{aligned} \mathbf{q}'_{j^*} \Upsilon^z(\phi) \mathbf{q}_{j^*} &= \mathbf{q}'_{j^*} \frac{\mathbf{c}_{z0}(\phi) \mathbf{c}'_{z0}(\phi)}{\mathbf{c}'_{z0}(\phi) \mathbf{c}_{z0}(\phi)} \mathbf{q}_{j^*} \\ &= m(\phi) \mathbf{q}'_{j^*} \mathbf{c}_{z0}(\phi) \mathbf{c}'_{z0}(\phi) \mathbf{q}_{j^*} \\ &= m(\phi) (\mathbf{c}'_{z0}(\phi) \mathbf{q}_{j^*})^2, \end{aligned} \quad (\text{B.38})$$

where  $m(\phi) = \frac{1}{\mathbf{c}'_{z0}(\phi) \mathbf{c}_{z0}(\phi)}$  is a positive scalar; the last equality derives from  $\mathbf{q}'_{j^*} \mathbf{c}_{z0}(\phi) = (\mathbf{q}'_{j^*} \mathbf{c}_{z0}(\phi))' = \mathbf{c}'_{z0}(\phi) \mathbf{q}_{j^*}$ . As a result, the whole set of constraints on the FEVD is reduced to

$$\underline{k}_{j^*}^z \leq m(\phi) (\mathbf{c}'_{z0}(\phi) \mathbf{q}_{j^*})^2 \leq \bar{k}_{j^*}^z \text{ for } z \in \Lambda_{j^*}^{(b)}. \quad (\text{B.39})$$

Condition (b) also establishes that for any variable  $z \in \Lambda_{j^*}^{(b)}$ , responses  $g_{zj^*}^h(\phi, \mathbf{Q})$  are sign-restricted for  $h = 0, \dots, \tilde{h}$ . Since  $g_{zj^*}^h(\phi, \mathbf{Q}) = \mathbf{c}'_{zh}(\phi) \mathbf{q}_{j^*}$  and  $\tilde{h} = 0$ , this implies

$$\mathbf{c}'_{z0}(\phi) \mathbf{q}_{j^*} \geq 0 \text{ for any } z \in \Lambda_{j^*}^{(b)}, \quad (\text{B.40})$$

where, without loss of generality, it is assumed that the sign of restrictions is positive. Combining (B.39) and (A.40) shows that the whole set of bounds on the FEVD under condition (b) is reduced to some linear inequalities in  $\mathbf{q}_{j^*}$ :

$$\sqrt{\frac{\underline{k}_{j^*}^z}{m(\phi)}} \leq \mathbf{c}'_{z0}(\phi) \mathbf{q}_{j^*} \leq \sqrt{\frac{\bar{k}_{j^*}^z}{m(\phi)}}, \quad (\text{B.41})$$

$$\mathbf{c}'_{z0}(\phi) \mathbf{q}_{j^*} \geq 0 \text{ for } z \in \Lambda_{j^*}^{(b)}. \quad (\text{B.42})$$

For  $\tilde{h} > 0$ , a similar argument can be used for proving that bounds on the FEVD can be reduced to a set of linear constraint on  $\mathbf{q}_{j^*}$ .

As a result, the whole set of identifying restrictions is reduced to the following:

$$\mathbf{q}'_{j^*} \mathbf{\Upsilon}^z(\boldsymbol{\phi}) \mathbf{q}_{j^*} \leq \bar{k}_{j^*}^z \text{ for } z \in \Lambda_{j^*}^{(a)}, \quad (\text{B.43})$$

$$\sqrt{\frac{k_{j^*}^z}{m(\boldsymbol{\phi})}} \leq \mathbf{c}'_{z0}(\boldsymbol{\phi}) \mathbf{q}_{j^*} \leq \sqrt{\frac{\bar{k}_{j^*}^z}{m(\boldsymbol{\phi})}} \text{ and } \mathbf{c}'_{z0}(\boldsymbol{\phi}) \mathbf{q}_{j^*} \geq 0 \text{ for } z \in \Lambda_{j^*}^{(b)}, \quad (\text{B.44})$$

$$\mathbf{S}_{j^*}(\boldsymbol{\phi}) \mathbf{q}_{j^*} \geq \mathbf{0}. \quad (\text{B.45})$$

The set  $\{\mathbf{q}_{j^*} \in \mathcal{R}^n \mid \mathbf{q}'_{j^*} \mathbf{\Upsilon}^z(\boldsymbol{\phi}) \mathbf{q}_{j^*} \leq \bar{k}_{j^*}^z \ \forall z \in \Lambda_{j^*}^{(a)}\}$  defined by constraint (B.43) is convex because by construction  $\mathbf{\Upsilon}^z(\boldsymbol{\phi})$  is positive semi-definite. Restrictions (B.44) and (B.45) impose linear constraints on  $\mathbf{q}_{j^*}$  and  $\{\mathbf{q}_{j^*} \in \mathcal{R}^n \mid \sqrt{\frac{k_{j^*}^z}{m(\boldsymbol{\phi})}} \leq \mathbf{c}'_{z0}(\boldsymbol{\phi}) \mathbf{q}_{j^*} \leq \sqrt{\frac{\bar{k}_{j^*}^z}{m(\boldsymbol{\phi})}} \ \forall z \in \Lambda_{j^*}^{(b)}, \ \mathbf{c}'_{z0}(\boldsymbol{\phi}) \mathbf{q}_{j^*} \geq 0 \ \forall z \in \Lambda_{j^*}^{(b)}, \ \mathbf{S}_{j^*}(\boldsymbol{\phi}) \mathbf{q}_{j^*} \geq \mathbf{0}\}$  is as such a convex set (Giacomini and Kitagawa, 2018). Since the intersection of convex sets is always convex, the intersection between the unit circle defined by  $\mathbf{q}_{j^*}$  (remark:  $\|\mathbf{q}_{j^*}\| = 1$ ) and the sets induced by restrictions (B.43), (B.44), and (B.45) determines a convex set:

$\{\mathbf{q}_{j^*} \in \mathcal{R}^n \mid \mathbf{q}'_{j^*} \mathbf{\Upsilon}^z(\boldsymbol{\phi}) \mathbf{q}_{j^*} \leq \bar{k}_{j^*}^z \ \forall z \in \Lambda_{j^*}^{(a)}, \ \sqrt{\frac{k_{j^*}^z}{m(\boldsymbol{\phi})}} \leq \mathbf{c}'_{z0}(\boldsymbol{\phi}) \mathbf{q}_{j^*} \leq \sqrt{\frac{\bar{k}_{j^*}^z}{m(\boldsymbol{\phi})}} \ \forall z \in \Lambda_{j^*}^{(b)}, \ \mathbf{c}'_{z0}(\boldsymbol{\phi}) \mathbf{q}_{j^*} \geq 0 \ \forall z \in \Lambda_{j^*}^{(b)}, \ \mathbf{S}_{j^*}(\boldsymbol{\phi}) \mathbf{q}_{j^*} \geq \mathbf{0}, \ \|\mathbf{q}_{j^*}\| = 1\}$  is convex and is as such path-connected. Since the impulse response is a continuous function of  $\mathbf{q}_{j^*}$ ,  $IS_g(\boldsymbol{\phi} \mid \mathbf{S}, \boldsymbol{\Gamma})$  is an interval, as the range of a continuous function with a path-connected domain is always an interval (Propositions 12.11 and 12.23 in Sutherland (2009)). Convexity of  $IS_g(\boldsymbol{\phi} \mid \mathbf{S}, \boldsymbol{\Gamma})$  follows because an interval defined on  $\mathcal{R}$  is always convex. Given the arguments above, the proof for  $\Lambda_{j^*}^{(ab)} \neq \emptyset$  is trivial. ■

# School of Economics and Finance



This working paper has been produced by  
the School of Economics and Finance at  
Queen Mary University of London

Copyright © 2019 Alessio Volpicella all  
rights reserved.

School of Economics and Finance  
Queen Mary University of London  
Mile End Road  
London E1 4NS  
Tel: +44 (0)20 7882 7356  
Fax: +44 (0)20 8983 3580  
Web: [www.econ.qmul.ac.uk/research/workingpapers/](http://www.econ.qmul.ac.uk/research/workingpapers/)